Selective modulation of alloreactive T cells in preclinical models of acute Graft-versus-Host Disease

Selektive Modulation von alloreaktiven T-Zellen in präklinischen Modellen der akuten Graft-versus-Host Erkrankung

Doctoral thesis for a doctoral degree
at the Graduate School of Life Sciences,
Julius-Maximilians-Universität Würzburg,

submitted by

Musga Qureischi
from
Kabul, Afghanistan

Würzburg, 16.02.2021

Submitted on: …….

Office stamp

Members of the Promotionskomitee:

Chairperson:	Prof. Dr. Georg Gasteiger
Primary supervisor:	Prof. Dr. Dr. Andreas Beilhack
Supervisor (Second)	PD Dr. Friederike Berberich-Siebelt
Supervisor (Third)	Prof. Dr. Harald Wajant

Date of Public Defence: ……

Date of Receipt of Certificates: ……

Acknowledgement

The completion of this PhD thesis would not have been possible without the cooperation and contribution of several people. I would like to take the opportunity and express my gratitude to all of them.

I want to thank my primary supervisor Prof. Dr. Dr. med. Andreas Beilhack for giving me the opportunity to perform my thesis in his laboratory and for introducing me to the field of HCT and immunotherapy. I am very grateful for his valuable advice on my project and his support during my PhD.

I am deeply thankful to PD Dr. Friederike Berberich-Siebelt for all her support during my study time in Würzburg. I thank her for the constant scientific exchange and education in T cell signaling and all the personal advice she gave me during the last years.

I want to thank Prof. Dr. Harald Wajant for introducing me into the world of TNF receptors and antibody engineering. Working with him and in his laboratory has broadened my scientific horizon. I appreciated his valuable input on my thesis enormously.

I appreciate the great support of my colleagues and friends from the lab: Thanks to Dalia, Estibaliz, Josefina and Zeinab for all the exciting scientific discussions, for the technical help and for the personal support every one of you gave me. I appreciate your friendship and I will be missing working with you!

I would like to mention Carolin and Sabine and say thank you for all the effort they put in organizing the lab. I also thank all the other members of the Beilhack laboratory for the memorable time.

I am very thankful to Benjamin from Berberich-Siebelt lab for always being willing to help me with my SUMO experiments. Thanks for the pleasant company during the many hours of ex vivo in the OP room!

During my research stay in the Wajant laboratory I was greatly supported by Dani III, Johannes, Juliane, Simone, Tina and Hanna. Thanks to Mohamed II for welcoming me so warmly. I have always enjoyed the coffee breaks in the Wajant Lab!

I thank the Graduate School of Life Sciences (GSLS) for awarding me with a fellowship from the German Excellence Initiative and for allowing me to attend several conferences, research schools and workshops. Furthermore, I would like to thank especially Dr. Gabriele Blum-Oehler for all her personal support during my PhD. This

work was additionally funded by an unrestricted donation by Merete and Alexander Knauf.

I am grateful to Prof. Dr. Thomas Hünig for his inspiring lectures and Prof. Dr. Thomas Herrmann for encouraging and supporting me in the field of immunology since my early bachelor's studies. Both together, elicited the fascination of immunology in me many years ago.

A special thanks goes to my parents for always being supportive and for giving me the freedom to do what I desire. I am deeply thankful to my lovely sister Leena for all her love and care during my PhD. Finally, I want to express my gratitude to my husband Florian for all his encouragement and moral support on every single day of my PhD. Thank you for always believing in me.

Table of contents

1 Affidavit

I hereby confirm that my thesis entitled ‘Selective modulation of alloreactive T cells in preclinical models of acute Graft-versus-Host Disease’ is the result of my own work. I did not receive any help or support from commercial consultants. All sources and / or materials applied are listed and specified in the thesis.

Furthermore, I confirm that this thesis has not yet been submitted as part of another examination process neither in identical nor in similar form.

Würzburg, 16.02.2021

Eidesstattliche Erklärung

Hiermit erkläre ich an Eides statt, die Dissertation „Selektive Modulation von alloreaktiven T-Zellen in präklinischen Modellen der akuten Graft-versus-Host Erkrankung“ eigenständig, d.h. insbesondere selbständig und ohne Hilfe eines kommerziellen Promotionsberaters, angefertigt und keine anderen als die von mir angegebenen Quellen und Hilfsmittel verwendet zu haben.

Ich erkläre außerdem, dass die Dissertation weder in gleicher noch in ähnlicher Form bereits in einem anderen Prüfungsverfahren vorgelegen hat.

Würzburg, 16.02.2021

2 List of Figures

3 List of Tables

4 List of Abbreviations

µg	Mikrogram
Ab	Antibody
AF	Alexa fluor
Ag	Antigen
aGvHD	Acute graft-versus-host disease
Allo-HCT	Allogeneic hematopoietic cell transplantation
APC	Allophycocyanine
B6	C57BL/6
BALB	Bagg albino
BLI	Bioluminescence imaging
BM	Bone marrow
BSA	Bovine serum albumin
BW	Body weight
CC-R	C-C motif chemokine receptor
CD	Cluster of differentiation
cLN	Cervical lymph node
CTL	Cytotoxic T lymphocyte
Cy	Cyanine
DC	Dendritic cell
DNA	Deoxyribonucleic acid
ed	Extracellular domain
EDTA	Ethylenediaminetetra acid
FACS	Fluorescence activated cell sorting
FC	Flow cytometry
FCS	Fetal calf serum
FITC	Fluorescein isothiocyanate
FMO	Fluorescence minus one
Foxp3	Forkhead box p3
g	Gram
GIT	Gastrointestinal tract
GpL	Gaussia princeps luciferase
GvHD	Graft-versus-host-disease
Gy	Gray
h	Human
HBSS	Hank's buffered salt solution
HCT	Hematopoietic cell transplantation

HDAC	Histone deacetylase
HLA	Human leukocyte antigen
HSC	Hematopoetic stem cell
IEL	Intraepithelial lymphocytes
HRP	Horse persoxidase
IFN-γ	Interferon gamma
IL	Interleukine
iLN	Inguinal lymph node
IR	Irradiation control
kg	Kilogram
LN	Lymph node
MAdCAM-1	Mucosal vascular addressin cell adhesion molecule 1
mg	Miligram
MHC	Major histocompatibility complex
min	Minute
ml	Milliliter
mLN	Mesenteric lymph node
mM	Millimolar
mu	Murine
NFAT	Nuclear factor of activated T cells
ng	Nanogram
NRS	Normal rat serum
PB	Pacific blue
PB	Peripheral blood
PBS	Phosphate buffer saline
PE	Phycoerythrin
PerCP	Peridinin chlorophyll
PFA	Paraformaldehyde
pLN	Peripheral lymph node
PMA	Phorbol 12-myristate 13-acetate
PP	Peyer's patch
RA	Retinoic acid
RLU	Relative light units
RPMI	Roswell park memorial institute
RT	Room temperature
S1P	Sphingosine-1-phosphate
S1PR1	Sphingosine-1-phosphate receptor 1
SD	Standard deviation
SDS-Page	Sodium dodecyl sulfate polyacrylamide gel electrophoresis
SLO	Secondary lymphoid organ
T	T cell(s)
Tcon	Conventional T cell
TCR	T cell receptor
TGF-β	Transforming growth factor beta
Th1	T helper cell type 1
Th17	T helper cell type 17
Th2	T helper cell type 2
TNF-α	Tumor necrosis factor alpha
Treg	Regulatory T cells
V_H	Variable heavy
V_L	Variable light

5 Declaration of author`s contribution

Part I & II

This work was conducted in the laboratory of Prof. Dr. Dr. Andreas Beilhack (University Hospital Würzburg, Department of Internal Medicine II). The experimental work has been performed by me and technical assistance was given by Estibaliz Arellano-Viera, Carolin Graf, Josefina Pena-Mosca and Dalia Sheta. All histopathological analysis (including tissue fixation, staining and GvHD grading) were performed by Dr. Simone Reu and her team (Institute of Pathology, University Würzburg). The experiments in the B6→BALB/b mouse model were performed by Carina Bäuerlein. Data analysis and figure preparation were done by me. Zeinab Mokhtari performed the k-mean clustering analysis. Figures and text are part of the manuscript Bäuerlein CA*, Qureischi M* et al., Front Immunol., 2021, "A T-cell Surface Marker Panel Predicts Murine Acute Graft-versus-Host Disease".

Part III

Molecular cloning was done by me under the scientific supervision of Prof. Dr. Harald Wajant in his laboratory (University Hospital Würzburg, Department of Internal Medicine II, Division of Molecular Medicine). Technical support was given by Daniela Weisenberger. Antibody production, purification, binding and cytotoxicity assays were performed by me with technical support of Johannes Nelke and Alventina Rosenthal.

Part IV

PD Dr. Friederike Berberich-Siebelt (Institute of Pathology, University Würzburg) supervised the project "NFATc1 SUMOylation" and experiments were performed by me with technical support of Benjamin Lunz and Yin Xiao. **Figure 32-35, Figure 35 A** and **Figure 36** were published in my own Master's Thesis, which was conducted at the Institute of Pathology of Würzburg University ("Rolle der NFATc1 SUMOylierung in präklinischer Stammzelltransplantation", 2016). The results of the Master Thesis were further corroborated during my PhD and extended by several experiments. Alloreactive T cells were isolated and FACS sorted by me. RNA isolation as well as sequencing was performed by Matthias Klein (Institute for Immunology, Mainz). Stefan Klein-Hessling (Institute of Pathology, University Würzburg) performed the RNAseq data analysis. Figures are part of the manuscript Xiao Y*, Qureischi M*, Dietz L* et al., JEM 2021, "Lack of NFATc1 SUMOylation prevents autoimmunity and alloreactivity".

*equal contribution

6 Abstract

Hematopoietic cell transplantation (HCT) is a curative therapy for the treatment of malignant and non-malignant bone marrow diseases. The major complication of this treatment is a highly inflammatory reaction called Graft-versus-Host Disease (GvHD). Here, transplanted donor T cells cause massive tissue destruction and inflammation in the main target organs liver, skin and the intestine. Currently, this inflammatory reaction can be treated successfully using strong immunosuppressive agents. One efficient group of immunosuppressants are calcineurin inhibitors such as Cyclosporin A (CsA) and Tacrolimus (FK506). These treatment strategies target all T lymphocytes subsets equally and do not separate GvH from the desirable Graft-versus-Leukemia (GvL) effect. Therefore, we aimed to find immunological targets on alloreactive T cells in order to develop novel treatment strategies, which selectively modulates alloreactive T cells without impairing the GvL effect or hematopoietic immune reconstitution.

The aim of this thesis was to develop a predictive marker panel to track alloreactive T cells in the peripheral blood (PB) of murine allo-HCT recipients. In clinically relevant model of aGvHD we demonstrated that alloreactive T cells have a distinct surface marker expression profile and can be detected in the PB before aGvHD manifestation. Based on our data, we propose a combinatory panel consisting of 4 surface markers ($\alpha4\beta7$ integrin, CD162E, CD162P und CD62L) on circulating $CD8^+$ T cells to identify the risk of aGvHD after allo-HCT.

Since tumor necrosis factor receptor superfamily (TNFR SF) members are involved in several immunological processes, we did extensive surface marker expression analysis of several TNFR superfamily members and other immunomodulatory molecules on conventional and regulatory T cells (Tcons vs. Tregs) on different time points during aGvHD progression. The aim of this study was to find subset-specific immunomodulatory molecules on recently activated Tcons and Tregs. We found that GITR, 4-1BB and CD27 were highly expressed on alloreactive and naïve Tregs. In contrast, PD1 expression was highly upregulated on recently activated alloreactive Tcons. The data of this study serves as basis for future approaches, which aim to develop T cell subset specific therapeutic antibody fusion proteins.

$\alpha4\beta7$ integrin and CD162P (P-Selectin ligand) are highly upregulated on alloreactive T cells and mediate the infiltration of these cells into GvHD target organs. We developed recombinant (antibody) fusion proteins to target these two homing molecules and could

show that antibody-based fusion proteins are superior to ligand-based fusion proteins regarding production efficiency and binding affinity. Therefore, we propose for future studies to focus on the described antibody-based fusion proteins for the selective targeting of T cells.

Since the widely used calcineurin inhibitors are impairing the desirable GvL effect, we investigated if selective NFATc1 inhibition might be a novel strategy to prevent or reduce alloreactivity, while hopefully maintaining the GvL effect. In particular, we addressed the role of the isoform NFATc1 and inhibited its posttranslational modification by SUMO (Small Ubiquitin-related Modifier). Indeed, inhibition of NFATc1 SUMOylation resulted in reduced inflammation and increased Treg frequencies in a murine MHC major mismatch aGvHD model.

Conclusively, we showed that alloreactive T cells can be identified by their surface profile in the PB of allo-HCT recipients before aGvHD symptoms appeared. Furthermore, we introduced a approach to selectively target alloreactive T cells by antibody fusion proteins, which might serve as a novel strategy to separate GvH from GvL. Additionally, we demonstrated that averted posttranslational modification of NFATc1 by SUMOylation serves as potential target to reduce alloreactivity of T cells.

7 Zusammenfassung

Die hämatopoetische Stammzelltransplantation ist eine weltweite Therapiemaßnahme für die Behandlung von malignen und nicht-malignen Knochenmarkserkrankungen (z.B. Leukämien). Eine schwerwiegende Komplikation dieser Therapieform ist die Transplantat-gegen-Wirt Erkrankung (engl. Graft-versus-Host Disease, GvHD). Hierbei greifen Spender-T-Lymphozyten den Körper des Empfängers an und verursachen massive Entzündungsreaktionen in den GvHD Zielorganen Leber, Haut und Darm. Diese überschießende Immunreaktion kann klinisch behandelt werden, indem stark immunsuppressive Medikamente wie Cyclosporin A (CsA) und Tacrolimus (FK506) eingesetzt werden. Jedoch greifen diese Medikamente alle T-Zellen gleichermaßen an und vermindern ebenfalls die gewünschte anti-Tumorantwort der Spender-T-Lymphozyten (engl. Graft-versus-Leukemia effect, GvL effect).

Ein Ziel dieser Arbeit war die Entwicklung eines prädiktiven FACS Tests, um T-Zellen im peripheren Blut (PB) von Stammzellempfängern anhand ihrer Oberflächenmoleküle zu identifizieren. Dazu haben wir ein klinisch relevantes Mausmodell für aGvHD herangezogen und konnten zeigen, dass eine Kombination von Migrations- und Aktivierungsmolekülen ($\alpha4\beta7$-Integrin, CD162E, CD162P und CD62L) alloreaktive T-Zellen im Blut eindeutig identifizieren konnten, bevor aGvHD Symptome entstanden.

Einige Proteine der TNFR Superfamilie sind auf Immunzellen exprimiert und regulieren diverse immunologische Prozesse. Wir haben konventionelle T-Zellen (Tcons) und regulatorische T-Zellen (Treg) an unterschiedlichen Zeitpunkten aus transplantierten Mäusen isoliert und die Expression von Proteinen der TNFR Superfamilie untersucht, um potenzielle therapeutische Zielstrukturen auf Spender-Lymphozyten zu identifizieren. Wir konnten zeigen, dass GITR, 4-1BB und CD27 auf aktivierten, alloreaktiven wie auch auf naiven Tregs exprimiert wurde. Wohingegen, die PD1 Expression vor allem auf aktivierten Tcons induziert wurde. Die Daten dieser Studie dienen als Grundlage für künftige Strategien um T-Zellen mit Hilfe von Antikörper Fusionsproteinen selektiv zu modulieren.

Unsere Daten zeigten, dass die Expression von $\alpha4\beta7$-Integrin und CD162P auf alloreaktiven T Zellen im Zuge der aGvHD-Pathogenese induziert wird. Weiterhin erstellten wir rekombinante therapeutische Antikörper Fusionsproteine gegen die oben genannten Migrationsmoleküle. Wir zeigten hier, dass Produktionseffizienz und Bindungsaffinität von Antikörperformaten besser waren als von Liganden-basierten

Fusionsproteinen. Demnach empfehlen wir für künftige Studien Antikörperformate heranzuziehen und die hier aufgeführten Antikörper Konstrukte weiter zu entwickeln.
Calcineurin Inhibitoren sind potente Immunsupressiva, die zur Behandlung von aGvHD eingesetzt werden. Diese Immunsuppressiva beeinträchtigen jedoch den GvL Effekt signifikant. Da Calcineurin Inhibitoren indirekt den NFAT Signalweg hemmen, haben wir hier die selektive Inhibition von NFAT in alloreaktiven T-Zellen untersucht. Wir zeigten, dass eine fehlende posttranslationale Modifikation von NFATc1 über SUMOylierung (Small Ubiquitin-related MOdifier) zu einer verminderten Alloreaktivität von T-Zellen führte. Diese Spender-T-Zellen zeigten eine verringerte Effektorfunktion, wobei die protektiven Tregs durch die fehlende SUMOylierung nicht beeinflusst wurden.
Zusammenfassend konnte gezeigt werden, dass alloreaktive T-Zellen über ihr spezifisches Oberflächenmarkerprofil im Blut identifiziert werden konnten bevor aGvHD Symptome entstanden. Weiterhin beschreiben wir eine neue Strategie, um alloreaktive T-Zellen mittels Antikörper-basierten Fusionsproteinen spezifisch zu modulieren. Darüber hinaus zeigten wir, dass eine Verhinderung der NFATc1 SUMOylierung die Alloreaktivität von T-Zellen deutlich reduzierte, ohne den protektiven Effekt von Tregs zu vermindern.

8 Introduction

8.1 The Immune system

The immune system is a host defense mechanism, which protects the human body against foreign substances and a variety of pathogens like bacteria, viruses and fungi. In general, all immune cells are derived from hematopoietic stem cells and go through complex differentiation steps in the primary lymphoid organs. Early during development the hematopoietic stem cells differentiate into myeloid or lymphoid progenitors (Abbas et al., 2017).

8.1.1 T cells

T cells derive from lymphoid progenitors, which are located in the bone marrow. In early T cell differentiation, the progenitors migrate from the bone marrow to the thymus, where several maturation steps take place. Importantly, central tolerance is achieved by several selection processes and no thymocyte, which recognizes self-peptides, should be able to leave the thymus. However, a special subtype, i.e. regulatory T cells (Tregs), also differentiating in the thymus, ensure peripheral tolerance if needed.
Once the progenitors matured to naive T cells, they downregulate the surface molecule CD62L enabling the migration from the thymus into periphery, where they recirculate through the secondary lymphoid organs (SLO) searching for their cognate antigen (Abbas et al., 2017). Most of the T cells express the $\alpha\beta$ T cell receptor (TCR). The TCR can bind only peptide fragments, which are presented by MHC (Major Histocompatibility Complex) molecules on the surface of other cells. All nucleated cells express the MHC I complex. The MHC II complex is expressed mostly on the surface of Macrophages (Mϕ), B cells and Dendritic Cells (DCs) (Germain, 2002). Depending on their MHC restriction T cells are divided into $CD4^+$ (interacts with MHC II) or $CD8^+$ (interacts with MHC I) T cells (Koch et al., 2011). There is a small population of thymocytes, which express a TCR composed of a γ- and a δ-chain. The $\gamma\delta$ T cell population also express the CD3 complex for signaling but in contrast to the $\alpha\beta$ T cells, the $\gamma\delta$ T cells recognize glycolipids and intact peptides (Abbas et al., 2017).
After antigen recognition and activation, naïve $CD4^+$ T cells can develop into different T helper (Th) subsets (Figure 1). The Th cell subsets are of particular importance during inflammatory immune responses. For example, B cells, engaging with T cells via MHC II-TCR binding, require signals from the $CD4^+$ T cells for efficient antibody

production. One prominent interaction is the CD40L-CD40 pairing. Furthermore, the recruitment of Mϕ and granulocytes is mediated by $CD4^+$ T cells. $CD4^+$ Th subgroups are developing according to the faced pathogen and the cytokine environment (Abbas et al., 2017). Th1 cells develop after an infection with intracellular viruses or bacteria and in the presence of IL-12 and IFN-γ. Th1 cells are characterized by the expression of the transcription factor T-bet, STAT1 and STAT4. They produce mainly the cytokine IFN-γ, which recruits Mϕ and improves phagocytosis. Th1 cells further secrete high amounts of IL-2, lymphotoxin-α and contribute to IgG1, IgG2a, IgG2b, IgG3 and IgE secretion in B cells (Afkarian et al., 2002; Luckheeram et al., 2012). Th2 cells develop after infection with parasites and in the presence of IL-4 and IL-6. Th2 cells are involved in immune responses against parasites, allergic immune responses and asthma. Th2 cells induce in B cells the production of IgG, IgA and especially IgE antibodies and produce mainly the cytokines IL-4, IL-5 and IL-13. The master transcription factor of Th2 cells is the protein GATA3 (Luckheeram et al., 2012; Szmeja, 2008).

Since the first classical characterization of Th cells into Th1 and Th2, by Mosmann and Coffman in 1986, researchers have been identifying more and more subpopulations (such as Th19, Th9 and Tfh) (Abbas et al., 2017; O' Shea et al., 2010). Previously a new subset, so called Th17 cells, were discovered. These cells produce the cytokine IL-17 and IL-21 and depending on the context also GM-CSF, IFN-γ or IL-22 (Aggarwal, 2003; Harrington et al., 2005).

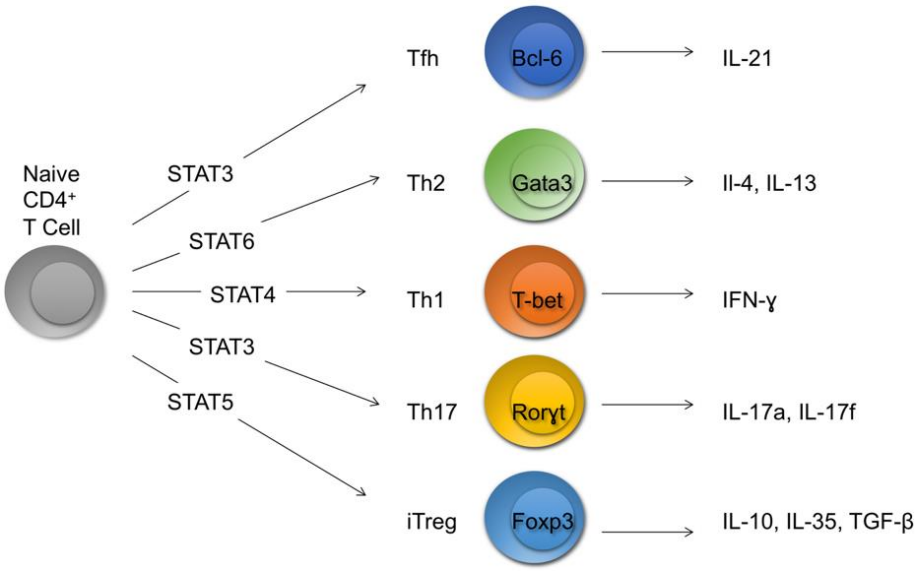

Figure 1: T cell differentiation.
Classical view of T cell differentiation into several T helper subsets. After antigen exposure $CD4^+$ T cells differentiate into different T helper subsets depending on the cytokines present during their activation. Each T helper subset is characterized by the specific expression of a transcription factor, also called lineage marker and a lineage-specific cytokine profile. Modified from (O'Shea et al., 2009).

Regulatory T cells (Treg) are of major importance in the control of immune reactions and autoimmunity. The dominant Treg populations are defined by the expression of the transcription factor forkhead box 3 protein (Foxp3) and constitutively express the high-affinity IL-2 receptor CD25 (Brodie et al., 2010). The cells are defined as $CD4^+CD25^+$ $Foxp3^+$ T cells (Hori et al., 2003). Tregs have a variety of effective suppressor functions. For example, Tregs express high levels of CTLA-4 which competes with the costimulatory molecule CD28 and binds CD80/86 on activated DCs, Mϕ and B cells inducing an inhibitory signaling cascade in the APCs (Sakaguchi et al., 2009). Moreover, Tregs also secrete high amounts of the anti-inflammatory cytokine IL-10 and TGF-β, which inhibit the effector function of Th cells. Tregs highly depend on the cytokine IL-2, which is only produced by conventional T cells (Tcon) and not by Tregs themselves. As Tregs express high amounts of CD25 (high affinity IL-2 receptor α-chain) molecules on their surface, they can consume mostly all IL-2, which indirectly leads to the downregulation of the effector T cell proliferation (Pandiyan et al., 2007; Scheffold et al., 2007). Therefore, Tregs are crucial for the control of autoimmunity, allergic inflammation, infection and tumor.

$Foxp3^+$ Tregs can be subdivided into thymic and peripheral Tregs. Thymic Tregs (tTregs) develop in the thymus and leave the thymus as already differentiated Treg cells. Tregs can also develop in the periphery from naive $CD4^+$ T cells (after antigen recognition) in the presence of the cytokines IL-2 and TGF-β. These cells are known as peripheral Tregs (pTregs). Both Treg subsets do not only control the immune reaction against foreign antigens but also the strength of an immune reaction. Importantly, however, Tregs and predominantly tTregs regulate the peripheral tolerance against self-antigens (Curotto de Lafaille et al., 2009).

$CD8^+$ T cells are important effector cells and mediate cellular immune responses. As these cells have a direct killing ability, they are also called cytotoxic T lymphocytes (CTL). Naive $CD8^+$ cells are activated in the periphery by exogenous antigens, which are presented by MHC I molecules (Jondal et al., 1996). The specific lysis of target cells can be induced by the secretion of Granzymes and Perforin, which will both lead to apoptosis in the target cell. Moreover, apoptosis can be specifically induced via the interaction of FasL/Fas. Additionally, CTLs secrete cytokines like IFN-γ and TNF-α to activate and attract cells of the innate immune system, like neutrophils and Mϕ (Barry et al., 2002; Berke, 1995; Shresta et al., 1998).

8.1.2 Leukocyte rolling and attraction

In general, immune cells are patrolling throughout the body in constant search of antigens and can enter all kind of tissues from the circulation via the vascular system. During inflammation, this process is even enhanced by the secretion of chemokines and cytokines. Chemokines are chemo attractant cytokines, which are released by the endothelium or immune cells and can induce directed cell chemotaxis. Furthermore, the chemokine receptors are G-coupled receptors and their stimulation leads to changes in cell adhesion and the cytoskeleton of the cells enabling a strong binding of the leukocyte integrin to their ligands on endothelial cells (Abbas et al., 2017).

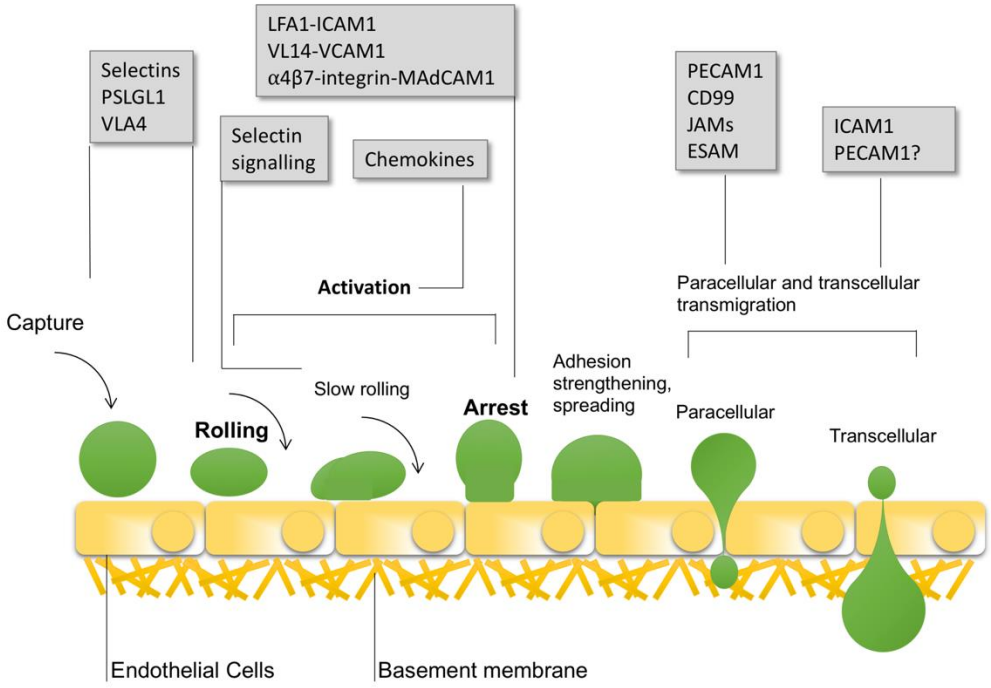

Figure 2: Leukocyte trafficking.
Leukocytes roll on endothelial cells using selectins. Once the cell is activated by chemokines and cytokines, the integrins change from their resting confirmation into an active confirmation and lead to a stable adhesion of the cell to the tissue. Next, cells can enter the tissue via paracellular or transcellular transmigration (modified from Rivera-Nieves et al., 2008).

The expression of tissue specific selectins and integrins together with the local secretion of cytokines mediates leukocyte trafficking to distinct sites. Naturally, the expression levels of selectins and integrins differs between steady state and inflammation. Cells in the SLOs express CD62L, CCR7, CXCR4 and LFA-1 and most of the cells are naïve under healthy conditions (Fu et al., 2016). After antigen recognition, TCR signaling and costimulation, the T cells undergo extensive proliferation and change their phenotype from naïve into effector. In order to egress from the lymph nodes, T cells downregulate CD62L and CCR7 (von Adrian et al.,

2003). For entering tissue specific sites, activated T cells upregulate organ-specific surface proteins such as P-Selectin Ligand for homing to the skin (Fu et al., 2016) and $\alpha4\beta7$ integrin for homing into the intestine (Beilhack et al., 2008; Hammerschmidt et al., 2008). In general, activated T cells show higher expression of homing receptors compared to naive T cells.

8.1.3 Intestinal immunity in inflamed and non-inflamed tissue

Besides primary and secondary lymphoid organs, there is also the mucosa-associated tissue (MALT), which is involved in regulating mucosal immunity. This lymphoid-associated tissue is found in the gastrointestinal tract, the lung and on other mucosal sites of the body (Abbas et al., 2017). The gastrointestinal tract (GI tract) hosts commensals and is exposed to food antigens daily. Immune response especially in highly microbe-exposed organs, need to be strictly controlled and tolerance needs to be maintained. Classically, the induction of immune responses in the GI tract are generated in lymphoid follicles within the intestine, which are called Peyer's patches (PP). The effector sites are mainly located in the *lamina propria* and the epithelium (Abbas et al., 2017; Mason et al., 2008). During an immune response in the GI tract, DCs present antigens via MHC II to T cells and upregulate costimulatory molecules in the Peyers Patches and in the mesenteric lymph nodes (mLN). After full activation in these two priming sites, T cells can home to mucosal sites of the body. Specific migration of effector T cells to their target sites is enabled by the upregulation of homing receptors on activated T cells. Under steady state the intestinal epithelial cells express CCL25 and CCL28, which bind CCR9 on T cells and enables T cell trafficking to the small and large intestine (Habtezion et al., 2015). Moreover, intestinal endothelial cells express mucosal-associated cell adhesion molecule 1 (MAdCAM-1), which interacts with the $\alpha4\beta7$ integrin and mediates direct homing of T cells from the circulation into the intestine. MAdCAM-1 is constitutively expressed in the small intestine, colon and mesenteric lymph nodes and is upregulated during inflammation (e.g. induced by TNF-α) (Connor et al., 1999). Additionally, endothelial cells in the gastrointestinal tract constitutively express and upregulate E- (CD62E) and P-Selectin (CD62P) to recruit leukocytes via rolling to the sites of inflammation (Fukatsu et al., 2000).

8.2 Hematopoietic cell transplantation (HCT)

8.2.1 Clinical relevance

Any treatment in which hematopoietic stem cells (HSC) of a healthy donor are transferred into a non-identical recipient in order to replace the recipients immune system is defined as allogeneic hematopoietic cell transplantation (allo-HCT) (Singh et al., 2016; Sureda et al., 2015). HCT is an established and curative therapy for the treatment of malignant hematopoietic diseases (Leukemia, Multiple Myeloma or Hodgkin's Lymphomas) and non-malignant conditions (anemias or other inherited immune disorders) (Copelan, 2006; Jenq et al., 2010). The number of allo-HCTs increases constantly. A retrospective observational study showed that one million HCTs (58% autologous and 42% allogeneic) were performed in the past 50 years by 1516 transplant centers in 75 countries (Gratwohl et al., 2015). Especially in case of cancer, HCT is not only replacing the malignant immune system of the host but also providing a strong GvL effect, which can be highly beneficial to target remaining tumor cells (Singh et al., 2016).

Before allo-HCT, the recipient undergoes total body irradiation (TBI) of 8-14 Gy and/or chemotherapeutic agents (e.g. Busulfan). The conditioning regiment eradicates tumor cells as well as healthy immune cells and makes "space" for the bone marrow of the healthy donor (Kröger et al., 2011). The type of allo-HCT is defined by the stem cell source and the donor match. These factors strictly determine the outcome of an allo-HCT. The decision between autologous or allogeneic transplantation depends on the underlying disease and the availability of matching donors. Suitable donors are defined by genetic matches of the major histocompatibility complex (MHC), also called human leukocyte antigen (HLA) in humans (Choo, 2007).

The major histocompatibility complex (MHC) encodes for a group of proteins, which are of high immunological relevance in transplantation setting as they determine the transplantation outcome. In humans, the MHC molecules are known as HLA (Human Leukocyte Antigen) (Abbas et al., 2017). The HLA-A, -B, -C genes encode for MHC I molecules, which are expressed by almost all nucleated cells in the body. HLA-DQ, -DR and -DP encode for MHC II molecules, which are mainly on the surface of professional APCs such as Mϕ, B cells and DCs. HLA/MHC molecules present peptides on their cell surface to T cells and are the most polymorphic genes in the human genome. Because of a selection process during T cell maturation in the thymus

(MHC restriction), $CD4^+$ T cells recognize MHC II molecules, whereas $CD8^+$ T cells recognize MHC I molecules (Abbas et al., 2017). For donor selection, the healthy donors' HLA genes are either sequenced by polymerase chain reaction (PCR) or next-generation sequencing (NGS) (Choo, 2007). Furthermore, host and donor compatibility can be determined by an *in vitro* mixed lymphocyte reaction (MLR). The molecules which are of particular importance for transplantation are HLA-A, HLA-B, HLA-C, HLA-DR. Therefore, especially both alleles of these loci are typed (total 8 loci and if HLA-DQ is included 10 loci) and the higher the match between the donor and recipient, the less rejection is expected (Choo, 2007). A match of 8/8 or 10/10 is considered as identical donor, which is likely to be found in a sibling or family donor. Patients who do not find a 8 or 9 out of 10 match, undergo haplo-identical transplantation, which increases post-transplant rejection and complications (Ottinger et al., 2003). Once HSC were infused intravenously, the cells distribute all over the body and engraft in the bone marrow niche. Within this bone marrow environment, they can develop into every cell type of the hematopoietic system. In the most cases, the healthy donor stem cells are isolated from the peripheral blood (PB), where they have been mobilized by granulocyte-macrophage stimulating factor (G-CSF, GM-CSF) or directly from the bone marrow. HSCs are selected by the CD34 marker, which is a general human hematopoietic cell marker (Kröger et al., 2011).

8.3 Graft-versus-Host Disease (GvHD)

Besides infectious diseases, the most severe immunological complication that can occur after allo-HSCT is Graft-versus-Host Disease (GvHD) leading to high morbidity and mortality (Jenq et al., 2010). Here, the co-transplanted donor T cells recognize the host as "foreign" and cause inflammation and massive organ damage (Ghimire et al., 2017; Léger et al., 2004; Teshima et al., 2016). About 35-50% of allo-HSCT recipients can develop aGvHD (Jacobsohn et al., 2007; Omer et al., 2016).

However, GvHD can also develop in patients despite complete HLA-matching. Here, so called minor histocompatibility antigens (miHAgs) can cause alloreactive activation of T cells. The miHAg peptides are associated with MHC I and MHC II antigens and expressed on the surface of almost every cell type and tissue. These peptides can be recognized as foreign by transplanted T cells and induce strong immune responses even in HLA matched patients. Furthermore, miHAg peptides are genetically highly polymorphic leading to a high variance in the translated miHAg peptides (Chao, 2004;

Turpeinen et al., 2013). Therefore, miHAgs are of high clinical relevance and determine HCT and solid transplantation outcomes.

Historically, GvHD was differentiated by the timing when the symptoms appeared into acute and chronic GvHD. In general, acute GvHD (aGvHD) develops within the first 100 days after transplantation, whereas chronic GvHD (cGvHD) appears 100 days after transplantation (Greinix et al., 2011; Schroeder et al., 2011). Following chapters will focus on aGvHD.

8.3.1 Pathophysiology of acute Graft-versus-Host Disease (aGVHD)

Main target organs of aGvHD are skin (81%), GI tract (54%) and liver (50%) (Ghimire et al., 2017; Martin et al., 1990). According to Ferrara et al., there are three distinct events happening during the development of aGvHD (**Figure 3**). In the first place, the host conditioning (e.g. irradiation or chemotherapy) induces massive tissue damage during the first days after transplantation. This leads to breakdown of epithelial barriers (especially in mucosal sides like the GI tract) and to a local inflammation. The damaged tissue as well as epithelial cells secrete high levels of TNF-α and IL-1 creating a highly inflammatory environment (Ferrara et al., 2009). Furthermore, damage-associated molecular patterns (DAMPs) and pathogen-associated molecular patterns (PAMPs) like lipopolysaccharides, CpG or Flagellin are released. All these mechanisms together lead to the activation of host APCs resulting in increased expression of MHC II and costimulatory molecules on these cells. These APCs then interact with the donor T cells in the secondary lymphoid organs of the host (Ball et al., 2008; Ferrara et al., 2009; Zeiser et al., 2016). Here, the transfused donor $CD4^+$ and $CD8^+$ T cells get activated via TCR engagement with MHC or minor antigens presented on the surface of APCs (Ferrara et al., 2009; Shlomchik et al., 1999). Furthermore, T cells receive co-stimulatory signals by the engagement of CD28 to CD80/86 on APCs. The released cytokines in the T cells environment serve as a third T cell activation signal. All these mechanisms together lead to the activation of several intracellular signaling pathways (NFAT, NFKB, mTOR) in the T cells triggering cell proliferation and IL-2 production (Abbas et al., 2017).

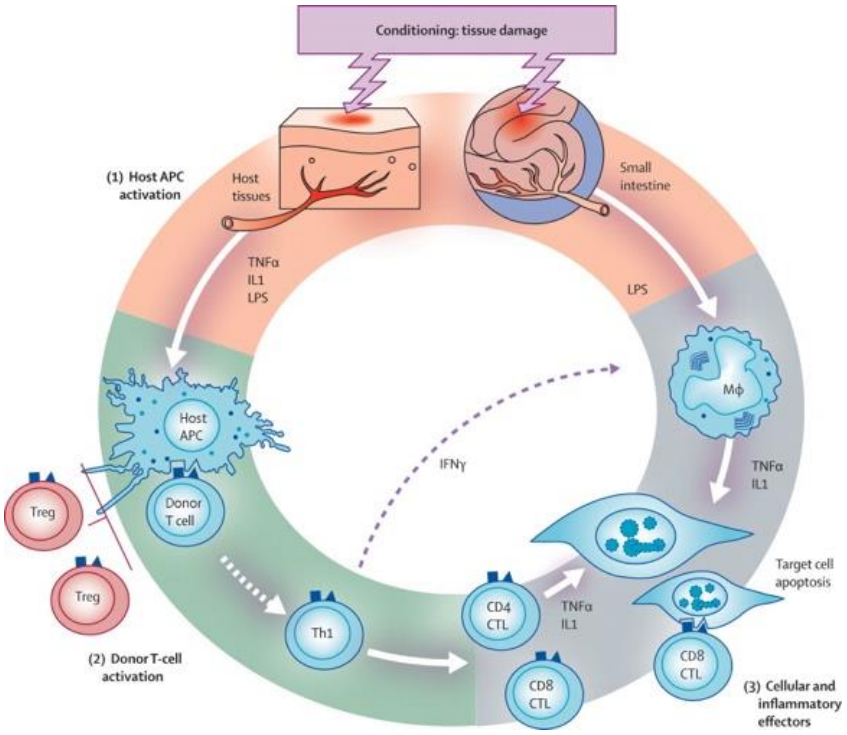

Figure 3: GvHD pathophysiology.
Overview of the GvHD pathophysiology. GvHD development can be subdivided into three distinct phases: Phase I describes the conditioning induced tissue damage. In Phase II the donor T cells get activated by host APCs. Phase III describes the inflammatory effector phase, in which alloreactive T cells attack the host tissue (from Ferrara et al., 2009).

Finally, during the third phase, alloreactive donor T cells migrate into the periphery by the upregulation of integrins and selectins. Once they arrived in the aGvHD target organs, alloreactive T cells exhibit their effector function and induce tissue destruction (**Figure 3**) (Ferrara et al., 2009). The tissue damage is mainly mediated by CTLs and recruited NK cells. CTLs induce apoptosis by ligation of Fas to FasL on host cells (Ball et al., 2008; Ferrara et al., 1999; Zeiser et al., 2017). The intestine is one of the first organ, which is infiltrated by alloreactive T cells and inflammatory T cell responses in the intestinal tract contribute significantly to aGvHD progression.

8.3.2 Alloreactive T cells in the GI tract

The intestine is a large organ with an immense surface area. The immune system in the GI tract needs to protect the body against foreign oral antigens and maintain the tolerance against commensal microbiota. After pre-transplant conditioning regimen, the protective barriers (especially on mucosal sites) collapse and inflammation is induced by several bacterial stimuli, which cross these disrupted epithelial barriers. In experimental models and clinical settings, it has been observed that the GI tract plays a major role in aGvHD progression and it is speculated that the events in the GI tract

might also amplify systemic aGvHD progression. Studies showed, that aGvHD progression could be reduced when recipients were treated with antibiotics before day 20 after allo-HCT (van Bekkum et al., 1974). The antibiotic treatment reduced the gut inflammation significantly and highlighted the important role of the gut microbiota during aGvHD progression (Moller et al., 1982; Strob et al., 1983). These observations have been further investigated by recent work of Marcel van den Brink and colleagues showing the importance of the gut microbiota composition and how this can influence and modulate allo-HCT outcomes (Mathewson et al., 2016; Peled et al., 2016; Taur et al., 2015).

Certainly, intestinal recruited T cells contribute massively to the aGvHD progression by amplifying the inflammation and the tissue damage. $CD4^+$ as well as $CD8^+$ T cells home (after activation in the secondary lymphoid organ) into the intestine (and other aGvHD target organs). For the specific homing to the target organs these cells upregulate integrins and selectins. Integrins are transmembrane proteins and expressed on almost all immune cells. Integrins are heterodimeric and contain a α-unit and a β-unit. Ligands on endothelial cells are ICAM-1, ICAM-2, VCAM-1 and MAdCAM-1. For the homing to mucosal sites the $\alpha4\beta7$ heterodimer binds MAdCAM-1 on intestinal endothelial cells and mediated homing into the intestine (Berlin et al., 1993; Fuchs et al., 2019). Previous work showed that a single knock out for the $\beta7$ monomer (Artis et al., 2000; Waldman et al., 2006) or a double knock out for the $\alpha4\beta7$ heterodimer (Petrovic et al., 2004) on T cells improves the outcomes in murine models of inflammatory conditions such as intestinal inflammation and aGvHD.

8.3.3 Clinical manifestation of aGvHD

The first signs of aGvHD in patients is mostly observed in the skin and GI involvement is typically shown as diarrhea and anorexia. The amount of liver damage is reflected in an increase of liver enzymes and bilirubin levels in the blood. Typically, aGvHD can be diagnosed by histological analysis of organ biopsies and the severity can be graded by pathological grading systems (Ball et al., 2008; Ferrara et al., 1999; Paczesny et al., 2009). Many researchers worldwide are developing several approaches to predict HCT outcomes and the risk of aGvHD after allo-HCT. For instance, soluble ST2 and TIM3 levels are established biomarkers for steroid-refractory GvHD (Abu Zaid et al., 2017; Vander Lugt et al., 2013). Several other serum markers correlate with aGvHD manifestation such as: REG3α (Aziz et al., 2020; Hartwell et al., 2018; Major-Monfried

et al., 2018), soluble TNF-α (Choi et al., 2008), soluble BAFF (Saliba et al., 2018), soluble IL-2 (Budde et al., 2017) and IL-2R (Berger et al., 2013) and circulating miRNA levels (Li et al., 2013). Yet, it remains difficult to determine biomarkers for the prediction of aGvHD since aGvHD pathophysiology involves many immunological mechanisms. Furthermore, the patients receiving HCT have a very heterogeneous disease history. Therefore, the identification of aGvHD specific markers with a high predictive value is still a field of active research.

8.3.4 Experimental aGvHD

Experimental aGvHD serves as ideal platform to study (hyper-) acute T cell activation and patterns of T cell migration *in vivo.* Murine mouse models are essential in order to develop new treatment strategies, investigate new molecular mechanisms and to understand the pathogenesis of aGvHD (Schroeder et al., 2011; Socié et al., 2009).
To induce aGvHD in murine recipients, allogeneic T cells are co-transplanted with T-cell depleted BM into a recipient in which the immune system had been eliminated by chemotherapy or irradiation. There are several ways to induce aGvHD *in vivo* using well-established and well-characterized mouse models (Schroeder et al., 2011). In this work, we were using X-ray irradiation as immunosuppressive treatment prior to HCT. The myeloablatively irradiated hosts received stem cells derived from bone marrow (isolated from femur and tibia bones) of a healthy donor. To study alloreactive T cell responses we employed two different mouse models with different severities. To induce hyperacute aGvHD we transplanted bone marrow cells and enriched splenic T cells of a B6 (H-2^b) donor and injected them into a fully MHC mismatched BALB/c (H-2^d) recipient. In this fully MHC mismatch model, the disease established within one week after allo-HCT. Notably, this fully MHC mismatch situation is not given in human settings. Therefore, we employed a minor histocompatibility antigens (miHAg) mismatch model, which represent the human aGvHD kinetics much closer. For this purpose, we transplanted BM and splenocytes from B10.D2 (H-$2K^d$) donors into BALB/c (H-$2K^d$) recipients. In this model, mice showed aGvHD manifestation around d20-d25. In both models $CD4^+$ and $CD8^+$ T cells contribute to aGvHD manifestation.

8.4 Antibodies

Antibodies are glycoproteins, which play a major role in the adaptive immune response of vertebrates. Antibodies can recognize foreign structures, called antigens, in their

native conformation. These antigens can be derived from pathogens like viruses and bacteria or malignant cancer cells, which for instance express specific tumor antigens (Kaufmann, 2014).

Antibodies are expressed as cell surface receptors on B cells. After first antigen contact and binding to Th cells, B cells undergo differentiation into effector cells and secrete large amounts of one unique antibody clone. These secreted antibodies can bind to pathogens and opsonize these for phagocytic immune cells. Furthermore, the antibodies can bind to target structures on other cells and induce antibody-dependent cell cytotoxicity (ADCC) or complement-dependent cytotoxicity (CDC) via binding to Fc receptors or complement proteins (Abbas et al., 2017). Because of their beneficial properties, antibody-based treatment strategies are getting more into clinical focus.

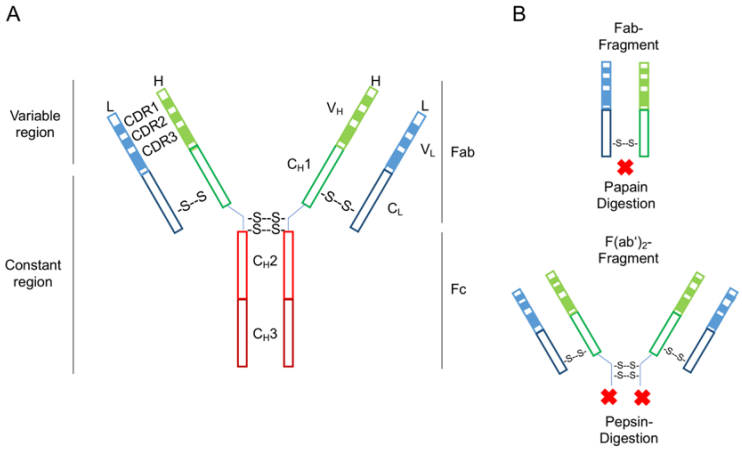

Figure 4: Structure of IgG-antibody.
A Schematic display of a full-length IgG antibody (here IgG1) which exists of two identical heavy (H) and light (L) chains. The variable region of the heavy (V_H) and light chain (V_L) are representing the antigen binding site. **B** Fab and F(ab')2-Fragments, which can be generated by the enzymatic digestion with papain or pepsin, respectively. C_H1-3 = constant region of the heavy chain; C_L = constant region of the light chain; S-S = disulfide bonds; CDR = complementarity determining region; Fab = fragment antigen binding; Fc = fragment crystallizable

There are five different Ig classes (IgA, IgD, IgE, IgM) in humans. 10-20 % of all plasma proteins are immunoglobulins. After an infection and the activation of the immune system it takes up to three weeks to generate antibodies against a certain antigen. Once the immune response is terminated, some of the B cells differentiate into plasma cells and migrate to the bone marrow where they persist during the entire life. If the same antigens induce another immune response, these plasma cells can rapidly be activated and antibody production is induced immediately in large quantities.

From structural perspective, all IgG antibodies contain a Y-form and consist of four polypeptide chains (150 kDa): two identical heavy chains (HC, 50 kDa) and two identical light chains (LC, 25 kDa) (Elgert, 2009). The HC of IgG, IgA and IgE

antibodies contain three constant regions (constant heavy; C_H1, C_H2, C_H3) and a variable region (variable heavy; V_H). Only the light chains have one constant region (C_L, constant light) and one variable region (V_L, variable light). The polypeptide chains are connected via disulfide bonds, which are located in the hinge region above C_H2. The disulfide bonds, which connect heavy and light chain are located around C_H1 and C_L. IgG antibodies exist in the subclasses IgG1, IgG2, IgG3 and IgG4, which are highly conserved but have differences in the hinge region, parts of the C_H2 and in the numbers of disulfide bounds (Roux et al., 2018; Schroeder et al., 2009).

8.4.1 Monoclonal antibody against $\alpha4\beta7$ integrin

As described before, the $\alpha4\beta7$ integrin on leukocytes interacts with MAdCAM-1 on endothelial tissues and guides T cells into the inflamed and non-inflamed mucosa of the intestine. Not only in aGvHD, but also in other diseases like crohn's disease (CD) and ulcerative colitis (UC), the intestine is the major organ of inflammation. The group of Marcel van den Brink showed in 2004 that the complete knock out of the $\alpha4\beta7$ integrin on donor T cells induced less inflammation in the intestine and liver after allo-HCT. At the same time the GvL effect was preserved (Petrovic et al., 2004). Furthermore, a humanized antibody targeting the integrin monomer $\beta7$ was developed in 2011. This antibody could selectively block the T cell homing into the intestine and provides a alternative treatment option for IBD (Gorfu et al., 2009; Stefanich et al., 2011). Vedolizumab is a humanized monoclonal antibody against $\alpha4\beta7$ and under current clinical investigation for the treatment of intestinal inflammation after allo-HCT (NCT03657160, Clinicaltrials.gov). Since Vedolizumab is a highly gut-selective immunomodulator, one of the biggest concerns are induced intestinal infections. Indeed, first studies in patients with gastrointestinal GvHD showed a high susceptibility to infections upon treatment. Nevertheless, overall response rate was still very high (64 % 8 weeks after the first injection). So far only very small patient groups have been treated with Vedolizumab and more clinical data is needed to really determine safety and effectiveness of this new therapy for the treatment of GI GvHD (Danylesko et al., 2019; Fløisand et al., 2019). However, one explanation for the observed side effects upon Vedolizumab treatment might be the lack of selectivity and the blockade of not only T cells but also other immune cell types. For instance, NK cells, neutrophils and macrophages are promoting innate immune responses against bacterial infections in the intestine, which occur due to the conditioning regimen. Furthermore, special types

of immune cells also promote wound healing and tissue repair. Therefore, targeting homing pathways remains a highly promising approach to treat organ-specific inflammatory reactions but an immune cell subset-specificity would be very desirable.

8.5 NFAT signaling in T lymphocytes

NFAT (Nuclear factor of activated T cells) transcription factors are family of proteins involved in the regulation of several immunological processes. Historically NFAT proteins were discovered as regulator of IL-2 transcription in T cells resulting into T cell activation and proliferation (Serfling et al., 2007). NFAT transcription factors are present in the cytosol in a phosphorylated, inactive form. TCR ligation induces an increase of intracellular Ca^{2+} levels and lead to the activation of the phosphatase calcineurin. This results in dephosphorylation of NFAT proteins enabling their translocation into the nucleus. Calcineurin inhibitors are a class of immunosuppressive agents which interfere in this process by blocking the phosphatase activity and consequently inhibiting T cell activation and proliferation by indirect suppression of NFAT activation (Wall et al., 1981). Patients suffering from aGvHD are treated with calcineurin inhibitors such as Cyclosporin A (CsA) and Tacrolimus (FK506) (Hogan et al., 2004). However, this treatment can cause severe side effects and importantly, inhibit the desirable GvL effect. In collaboration with the Berberich-Siebelt laboratory, we demonstrated previously that donor T cells with a lack of NFATc1 and/or NFATc2 showed reduced alloreactivity by maintaining the desirable GvL effect. In line with the known mutual role of Tregs in repressing aGvHD, but allowing GvL, Treg frequencies remained unaltered in this study (Vaeth et al., 2015). Previous *in vitro* studies showed that the posttranslational modification of NFAT proteins by SUMO (Small Ubiquitin-like Modifiers) can influence the transcriptional activity of the isoform NFATc1/C. Here it is noteworthy that NFATc1 is expressed in distinct forms and that only the longer NFATc1/C is modified by SUMO. NFATc1/C is constitutively expressed in peripheral T cells, while the short NFATc1/A is present mainly in effector T cells (Serfling et al., 2000). *In vitro* experiments demonstrated that T cells, in which NFATc1/C could not be modified by SUMO, secreted more IL-2 (Nayak et al., 2009). Under normal conditions, SUMOylated NFATc1/C recruits HDACs (Histone deacetylases), which seems to occur site-specifically at the *Il2* locus leading to a repression of IL-2 expression. By averted NFATc1/C SUMOylation, the IL-2 locus remains accessible for the transcriptional machinery and IL-2 expression can be induced by NFATc1/C to the same extent as by

NFATc1/A (Nayak et al., 2009). These observations have been gained mainly through *in vitro* studies. To further study these mechanisms the laboratory of Dr. Friederike Berberich-Siebelt generated a new mouse strain. In this strain, NFATc1/C SUMOylation is averted *in vivo*. Like many other posttranslational modifications, SUMOylation occurs at lysines. Therefore, the codons encoding the lysines of the SUMO consensus sites within the extra-long C-terminus of NFATc1 were mutated towards arginine replacements, creating NFATc1/ΔS mice. Consistent with the former *in vitro* studies of retroviral transduced EL-4 cells, $CD4^+$ T cells from NFATc1/ΔS mice produced more IL-2 and less effector cytokines under various *in vitro* conditions. Finally, when NFATc1/ΔS mice were challenged with MOG_{35-55} peptide/CFA and pertussis toxin to induce experimental autoimmune encephalitis (EAE), the disease scores were less severe in comparison to their WT littermates. After these promising results in a model of chronic inflammation, we examined in close collaboration with the Berberich-Siebelt laboratory, the role of NFATc1 SUMOylation under the acute inflammatory condition of aGvHD.

9 Objective of the work

For many malignant bone hematopoietic diseases allo-HCT is the only curative treatment. The numbers of allo-HCTs are increasing worldwide (Gratwohl et al., 2015). However, mortality and morbidity after allo-HCT still remain high predominantly due to an inflammatory complication termed acute Graft-versus-Host Disease (aGvHD). Although, aGvHD can successfully be treated by strong immune suppressive agents, treatment can often result in opportunistic infections and disease relapse. The aim of this thesis was to identify novel targets, which can be used to selectively mitigate alloimmune responses after transplantation. To address these questions, we employed fully MHC mismatch and miHAg mismatch mouse models of hyperacute/acute GvHD to study the biology of alloreactive T cells.

The specific aims of the thesis are described as follows.

Part I: Development of a flow cytometry-based prognostic marker panel for the prediction of aGvHD

The overreaching goal of this part of the work is to identify prognostic markers for aGvHD because early diagnosis of aGvHD still remains very challenging. We aimed to develop a predictive surface marker panel, which identifies alloreactive T cells in the peripheral blood (PB) of allo-HCT recipients before aGvHD manifestation.

- At which time points after allo-HCT can alloreactive T cells be detected in the PB in mice?
- What is the specific surface expression profile of alloreactive T cells in the PB of murine allo-HCT recipients (MHC/miHAg mismatch vs. syngeneic recipients)?

Part II: Expression kinetics of immunomodulatory molecules on donor and host T cell populations

We did extensive analysis on immunomodulatory molecules on alloreactive T cells to identify novel targets for the development of new treatment strategies. Here, we focused on individual T cell populations (inflammatory $CD4^+Foxp3^-$/ $CD8^+$ $Foxp3^-$ Tcons and anti-inflammatory $CD4^+Foxp3^+$ Tregs).

- On which time points during aGvHD progression are immunomodulatory molecules upregulated on alloreactive T cells?
- Which immunomodulatory molecules are selectively expressed on Tcons vs. Tregs?

Part III: Development of therapeutic (antibody) fusion proteins to selectively target alloreactive T cells

We defined possible targets on T cells and aimed to develop new therapeutic (antibody) fusion proteins to selectively target alloreactive T cells.

- Which therapeutic (antibody) fusion protein formats are suitable to target homing molecules on alloreactive T cells?
- Which antibody effector domains can be used to selectively modulate alloreactive T cells?

Part IV: Modulation of alloreactive T cells via NFAT SUMOylation pathway

Calcineurin inhibitors (Cyclosporin A, Tacrolimus) are effective immunosuppressive agents, which are used to prevent and downregulate hyperacute T cell responses (during auto-/alloreactivity). Especially for the treatment of aGvHD, these drugs are very effective. However, they do not only suppress alloreactive T cells but also impair the desirable GvL effect. Furthermore, they impair the protective function of Tregs (Rothermel et al., 2003; Serfling et al., 2000). Previous studies using NFATc1 and/or NFATc2 donor T cells revealed reduced alloreactivity in mouse models of aGvHD, while preserving the desirable GvL effect (Vaeth et al., 2015). Here we asked, whether it is possible to target an individual NFATc1 isoform in order to develop a more specific treatment strategy with less side effects.

- Can the prevention of post-translational SUMOylation on NFATc1 proteins ameliorate aGvHD?
- Does blocked NFATc1 SUMOylation alter Treg frequencies and/or function?

10 Material& Methods

10.1 Material

Equipment	**Cat #**	**Company**
Accu-jet pro	26300	Brandt
Cell counting chamber (Neubauer)	P04-36500	Pan Biotech
Cell strainer, 70 um EASYstrainer™	542070	Greiner Bio-one
Centrifuge (Megafuge 40R) 150i	15253457	Thermo Fisher Scientific
Cryostat	CM1950	Leica
Micropipettes	042760930 642752433 942742768 342733754 042720454 942711302	VWR
Microscopy cover slips 21x26	01 01092	Marienfeld
Microtubes 1.5 ml	227261	Greiner Bio-one
Orbital shaker	PSU-10i	Grant Instruments
Scalpel blades, feather hashtag 10	BB510	B. Braun
Serological pipettes	760180 607180 606180	Greiner Bio-one
SuperFrostR Plus Microscope Slides	300859	R. Langenbrinck
Syringe, 1 ml 26GAx3/8" (0.45 x 10 mm) BD Plastipak™	300015	Becton Dickinson
Syringe, 1 ml insulin (30Gx1/2", 0.3mm x 12mm) Omnican® 100	9151141	Braun
Trypan blue solution	11413D	Thermo Fisher
Falcon tubes 15 ml	188271	Greiner Bio-one
Falcon tubes 50 ml	227261	Greiner Bio-one
U-bottom 96-well plates	83.3922.500	Sarstedt
Water bath	WNB14	Memmert
X-Ray irradiation source	CP-160	Faxitron
Cell counting chamber (Neubauer)	ZK03	Hartenstein

10.2 Chemical reagents

Chemical reagent	**Cat #**	**Company**
1kb DNA-Ladder	11823963	Fermentas St. Leon-Rot
2-Propanol	I9516	Sigma-Aldrich
Acetic acid		Sigma-Aldrich
Acetone	33201	Sigma-Aldrich
Acrylamide/Bisacrylamide	537020	Carl Roth GmbH
LB-Agar	X969.1	Carl Roth GmbH
Agarose Standard	232-731-8	Carl Roth GmbH
Albumin from chicken egg white	A5378	Sigma-Aldrich

Ammonium persulfate (APS)	A1142,0250	AppliChem
Ampicilin	HP62.1	Carl Roth GmbH
Avidin/Biotin blocking kit	SP-2001	Vector Laboratories
Blue Protein standard (Broad Range)	#P7718	New England Biolabs
Column performance check standard aqueous SEC1	AL0-3042	Phenomenex
Crystal violet (powder)	T123.2	Carl Roth GmbH
Cyclohexamide (CHX)	C7698-1G	Sigma-Aldrich
Dimethyl sulfoxide	A994.1	Carl Roth GmbH
Disodium Hydrogen Phosphate	A1046,1000	AppliChem
Dulbecco's PBS (Phosphate Buffered Saline)	D8537-500ML	Sigma-Aldrich
Entellan new	1.07961	Merck
Ethanol, absolute	2246	Sigma-Aldrich
Ethylenediaminetetraacetic acid (EDTA)	CN06.1	Carl Roth GmbH
FLAG® peptide	F3290-4MG	Sigma-Aldrich
Glycerin (86%)	4043.1	Carl Roth GmbH
Glycin	A1067,0500	AppliChem
Hydrochloric acid	T134.4	Carl Roth GmbH
Liquid blocker super PAP pen	N71310	Science services
Methanol	322415	Sigmal-Aldrich
Midori Green	617006	Advance Biozym
Nitrocellulose membrane	32-10402506	Schleicher & Schuell
O.C.T. Tissue Tek	4583	Sakura
Paraformaldhyde	P6148	Sigma-Aldrich
Pepton	8986.1	Carl Roth
Polyethylenimine (PEI)	23966	Polysciences Europe GmbH
Nonfat-Derived Milk bovine	M7409-1BTL	Sigma-Aldrich
Protein G, recombinant	539303-1MG	Merck-Millipore
Sodium chloride	A2942,1000	AppliChem
Sodiumdodecylsulfat (SDS)	0183.1	Carl Roth GmbH
N,N,N′,N′-Tetramethylethylenediamine	T9281-25ML	Sigma-Aldrich
Tris(hydroxymethyl)aminomethane (TRIS)	252859-100G	Sigma-Aldrich
Trypan blue	A0668,0025	Applichem
Trypsin/EDTA-Solution	T4174	Sigma-Aldrich
Tween-20	9127.1	Carl Roth

10.3 Enzymes

Enzymes	**Cat #**	**Company**
Calf Intestine Alkaline Phosphatase (CIAP)	18009019	Thermo Fisher
Restriction endonuclease (Cloning)		Fermentas, St. Leon-Rot

10.4 Cell Culture

Media/Cell Culture Supplement	Cat #	Company
DMEM	21969035	GIBCO™
Fetal bovine serum	102770-106	GIBCO™
IMDM	12440053	Thermo Fisher Scientific
Penicillin/ Streptamycin	15140-122	GIBCO™
RPMI 1640	21875-034	GIBCO™

10.5 Antibodies for flow cytometry

Antibody	Cat #	Company
anti-CD3ε-PB (17A2)	100213	BioLegend
anti-LPAM-1/α4β7-PE (DATK32)	120605	BioLegend
anti-CD25-PE (PC61)	102007	BioLegend
anti-CD44-APC (IM7)	103011	BioLegend
anti-CD62L-Percp/Cy5.5 (MEL-14)	104431	BioLegend
E-Selectin ligand-Fc chimera	724-ES-100	R&D Systems
P-Selectin ligand-IgG fusion protein	137-PS-050	R&D Systems
anti-human-IgG-FITC	ab81051	Abcam
anti-CD152/CTLA-4-APC (UC10)	17-1522-82	eBioscienc
anti-CD357/GITR-PE (DTA-1)	126309	BioLegend
anti-CD278/ICOS-PE (15F9)	107705	BioLegend
anti-CD134/OX40-APC (OX-86)	17-1341-82	eBioscience
anti-CD120/TNFR2-PE (3G7A02)	358403	BioLegend
anti-CD45.1-APC-Cy7 (A20)	110715	BioLegend
anti-CD90.1-APC-Cy7 (OX-7)	202519	BioLegend
anti-279/PD1-APC (RMP1-30)	109111	BioLegend
anti-CD69-Percp/Cy5.5 (H1.2F3)	104521	BioLegend
anti-CD4-PE/Cy7 (RM4-5)	100527	BioLegend
anti-CD8α-Percp/Cy5.5 (53-6.7)	100733	BioLegend

10.6 Commercial kits

Commercial Kits	Cat #	Company
BioLux® *Gaussia* Liciferase Assay Kit	E3300	New England Biolabs
Cell Trace™ Violet Cell Proliferation Kit	C34557	Thermo Fisher Scientific
DNA-Gelextraktion NucleoSpin Extract II Kit	740609.10	Machery-Nagel
Dynabeads™ Untouched™ Mouse T Cells Kit	11413D	Thermo Fisher Scientific
KOD Hot Start DNA Polymerase	71086-3	Merck Millipore
BD OptEIA™ IL-6 ELISA Set	555224	BD Biosciences

PageSilver™ Silver Staining Kit	35077.01	St. Leon-Rot
Pierce™ ECL Western Blotting Substrate	10590624	St. Leon-Rot
Pure Yield™ Plasmid Miniprep/Midiprep System	A2492	Promega
Rapid DNA Ligation Kit	K1422	Thermo Fisher Scientific
Zombie Aqua Fixable Viability Kit	423101	Biolegend

10.7 Solutions and buffers

Solution and buffers	**Preparation method**
Assay Diluent (ELISA)	1 x PBS 10% FCS
Assay Diluent (ELISA)	1 x PBS 10 % (v/v) FCS
Blotting Buffer	0.025 M Tris 0.192 M Glycin 20 % (v/v) methanol, pH 8,3
Buffer I (Mini-Prep, DNA Isolation)	50 mM TRIS/ HCl, pH 7,5 10 mM EDTA, pH 8,0 0,1 mg/ml RNase A
Buffer II (Mini-Prep, DNA Isolation)	0,2 M Natriumhydroxid 1% (w/v) SDS
Buffer III (Mini-Prep, DNA Isolation)	3 M Natriumacetat pH 4,8
Coating Buffer (ELISA)	0.1 M Sodium carbonat, pH 9.5
Crystal Violet	20 % (v/v) methanol 0.5 % (w/v) Crystal violet
D-Luciferin	5 g D-luciferin 165 ml Aqua ad injectabilia
Digestion Buffer	Collagenase P 15 mg DNase I 400 ng 50 ml FCS 500 ml HBSS without $Ca2^{+}/Mg2^{+}$
Dissociation buffer	55.836 mg of EDTA 66.5 ml HBSS without $Ca2^{+}/Mg2^{+}$ 3.5 ml FCS
Enrichement buffer	0.5 g BSA 0.375 g EDTA in 500 ml DPBS
Erythrocyte lysis buffer	89.9 g NH_4Cl 10 g $KHCO_3$ 0.37 g EDTA in 1 L deionized water
Laemmly Buffer (SDS-Page, 4 x)	8 % (w/v) SDS 10 % β- mercaptoethanol 40 % Glycerol 0.2 M Tris 0.04 % Bromphenol blue
LB Agar	1x LB Medium (5x) 1.5 % (w/v) Agar Agar in deionized water
LB Media (5 x)	10 g/l Pepton 5 g/l Yeast extract

	10 g/l Sodium chloride
PBS (Phosphate buffered saline)	0.02 M Natrium-Phosphat 0.7 % (w/v) Sodium chloride pH 7.2
PBST	1 x PBS 0.05 % (v/v) Tween-20
PBST in Milk	1 x PBS 0.05 % (v/v) Tween-20 5 % (w/v) milk poweder
Running gel buffer (SDS-Page)	1,5 M Tris 0,015 M SDS pH 8,8
Stacking gel buffer (SDS-Page)	0,5 M Tris 0,015 M SDS pH 6,8
TAE Buffer	2 M Tris 1 M Essigsäure 0,1 M EDTA pH 8,3
TBS (Tris buffered saline)	0,02 M Tris 8 % (w/v) Natriumchlorid pH 7,6

10.8 Cell lines

Cell line	**Source**
HEK293T	Lab Harald Wajant stock
HT1080	Lab Harald Wajant stock
TK1	ATCC
Wehi-3	ATCC

10.9 Anasthesia

Anasthesia	**Company**
Ursotamin (100 mg/ml)	Serumwerk
Xylavet (20mg/ml)	CP-pharma

Anasthesia was prepared as follows: 2 ml of Ursotamin and 2 ml of Xylavet were added to 21 ml DPBS. 10 µl per g body weight were injected i.p. (end concentration Ketamin 80 mg/kg, Xylazin 16 mg/kg).

11 Methods

11.1 Molecular cloning

11.1.1 Cloning of vectors and inserts

For the cloning of all recombinant fusion proteins and antibody formats a modified pCR3-expression vector (Invitrogen) has been used. For positive selection of recombinant vectors and inserts, the plasmid contained an ampicillin resistance gene. Additionally, the vector contained an immunoglobulin signaling peptide and a FLAG-Tag at the N-terminal end (Schneider et al., 1997) to allow detection and purification of the recombinant protein, respectively. First, the parental vector was digested with restriction enzymes. The restriction mix (containing digestion enzymes) was incubated together with the plasmid and the enzymes for 90 min at 37 °C. The calf intestinal alkaline phosphatase (CIAP) was added to the vector digest after 60 min incubation.
The inserts were digested with restriction enzymes without CIAP. For some plasmids, the inserts were amplified with the according primers via polymerase chain reaction (PCR) and digested with the according restriction enzymes.
The digestion products were separated by agarose gel electrophoresis and separated depending on the size of the DNA fragments. DNA was purified using DNA gel extraction kit "NucleoSpin Extract II". After purification, the vector and insert were ligated using the "Rapid DNA Ligation kit" (Thermo Fisher Scientific). In order to produce large amounts of the DNA plasmid, the ligation mix was transformed into competent *E. coli* using heat shock method and seeded on LB-Agar plates (containing 0.1 % ampicillin). The plates were incubated overnight at 37 °C. On the next days, several bacterial colonies were picked and DNA was isolated. A control digest confirmed the presence of the inserts in the vectors. To amplify the right plasmid, a positive clone was grown in 150 ml LB media overnight and DNA extraction and purification was done with the "PureYield™ Plasmid Midiprep System". The plasmids were sequenced by GATC Biotech.

11.1.2 Cloning of recombinant (antibody) fusion proteins

Table 1 summarizes all recombinant ligand-based fusion protein formats. All antibody-based fusion protein formats are summarized in Table 2.

Both developed formats consisted of a T cell recognition side against $\alpha 4\beta 7$ integrin or P-Selectin Ligand/P-Lig (CD162P). Furthermore, the recombinant proteins were fused to an effector domain or to the *Gaussia princeps* luciferase by molecular cloning.

Vector plasmid	Parental vector	Vector digest	Insert plasmid	Insert digest
MAdCAM-1(ed, mu)-FLAG-GpL	TNFR1(ed)-FLAG-GpL	Hind3 / BamH1	Synthetic gene MAdCAM-1(ed,mu)	Hind3 / BamH1
MAdCAM-1(ed, mu)-FLAG-TNC-FasL(h)	CD27(ed, mu)-FLAG-TNC-FasL(h)	Hind3 / BamH1	MAdCAM-1(ed, mu)-FLAG-FasL(h)	Hind3 / BamH1
MAdCAM-1(ed, mu)-FLAG-TNC-FasL(mu)	MAdCAM-1(ed, mu)-FLAG-TNC-FasL(h)	Ecor1 / Xba1	P-Selectin(ed, mu)-FLAG-TNC-FasL(mu)	Ecor1 / Xba1
MAdCAM-1(ed, mu)-FLAG-TNC-PD-1L(ed, mu)	MAdCAM-1(ed, mu)-FLAG-TNC-FasL(mu)	Ecor1 / Xba1	PCR template PDL1-pCMV6-Entry	Exor1 / Xba1
MAdCAM-1(ed, mu)-FLAG-TNC-scTNF80(mu)	MAdCAM-1(ed, mu)-FLAG-TNC-FasL(mu)-	Ecor1 / Xba1	scTNF80-FLAG-TNC(mu)	Ecor1 / Xba1
MAdCAM-1(ed, mu)-FLAG-FasL(h)	FLAG-RGD2-FasL	Hind3 / BamH1	MAdCAM-1(ed,mu)	Hind3 / BamH1
MAdCAM-1(ed, mu)-FLAG-FasL(mu)	MAdCAM-1(ed, mu)-FLAG-FasL(h)	Ecor1 / Xba1	P-Selectin (ed, mu)-FLAG-TNC-FasL(mu)	Ecor1 / Xba1
MAdCAM-1(ed, mu)-FLAG-scTNF80(mu)	MAdCAM-1(ed,mu)-FLAG-FasL(h)	Ecor1 / Xba1	scTNF80(mu)-FLAG-TNC	Ecor1 /Xba1
MAdCAM-1(ed, mu)-FLAG-PD1L(ed,mu)	MAdCAM-1(ed,mu)-FLAG-FasL(h)	Ecor1 / Xba1	PCR template PDL1-pCMV6-Entry	Ecor1 / Xba1
PD-1L(ed, mu)-FLAG-GpL	GpL-FLAG-CD40L	Ecor1 / Xba1	PCR template PDL1-pCMV6-Entry	Ecor1 / Xba1
PD1L(ed, mu)-FLAG-GpL	TNFR1(ed)-FLAG-GpL	Hind3 / BamH1	PCR template PDL1-pCMV6-Entry	Hind3 / Bgl2
P-Selectin(ed, mu)-FLAG-FasL(h)-(RGD2)	FLAG-FasL(h)	Hind3 / BamH1	Murine P-Selectin-pMK-RQ	Hind3 / BamH1
P-Selectin(ed, mu)-FLAG-FasL(mu)	P-Selectin(ed, mu)-FLAG-FasL(h)	Ecor1 / Xba1	P-Selectin(ed, mu)-FLAG-TNC-FasL(mu)	Ecor1 / Xba1
P-Selectin(ed, mu)-FLAG-GpL	TNFR1(ed)-FLAG-GpL	Hind3 / BamH1	P-Selectin(ed, mu)-FLAG-TNC-GpL	Hind3 / BamH1
P-Selectin(ed, mu)-FLAG-PD1L(ed, mu)	P-Selectin(ed, mu)-FLAG-FasL(h)	Ecor1 / Xba1	PCR template PDL1-pCMV6-Entry	Ecor1 / Xba1
P-Selectin(ed, mu)-FLAG-scTNF80	P-Selectin(ed, mu)-FLAG-FasL(h)	Ecor1 / Xba1	scTNF80(mu)-FLAG-TNC	Ecor1 /Xba1
P-Selectin(ed,mu)-FLAG-TNC-FasL(mu)	P-Selectin(ed, mu)-FLAG-TNC-rGel1(full)	Ecor1 / Xba1	CD40(mu)-FLAG-TNC-FasL(mu)	Ecor1 / Xba1
P-Selectin(ed,mu)-FLAG-TNC-scTNF80	P-Selectin(ed, mu)-FLAG-TNC-rGel1(full)	Ecor1 / Xba1	scTNF80(mu)	Ecor1 / Xba1
P-Selectin(ed,mu)-FLAG-TNC-PD1L(ed, mu)	P-Selectin(ed, mu)-FLAG-TNC-rGel1(full)	Ecor1 / Xba1	PCR template PDL1-pCMV6-Entry	Ecor1 / Xba1

Table 1: Vector and insert digest of ligand-based fusion proteins
ed = extracellular domain; h = human; mu = murine, GpL = *Gaussia princeps* luciferase

Vector plasmid	Parental vector	Vector digest	Insert plasmid	Insert digest
C1-HC-heavy-hIgG1-scFv-DATK32-hIgG1	18D1-VH-full-heavy-chain	Mfe1 / BamH1	PCR template C1-H-pcDNA3.1	Mfe1 / Bamh1
C19-FLAG-full-heavy-hIgG1(N297A)-scFv-DATK32	C19-full-HC-N297A-scTWEAK	Ecor1 / Xba1	PCR template scFv-DATK32	Ecor1 / Xba1
C4-HC-N297A-scFv-C19	C4-HC-full-heavy-scTNF80	Ecor1 / Xba1	PCR template C19(scFv)pMA-RQ	Ecor1 / Xba1
DATK32-FLAG-full-VH-FAB2	18D1-FLAG-VH-FAB2	Hind3 / BamH1	DATK32-FLAG-full-VH-hIgG1	Hind3 / BamH1
DATK32-FLAG-full-VH-hIgG1	18D1-FLAG-full-VH	Ecor1 / BamH1	PCR template DATK32-HC	Mfe1 / BamH1
DATK32-FLAG-full-VH-hIgG1(N297A)	18D1-FLAG-full-VH(N297A)	Ecor1 / BamH1	DATK32-FLAG-full-VH-hIgG1	Hind3 / BamH1
DATK32-FLAG-full-VH-hIgG1(N297A)-scFv-C19-	C4-full-HC-N297a-scFc-C19	Hind3 / BamH1	DATK32-FLAG-full-VH-hIgG1	Hind3 / BamH1
DATK32-FLAG-full-VH-hIgG1(N297A)-scFv-C19-	C4-full-HC-N297A-scFv-C19	Hind3 / BamH1	DATK32-FLAG-full-VH-hIgG1	Hind3 / BamH1
DATK32-FLAG-full-VH-hIgG1(N297A)-scTNF80(mu)	scTNF80(mu)-FLAG-TNC	Hind3 / BamH1	PCR template from DATK32-FLAG-full-hIgG1(N297A)	Hind3 / Ecor1
DATK32-FLAG-full-VH-hIgG1(N297A)-scTNF80(mu)	scTNF80(mu)-FLAG-TNC	Hind3 / BamH1	PCR template DATK32-FLAG-full-hIgG1(N297A)	Hind3 / Ecor1
DATK32-FLAG-full-VH-hIgG2	18D1-FLAG-full-VH-hIgG2	Hind3 / BamH1	DATK323-FLAG-full-VH-hIgG1	Hind3 / BamH1
DATK32-FLAG-full-VH-hIgG2	18D1FLAG-full-VH-hIgG2	Hind3 / BamH1	DATK32-FLAG-full-hIgG1	Hind3 / BamH1
DATK32-FLAG-full-VH-muIgG1	DATK32-FLAG-VH-FAB2	BamH1 / Xba1	PCR template K21-VH-FLAG-full-heavy	Bgl2 / Xba1
DATK32-FLAG-full-VH-muIgG2a	DATK32-FLAG-VH-FAB2	BamH1 / Xba1	synthetic gene muIgG2A	BamH1 / Xba1
DATK32-FLAG-full-VL (h)	18D1-FLAG-full-VL(h)	Ecor1 / BamH1	PCR template DATK32-LC	Mfe1 / BamH1
DATK32-FLAG-full-VL (mu)	DATK32-FLAG-full-VL(h)-GpL	BamH1 / Xba1	K21-FLAG-full-VL	BamH1 / Xba1
DATK32-FLAG-full-VL-GpL(w/o) (h)	18D1-FLAG-full-VL(h)-GpL	Ecor1 / BamH1	PCR template DATK32-LC	Mfe1 / BamH1
P-Selectin(ed, mu)- FLAG-constant-light	P-Selectin(ed, mu)-FLAG-FasL(h)	Ecor1 / Xba1	Fn14(ed)-FLAG-light	Ecor1 / Xba1
P-Selectin(ed, mu)-2xFLAG-Fc	P-Selectin(ed, mu)-FLAG-FasL(h)	Ecor1 / Xba1	TRAILR3-FLAG-Fc	Ecor1 / Xba1
P-Selectin(ed, mu)-FLAG-constant-heavy-hIgG1	P-Selectin(ed, mu)-FLAG-FasL(h)	Ecor1 / Xba1	Fn14(ed)-FLAG-heavy-hIgG1	Ecor1 / Xba1
P-Selectin(ed, mu)-FLAG-constant-light-GpL	P-Selectin(ed, mu)-FLAG-FasL(h)	Ecor1 / Xba1	Fn14(ed)-FLAG-light-GpL	Ecor1 / Xba1
P-Selectin(ed, mu)-FLAG-Fc-GpL	anti-CD40-Fc-FLAG-GpL	Hind3 / BamH1	P-Selectin(ed, mu)-FLAG-TNC-GpL	Hind3 / BamH1

Table 2: Vector and insert digest of antibody-based fusion proteins

ed = extracellular domain; h = human; mu = murine, GpL = *Gaussia princeps* luciferase

11.2 Biochemical methods

11.2.1 Culturing of HEK293T

Cells were cultivated under standard conditions (5 % CO_2 and 37 °C) in RPMI 1640 media with 10 % heat-inactivated fetal calf serum (FCS). For harvesting of adherent cells, the flasks were incubated with Trypsin/EDTA (10 mM) and centrifuged for 4 min at 310 x g. Afterwards, the cells were resuspended in fresh media and seeded in flasks (for culturing) or plates (for transfection). If the cells were not used for antibody production, trypsinized cells were cryopreserved with FCS containing 10 % DMSO and stored at -80 °C.

11.2.2 Antibody production in HEK293T

Seeded HEK293T cells were transiently transfected with polyethylenimine (PEI) and the desired plasmids. A 2 ml transfection solution was prepared as follows: 12 µg plasmid DNA (total amount) were pipetted to RPMI 1640 (containing 1 % P/S, 1 mg/ml PEI) and the mix was incubated for 10-15 min at RT. During this time, the media of confluent growing HEK293T cells was changed from RPMI1640 with 10 % FCS to RPMI1640 without FCS but with 1 % P/S. The transfection solution was carefully transferred to the cells and cells were cultured overnight. On the next day, media was exchanged and cells were cultured with RPMI 1640 containing 2 % FCS and 1 % P/S for 5-7 days. After this time, cells were collected in a falcon and centrifuged for 10 min at 4630 x g. The supernatant was transferred into a fresh falcon and stored at 4 °C until further analysis.

11.2.3 Anti-FLAG affinity chromatography

The recombinant fusion proteins were purified by anti-FLAG M2 agarose beads. The beads were washed with TBS and transferred into a chromatography column. Afterwards, the cellular supernatant was slowly transferred on top of the beads. The drop speed was adjusted to 20-25 sec and the column was kept at 4 °C until the total supernatant passed through. All FLAG-tagged proteins were bound to the column/beads and beads were washed with autoclaved TBS. The bound proteins were eluted by adding 100 µg/ml of a FLAG-peptide (in TBS) to the column. The drop speed was now adjusted to 2-3 drops per min. The recombinant fusion proteins were collected

in 700 µl fractions. After elution, the anti-FLAG M2 agarose beads were washed with PBS and stored in TBS (containing 50 % glycerol and 0.02 % sodium azide) at -20 °C until further usage. The eluates were dialyzed overnight at 4 ºC in PBS to remove remaining FLAG peptides. Afterwards, the concentration of the collected eluate fractions was determined by western blotting.

11.2.4 SDS polyacrylamide gel electrophoresis

The SDS-Page was prepared with one layer of stacking gel and one layer of running gel (374 mM Tris pH 8.8; 3.75 mM SDS, 12 % acrylamide). Polymerization was initiated by adding 0.1 % adenosine 5′-phosphosulfate sodium salt (APS) and 0.1 % TEMED. The running gel was immediately covered with isopropanol in order to create a straight surface. After polymerization, the isopropanol was removed and the stacking gel was added (6 % polyacrylamide in 123 mM Tris pH 6.8; 3.75 M SDS; 0.1 % APS; 0.1 % TEMED). To create sample bags a chamber was added to the stacking gel. The first chamber was loaded with a protein marker. Next, 15 µl of the supernatant was mixed with protein sample buffer containing β-mercaptoethanol and denatured for 5 min at 95 °C. The electrophoresis was done at 90-130 V for 100 min.

11.2.5 Blotting

The electro transfer of the proteins from the SDS-page to a nitrocellulose membrane was done in a wet blotting chamber system. The nitrocellulose membrane was drained in blotting buffer and put on top of the SDS-page together with additional whatman papers. The nitrocellulose membrane was positioned towards anode and the SDS-page towards cathode. The protein transfer was done at RT and a voltage of 400 mA for 150 minutes.

11.2.6 Protein detection

To prevent unspecific binding of the detection antibody, the nitrocellulose membrane was blocked with 5 % milk in 1 x PBST on a shaker at RT. Next, the nitrocellulose membrane was washed 3 x for 10 min with 1 x PBST and incubated over night at 4 °C with the primary anti-FLAG (M2) antibody on a shaker. On the next day, the membrane was washed 3 x for 10 minutes with 1 x PBST. Afterwards, the membrane was incubated with an HRP-conjugated (horseradish peroxidase) secondary antibody on a

shaker at RT. The nitrocellulose membrane was washed 3 x for 10 min with 1 x PBST. The protein detection was done with an enhanced chemiluminescence system.

11.2.7 Binding affinity study

To determine the affinity of the recombinant (antibody) fusion proteins to their target, the plasmids were molecularly fused to the *Gaussia princeps* luciferase (GpL). Cell lines, which constitutively expressed P-Selectin ligand (Wehi-3) or $\alpha 4\beta 7$ integrin (TK1) were used for the cellular binding studies. Cells were incubated with increasing concentrations of the recombinant (antibody) fusion proteins and the according control proteins for 90 min at 37 °C. Cells were washed 10 x with ice cold PBS and harvested in 50 µl RPMI1640 medium with 0.5 % FCS and transferred to black 96-well plates. GpL activity was measured using the "Gaussia Luciferase Assay Kit" according to the recommendations of the supplier. Light emission was measured within 10 sec after adding the substrate-buffer solution to the cells to minimize errors related to the decay of GpL activity (» T1/2 D 4 min) using a luminometer.

11.2.8 FasL-mediated cytotoxicity assay

To analyze the potential of Fas-induced apoptosis of the recombinant proteins (with a FasL effector domain), 2 x 10^4 HT1080 cells (express human Fas) were seeded in 96 well plates and cultivated overnight. Next morning, the cell supernatant was removed and cells were resuspended in fresh RPMI containing 7.5 µg/ml Chlorhexidine (CHX) for 30 min at 37 °C. Next, the diluted fusion proteins were added to the HT1080 cells. For 100% viability values, HT1080 cells were cultured with pure RPMI 1640 media (10 % FCS). As cytotoxicity control, cells were incubated with a mix of 200 ng/ml FasL-Fc, 200 ng/ml TRAIL-TNC, 200 ng/ml TNF-F and 2.5 µg/ml CHX. All conditions were incubated for approximately 20 hours at 37 °C. Afterwards, the supernatant was discarded and 70 µl of a crystal violet solution was added to the cells for 20 min at RT. Crystal violet solution was removed and cells were washed with distilled water and kept at RT for drying. The plates were measured with ELISA-Reader Lucy 2 at 595 nm.

11.2.9 ELISA

2 x 10^4 HT1080 cells were grown in a 96 well plate overnight in RPMI (10 % FCS and 1 % P/S). The next day, cell culture medium was changed and cells were stimulated

with scTNF80 variants for 6 h at 37 °C. The supernatants were analyzed for IL-6 with the OptEIA Human IL-6 ELISA Kits (BD Biosciences).

11.3 Working with primary cells

11.3.1 Cell centrifugation

Primary immune cells were centrifuged at 1200 rpm for 5 min at 4 ºC in a Megafire 40R (Thermo Fisher).

11.3.2 Cell counting

10 µl of the cell suspension was diluted with 90 µl of trypan blue for cell counting. 10 µl of this solution were transferred into a neubauer chamber and viable cells (not stained by trypan blue) were counted in all 4 quadrants.

$$D = \frac{N}{Q} \times V \times 10^4$$

D: cells/ml, N: Cell counts in all quadrants, Q: Number of quadrants, V: Dilution factor, 10^4: Volume factor for the calculation of cells/µl to cells/ml

11.3.3 Culturing of primary cells

All cells were cultured in RPMI 1640 (10 % FCS, 1 % P/S, 1 % L-Glutamine) and cultivated at 37°C and 5 % CO^2.

11.4 Murine *in vitro* and *in vivo* models

Murine recipients for HCT experiments were purchased from Charles River (Germany) or Janvier Laboratories (France). Transgenic mouse strains were bred in the animal facility of the ZEMM at Würzburg University Clinics. All donor and recipient mice were sex- and age-matched for HCT experiments.

11.4.1 Mouse strains

Used mouse strains for *in vivo* models and *ex vivo* analysis.

Mouse strain	**Origin**
BALB/c (BALB/cAnNRj)	Janvier Labs
B10.D2 (Hc0 H2d H2-T18c/oSnJ)	Jackson Laboratory
Albino C57BL/6.CD45.1L2G85/J	Bred in the Beilhack Laboratory
C57BL/6 Tg(CD90.1)L2G85/J	Bred in the Beilhack Laboratory
Nfatc1/C$^{\Delta SUMO/wt}$ (C57BL/6)	Bred in the Berberich-Siebelt Laboratory

Table 3: Mouse strains

11.4.2 T cell enrichment for transplantation

Dynabeads™ Untouched™ mouse T cells kit (Invitrogen™) was used according to manufacturer's instructions to enrich T cells from splenocytes. Purity of T cells was around 85-95 %, and more then 90 % T cells were alive after enrichment and before injection.

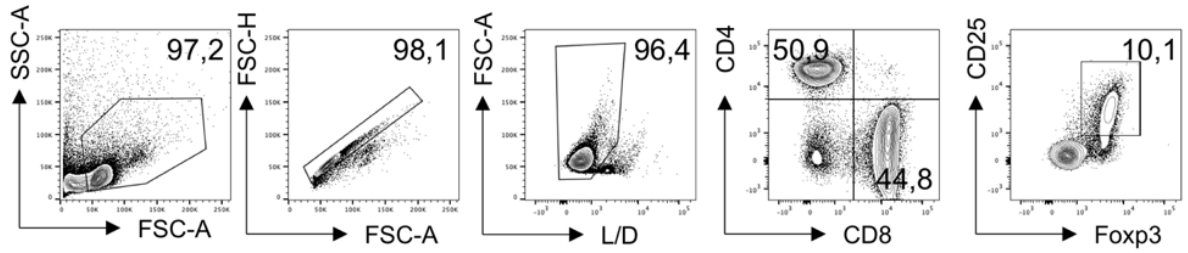

Figure 5: Purity FACS of enriched T cells before transplantation.
Representative FACS analysis of purified T cells. Purity was determined by total $CD4^+$ and $CD8^+$ frequencies (around 95 %).

11.4.3 Bone marrow isolation for transplantation

Bone marrow (BM) cells were isolated from *femur* and *tibia* bones of respective donor mice. More than 90 % of BM cells were alive at the time of injection.

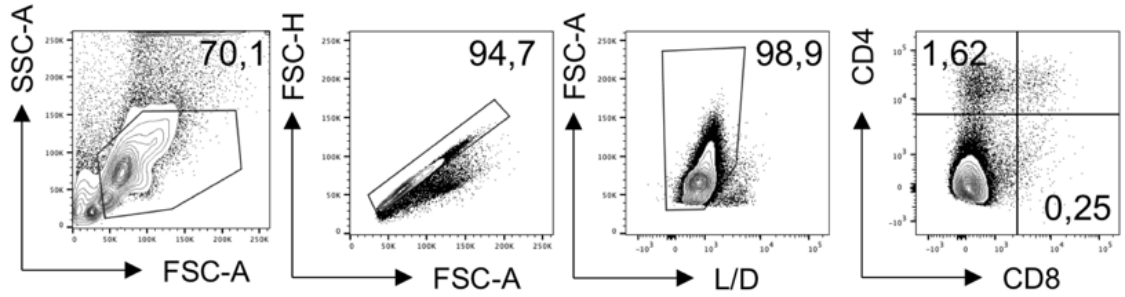

Figure 6: Isolated bone marrow cells.
Representative FACS analysis of bone marrow cells isolated from *femur* and *tibia* bones.

11.4.4 Hematopoietic stem cell transplantation: MHC major mismatch

All BALB/c HCT recipients were irradiated with 8 Gy (12.8 min) using a Faxitron CP-160 X-ray irradiation system (Faxitron X-Ray, Lincolnshire, IL, USA). Within the next 2 h after irradiation mice were retroorbitally transplanted with 6 x 10^5 luciferase positive T cells and 5 x 10^6 bone marrow cells.

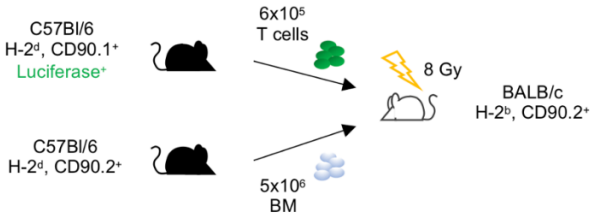

Figure 7: Scheme of MHC major mismatch allo-HCT mouse model.
BALB/c recipients were myoablatively irradiated with 8 Gy and intravenously injected with 5 x 10^6 bone marrow cells and 6 x 10^5 T cells. The donor cells expressed the congenic marker CD90.1.

11.4.5 Hematopoietic stem cell transplantation: miHAg mismatch

All recipients were irradiated with 8 Gy using a Faxitron CP-160 X-ray irradiation system (Faxitron X-Ray, Lincolnshire, IL, USA) before transplantation. Within the next 2 h mice received 30 x 10^6 splenocytes and 5 x 10^6 bone marrow cells from B10.D2 donors.

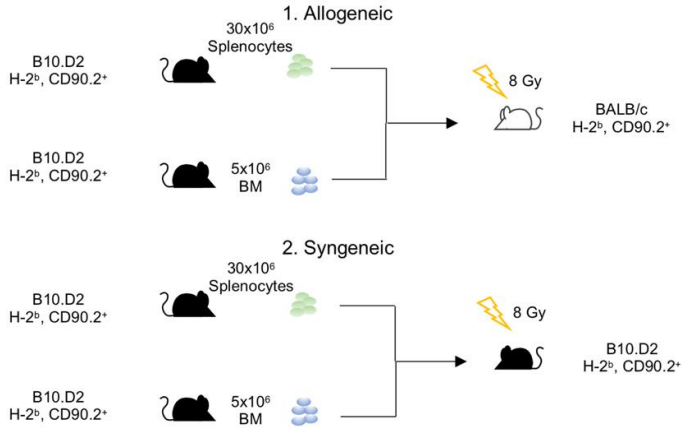

Figure 8: Scheme of miHAg mismatch allo-HCT and syngeneic HCT mouse model.
BALB/c (allogenic) and B10.D2 (syngeneic) recipients were myoablatively irradiated with 8 Gy and intravenously injected with 5 x 10^6 bone marrow cells and 30 x 10^6 splenocytes.

11.4.6 Scoring criteria to determine aGvHD severity

To determine the GvHD severity in murine recipients a clinical scoring system was used (Cooke et al., 1996).

	Intestinal aGvHD	**Skin aGvHD**	**Anemia**
Weight loss	1-2+	0-1	1-2+
Posture	2	0-1	2
Behavior	1-2	0	1-2
Ruffled fur	1-2	2	0-1
Skin	0	2	0
Eyes	0-1	1-2	0-1
Licking/ Scratching of the Skin	0	2	0
Stool	1-2	0	0
Anemia	0	0	1-2
Score Total	**6-11**	**7-10**	**5-10**
End point	**≥ 8**		

Table 4: Clinical scoring criteria to determine GvHD severity

11.5 Isolation of primary T cells

11.5.1 Peripheral blood collection

To obtain blood for multiple time point analysis, blood was taken from the tail vein (approx. 30-40 µl) and lysed in 3-4 ml of ice-cold lysis buffer. Cells were centrifuged at 330 x g at 4 °C and resuspended in 300 µl of PBS.

11.5.2 Mesenteric lymph nodes

Fat tissue and vessels were removed from the mesenteric lymph nodes (mLN). The mLN were kept in 500 µl PBS on ice until they were minced through a pre-wet 70 µm strainer. The strainer was washed with 10 ml PBS and the cell suspension was pelleted at 330 x g for 5 min at 4 °C and resuspended in 1 ml PBS.

11.5.3 Intestine

The small intestinal tube was opened and washed with PBS to remove intestinal content. It was cut into 2 cm segments and transferred into a 50 ml tube containing 30 ml dissociation buffer. The tube was shaked at 250 rpm for 20 min at 37 °C to isolate cells from the epithelial fraction. The cell suspension was meshed through a 100 µm strainer into a 50 ml tube. Both, incubation and filter steps were repeated with another 30 ml dissociation buffer. The two filtered cell suspensions were pelleted at 330 x g for 5 min at 4 °C and then pooled with the *lamina propria* (LP) fraction, which was enzymatically digested as follows: LP was cut into small pieces and incubated in 10 ml of digestion solution containing collagenase P and DNase I on an orbital shaker for 20 min at 37 °C. Afterwards, the falcons were vortexed for 15-20 sec and centrifuged at 330 x g for 5 min at 4 °C. The supernatant was discarded, the pellet was resuspended in 30 ml ice cold HBSS (10% FCS) and passed through a 100 µm strainer into a fresh falcon. Next, the falcon was centrifuged at 330 x g for 5 min at 4°C, the pellet was resuspended in fresh HBSS and pooled with the epithelial fraction.

11.5.4 Spleen

A 70 µm strainer was placed on a 50 ml falcon and pre-wetted with 2 ml of lysis buffer. The spleen was placed on the strainer, cut into pieces and minced through the strainer. The strainer was washed two times with 4 ml of lysis buffer. After 2 min of cell lysis,

10 ml of PBS was added to the falcon to stop the lysis. Splenocytes were pelleted for 5 min at 330 x g at 4°C and resuspended in 2 ml PBS for counting.

11.5.5 Serum collection for Bio Legend's LEGENDplex™

Serum cytokine concentrations were determined using BioLegend's LEGENDplex™ bead-based immunoassays according to the manufacturer's protocol. Samples were collected from tail vein on several days after allo-HCT. Data were acquired on a FACS Canto II (BD Biosciences) and analyzed with LEGENDplex™ data analysis software.

11.6 Flow cytometry

All flow cytometric analysis were performed on a BD FACS Canto II equipped with 405 nm, 488 nm and 633 nm lasers (Becton Dickinson, Heidelberg, Germany). Data was analyzed with the doftware FlowJo (Tree Star, Ashland, OR, USA).

11.6.1 Surface staining

Cells were pelleted and then blocked with normal rat serum (NRS) diluted in PBS (1:20) for 10 min and 4 °C. Antibodies were diluted in PBS and then added to the cells and incubated for another 20 min at 4 °C (dark). 100 µl of PBS was added for washing and cell were centrifuged at 330 x g at 4 °C. The supernatant was discarded and cells were resuspended in PBS for measurement or intracellular staining.

11.6.2 Intracellular staining

Cells were *ex vivo* restimulated with Phorbol-12-myristat-13-acetat (PMA) and ionomycin for 5 h at 37 °C in the presence of Brefeldin A. After stimulation, cells were harvested and blocked with NRS and surface staining was done as described before. To stain intracellular cytokines and the intracellular transfection factor Foxp3, cells were fixed and permeabilized with Fix & Perm Cell Fixation & Cell Permeabilization Kit from Thermo Fisher according to manufacturer's instructions. Antibodies were diluted in 1 x Perm buffer and intracellular staining mix was incubated overnight.

11.7 Imaging

11.7.1 *In vivo and ex vivo* bioluminescence imaging

Mice were injected with 150 μg/g bodyweight D-Luciferin mixed with anesthesia intraperitoneally. Luminescence signals were measured by an IVIS Spectrum CCD imaging system. Data analysis was performed using Living Image 4.0 software (Caliper Xenogen).

11.8 Next generation sequencing (NGS)

11.8.1 RNA-Seq assay

Donor $CD4^+$ T cells were enriched by FACS and sorted directly into RNA lysis buffer. Quantification of total RNA was assessed with the Qubit 2.0 and quality was checked using a RNA 6000 Nano chip on Agilent's bioanalyzer. Sequencing libraries were prepared from 600 ng total RNA using a NEBnext ultra RNA library prep kit and by following the manufacturer's instruction. The resulting barcoded cDNA libraries were sequenced on an Illumina HiSeq 2500 platform for 50 nucleotides (single end).

11.9 Statistics

Two groups were compared by the Wilcoxon-Mann-Whitney-Test U. For the comparison of miHAg mismatch versus syngeneic and healthy controls for several time points, a repeated two-way ANOVA was conducted with a posthoc analysis using a Bonferroni correction of the significance level. Applied statistical analysis for individual data sets are mentioned in the figure legend. Analysis was done using GraphPad Prism 7 software (La Jolla, USA).

12 Results

12.1 Part I: Development of a FACS-based predictive marker panel for aGvHD

The first part of this thesis aimed to develop a predictive peripheral blood test based on cellular surface markers for aGvHD. For this purpose, it was of high relevance to know the critical time points of donor T cell activation, migration and aGvHD manifestation in the employed mouse models. For our first analysis we used a well-defined MHC major mismatch aGvHD model (B6→BALB/c) to study the T cell biology under highly inflammatory conditions. To develop a predictive marker panel, we employed a clinically relevant model of aGvHD. In this model (B10.D2→BALB/c) the events of T cell activation, T cell migration and target organ infiltration are taking several days and enable tracking of T cells in the peripheral blood (PB) of HCT recipients for a period of two weeks before aGvHD manifestation.

12.1.1 aGvHD pathophysiology in a fully MHC major mismatch model

To study the surface receptor profile of alloreactive T cells in the SLOs we used a model of hyperacute GvHD (B6→BALB/c, n = 5 Major mismatch, n = 5 BM control, n = 5 IR control). 6 x 10^5 fully MHC mismatch *luc*+ T cells together with 5 x 10^6 BM cells from B6 donors ($H2^b$) were transplanted into myeloablative conditioned (8 Gy irradiation) BALB/c recipients ($H2^d$). As experimental controls, a group of mice was included, which received only BM cells (BM). Irradiated BALB/c mice served as controls for the myeloablative conditioning regimen (IR). As shown in **Figure 9** all groups lost equally up to 20% weight during the first week after irradiation and/or transplantation. Mice from IR group died due to anemia between d12-d15. Whereas mice, which received only BM cells from allogeneic donors regained weight one week after transplantation and could recover completely (**Figure 9 A**). The BM+T group lost 20-25% of weight and could not recover again and developed severe signs of aGvHD documented by aGvHD scoring (weight loss, ruffled fur, diarrhea and lethargy) within d5-d10 after allo-HCT and died between d8-d10.

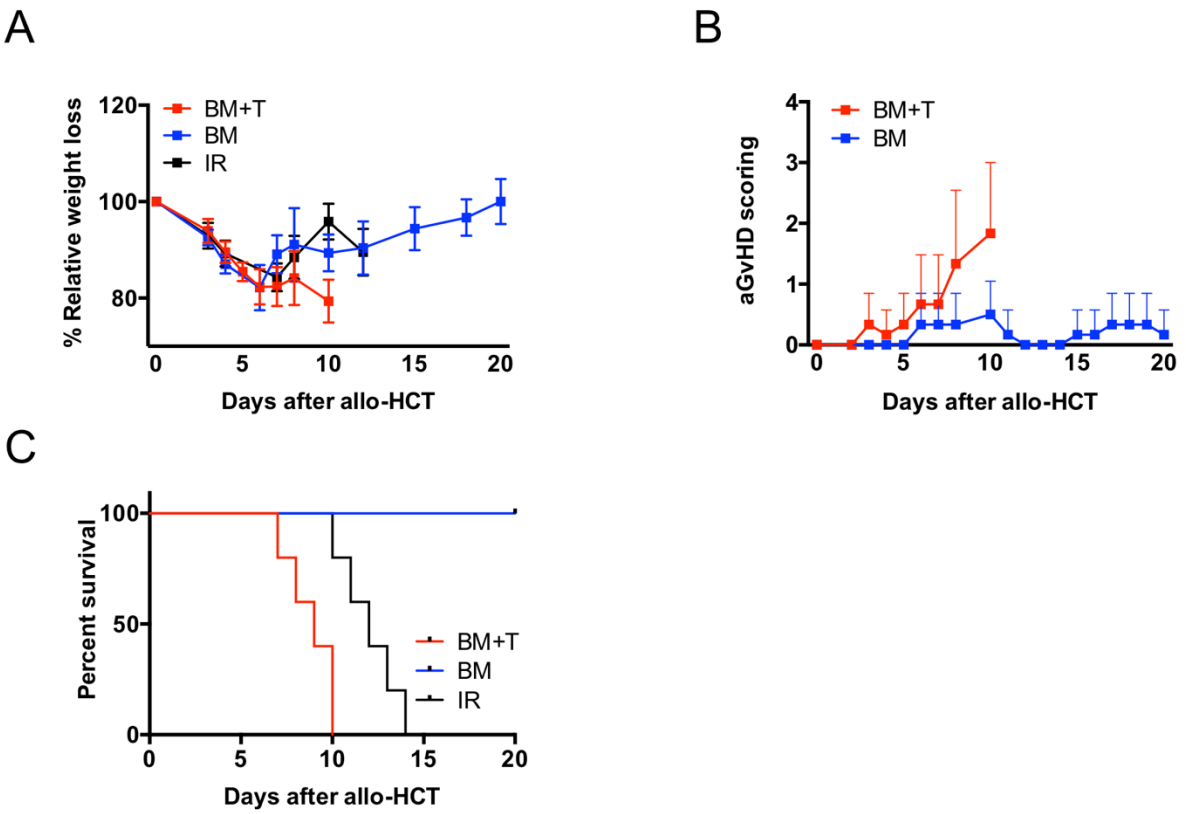

Figure 9: aGvHD development after MHC major B6→BALB/c allo-HCT.
BALB/c recipient mice were injected i.v. with 6 x 10^5 naïve T cells together with 5 x 10^6 BM cells from the same B6 donor strain (BM+T, red). The second BALB/c recipient group received allogeneic B6 BM only (BM, blue). One control group of BALB/c mice was irradiated and did not receive any cell transplantation (IR, black). **A** Weight loss is shown relative to d0 for BALB/c recipients. **B** Clinical aGvHD score highly increased in mice transplanted with BM+T (red) compared to mice transplanted with BM only (blue). Values represented as mean±SD (n = 5 for all groups). **C** Survival of mice after myeloablative irradiation and/or transplantation (n = 5/ group).

We used B6 donor T cells encoding the enzyme *luciferase* and the congenic marker CD90.1 enabling *in vivo* tracking and identification of donor T cells in the recipient. We monitored the migratory behavior of T cells closely by *in vivo* and *ex vivo* bioluminescence imaging (**Figure 10**). As reported previously, we confirmed that allogeneic T cells accumulate in the SLOs already by d2-d3 after allo-HCT in this model (Beilhack et al., 2005). During d4-d5 T cells migrated into the periphery and started to infiltrate the aGvHD target organs. Already on d6 full aGvHD manifestation could be observed in MHC major mismatch recipients. On d3.5 the main T cell signals were observed in the SLOs (iLN, spleen, mLN and PP) whereas on the following days the signals increased in the aGvHD target organs.

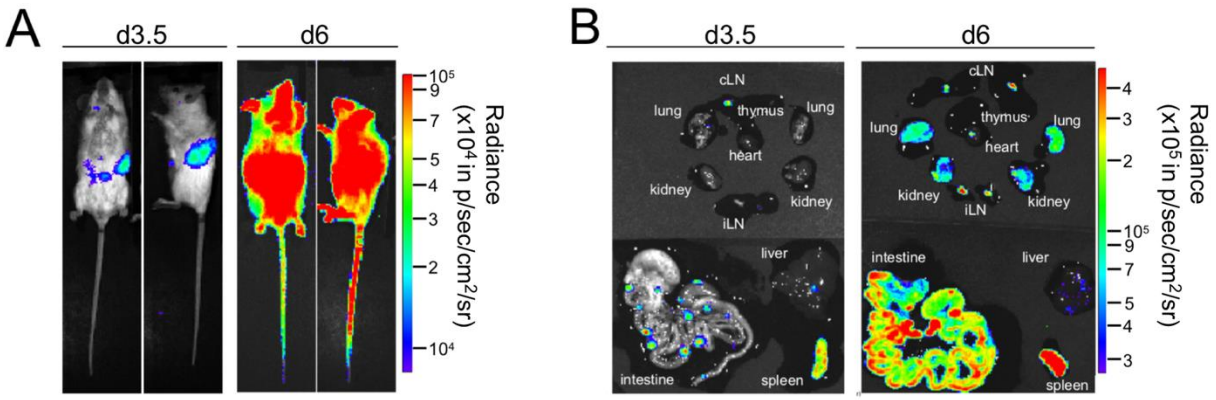

Figure 10: *In vivo* and *ex vivo* bioluminescence imaging of allo-HCT recipient.
BALB/c recipients were irradiated and received 6 x 10^5 T cells together with 5 x 10^6 BM cells from allogenic B6 donors. **A** Ventral and lateral view of one representative mouse of the allo-HCT (BM+T) recipient group on d3.5 and d6 after allo-HCT. Only transplanted CD90.1$^+$ donor T cells were expressing the enzyme luciferase. Signals were measured 10 min after i.p. injection of D-Luciferin. **B** To resolve T cell distribution in distinct organs mice were sacrificed 10 min after i.p. injection of D-Luciferin and organs were imaged within 3-5 min after isolation to detect bioluminescent donor T cells.

Thus, we confirmed timely coordinated events of allogeneic donor T cells proliferation (d3-d4) and T cell migration into the target organs (d5-d6) after MHC major mismatch allo-HCT. Since we were interested in the phenotype of T cells before they leave the SLOs and during the aGvHD effector phase we selected the time points d3.5 and d6 to further characterize of alloreactive T cells.

12.1.2 Alloreactive T cells upregulate homing receptors and activation markers after MHC major mismatch allo-HCT

Previous studies showed that CD4$^+$ and CD8$^+$ T cells are equally migrating out of the SLOs and infiltrating aGvHD target organs (Bäuerlein et al., 2013). We were interested in the unique surface marker profile of egressing CD8$^+$ T cells for the development of a predictive marker panel. CD8$^+$ T cells are major contributors to the aGvHD pathophysiology causing tissue damage and destruction in the aGvHD target organs. For surface marker profiling, T cells from inguinal and mesenteric lymph nodes (iLN and mLN) as well as from spleen of healthy vs. allogeneic transplanted mice were isolated on several time points after allo-HCT. We selected d3.5 as early time point because most of the cells were still in the activation and proliferation phase and did not migrate yet into the periphery (**Figure 11**).

To prepare for a prognostic peripheral blood test and to validate the FACS surface marker panel, we analyzed the expression of the activation markers on healthy and alloreactive T cells (n = 1 healthy; n = 3 B6→BALB/c). This preliminary study served as preparation for the follow up studies in the miHAg mismatch mouse model.

CD25 is the α-chain of the IL-2 receptor and its expression is induced on recently activated T cells. Less than 1 % of naïve T cells expressed CD25. On d3.5 after allo-HCT $CD8^+CD25^+$ frequencies reached 35.5 ± 8 % in mLN and 49.8 ± 6.4 % in spleen, whereas in iLN only 7.9 ± 3.9 % of $CD8^+CD25^+$ T cells were found (**Figure 11 B**). On d6 the frequencies in iLN increased to 49.8 ± 16.1 %, whereas the frequencies in mLN and spleen did not change drastically compared to d3.5 (62.3 ± 16.5 % and 44.6 ± 7.2 %, respectively).

CD44 is a marker for effector memory T cells (T_{EM}) and highly expressed on activated T cells (Ponta et al., 2003). On d3.5 in iLN of transplanted mice 58.9 ± 17.1 % of $CD8^+$ expressed CD44 (mLN 81.5 ± 2.4 % and spleen 76.1 ± 2.5 %). Healthy control mice showed around 30-50 % $CD8^+CD44^+$ in all organs on both measured time points (**Figure 11 C**).

CD69 has been described as immunomodulatory surface molecule and is induced early after activation on immune cells (Sancho et al., 2005). We measured CD69 expression on $CD8^+$ on d3.5 and d6 after allo-HCT. Around 30-45 % of donor $CD8^+$ T cells in iLN, mLN and spleen of allo-HCT recipients expressed CD69 on d3.5 after allo-HCT (**Figure 11 D**). In healthy mice only 2-4 % of $CD69^+CD8^+$ T cells were found in the SLOs. On d6 after transplantation $CD8^+CD69^+$ frequencies decreased to 5-7 % in iLN, mLN and spleen.

CD62L (L-Selectin) is a surface molecule on T cells and crucial for entering the SLOs (Sallusto et al., 1999). Since naïve T cells have to re-enter SLOs they express higher levels of CD62L compared to antigen-experienced cells. We observed CD62L expression on 85-95 % on $CD8^+$ in all organs of healthy controls. CD62L expression was significantly reduced on alloreactive T cells on d3.5 after allo-HCT and stayed low until d6 (**Figure 11 E**).

Because alloreactive T cells infiltrate the target organs during aGvHD progression, we analyzed the expression levels of the homing molecules $\alpha4\beta7$ integrin, CD162P (P-Selectin ligand) and CD162E (E-Selectin ligand) (**Figure 12**).

The highest frequency of $CD8^+\alpha4\beta7^+$ cells were found in the mLN on d3.5 (17.8 ± 3.2 %). On d6 after allo-HCT the $CD8^+\alpha4\beta7^+$ frequencies increased in all analyzed organs (29.1 ± 31.5 % in iLN; 40.8 ± 25.9 % in mLN; 58.7 ± 14.8 % in spleen). The levels of $\alpha4\beta7^+$ $CD8^+$ cells in the healthy control were around 1 % on all measured time points and in every organ (**Figure 12 B**).

GPR15 is a G-protein coupled receptor whose expression was reported on colonic T cells (Nguyen et al., 2015). Analysis of surface expression on d3.5 showed almost no upregulation of GPR15 on alloreactive T cells. In iLN, mLN and spleen only 2-3 % of $CD8^+$ cells expressed GPR15. The highest frequency of $GPR15^+$ donor cells were found in the iLN (19.2 ± 17.7 %) and mLN (12.9 ± 15.4 %) of transplanted mice.

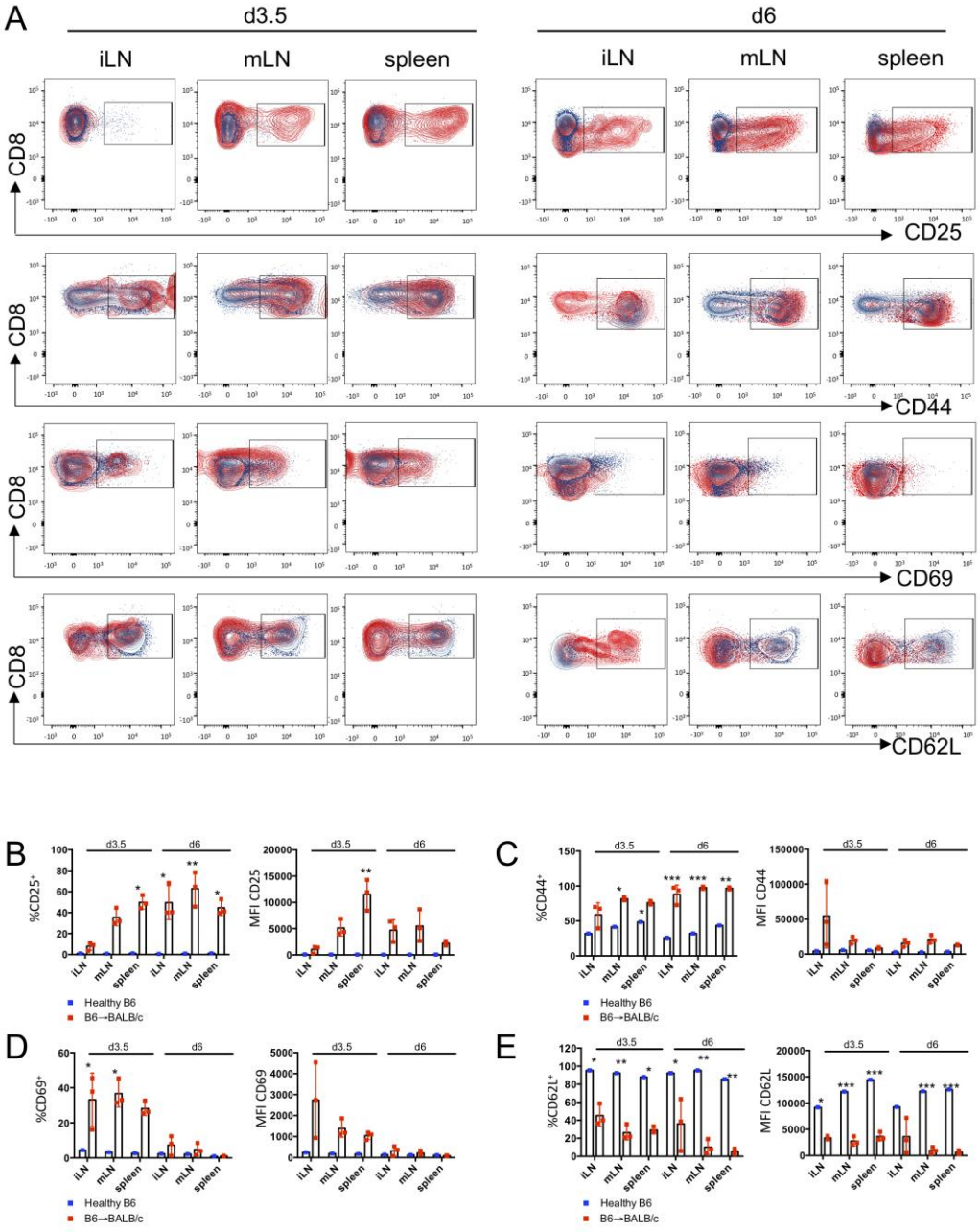

Figure 11: Alloreactive T cells are highly activated in the SLOs of allo-HCT recipients.
A Representative FACS plots of pregated $CD3^+CD8^+$ T cells. Cells were isolated from SLOs on d3.5 and d6 from healthy B6 mice (blue) or allo-HCT recipients (red) and analyzed by flow cytometry for cell surface expression of CD25, CD44, CD69 and CD62L. **B, C, D** and **E** show individual values (% or MFI) of the respective markers on living $CD3^+CD8^+$ T cells. All values were displayed as mean ± SD (n = 1 healthy B6, n = 3 B6→BALB/c for each time point). Statistical significance was tested by unpaired t-test and indicated for significance as *, $P \leq 0.05$; **, $P \leq 0.01$; ***, $P \leq 0.001$.

Next, we analyzed whether donor $CD8^+$ express the P-Selectin ligand (CD162P), which is involved in leukocyte rolling and mediates adhesion and transendothelial migration of leukocytes by binding to P-Selectin on endothelial cells (Moore, 1998). On d3.5 (initiation phase) almost 15.3 ± 11.2 % of T cells in the iLN expressed CD162P (11.5 ± 2.4 % in mLN and 22.8 ± 13.1 % in spleen). On d6 after transplantation the frequencies of $CD162P^+$ T cells reached up to 56 ± 26 % in iLN and to 80.4 ± 8.4 % in mLN and to 62.9 ± 8.5 % in spleen. The $CD162P^+$ frequency in $CD8^+$ T cells of the untreated controls never exceeded 1 %.

On d3.5 after allo-HCT 20-40 % of donor T cells expressed the skin homing molecule CD162E. The highest frequency of $CD8^+CD162E^+$ T cells was found in the spleen of transplanted mice (around 34.6 ± 7.4 %). On d6 most of the effector cells had already migrated to the aGvHD target organs and only few cells remained in the SLOs. Relative $CD8^+CD162E^+$ cell frequencies reached up to 76.3 ± 11.2 % in spleen (66.7 ± 10.3 % in iLN and 77.4 ± 12.1 % in mLN). For all measured time points $CD162E^+$ frequency was significantly higher on donor T cells compared to T cells from healthy controls. Only 1-2 % of $CD162E^+$ $CD8^+$ T cells were found in healthy mice in all analyzed organs. Thus, $\alpha 4\beta 7$ integrin, CD162P and CD162E were significantly upregulated on donor T cells and allowed specific identification of alloreactive T cell early after transplantation. Furthermore, alloreactive T cells in the SLOs were highly activated and expressed high levels of CD25 and CD69. CD62L was significantly downregulated on these cells.

To confirm our results and to analyze the surface expression under more clinically relevant conditions, we utilized a second model of aGvHD (Eyrich et al., 2005; Korngold et al., 1980). aGvHD in this model is less acute since MHC molecules between donor and host are matched and aGvHD is induced by recognition of mismatches in minor histocompatibility antigens (miHAg). The events of T cell activation, proliferation and organ infiltration occur in a spatiotemporal organized fashion after MHC matched and miHAg mismatched allo-HCT (Bäuerlein et al., 2013). Therefore, employing a miHAg allo-HCT model allowed us to track donor T cells in the PB before aGvHD symptoms occurred.

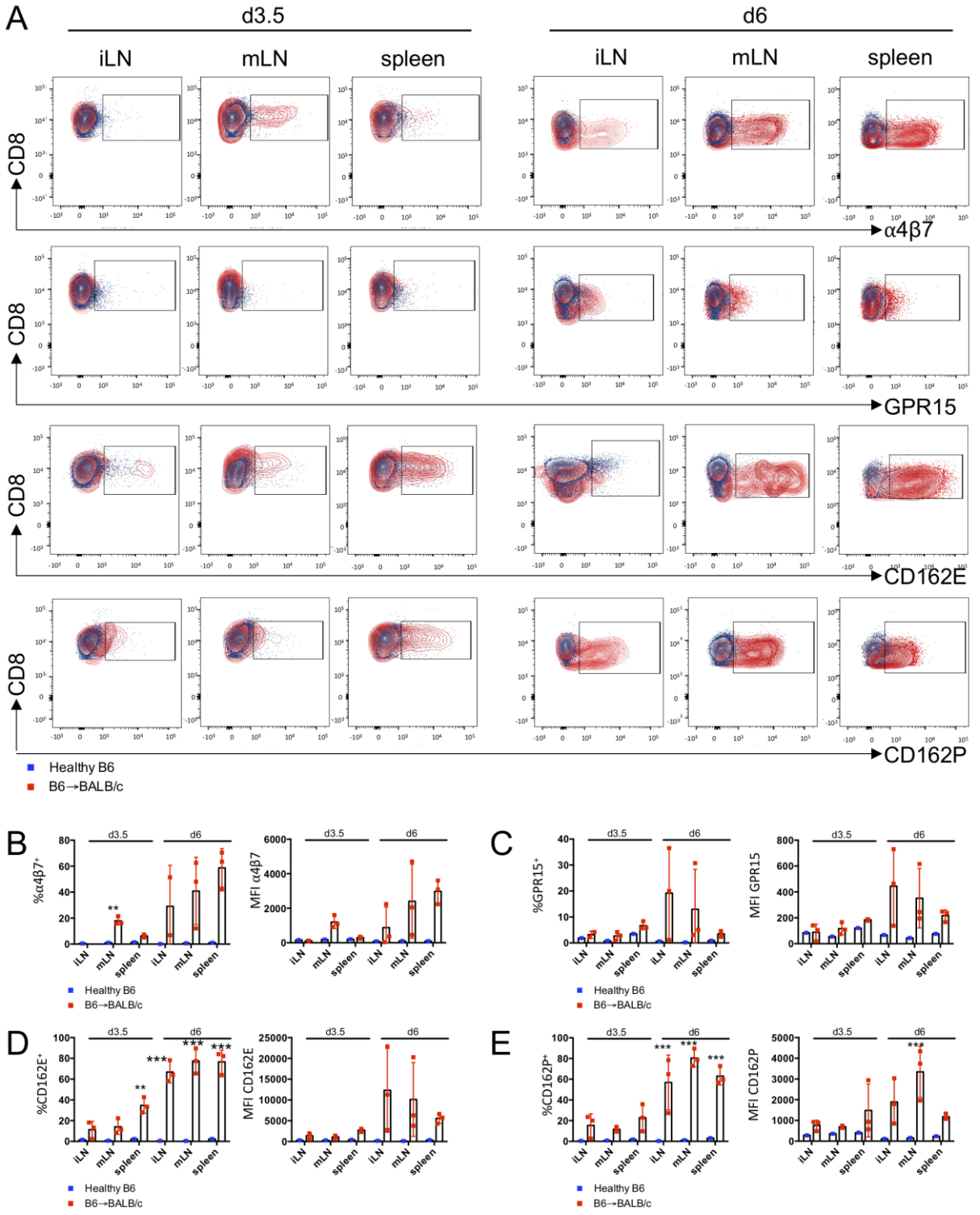

Figure 12: Alloreactive T cells highly upregulate homing receptors early after allo-HCT.
A Representative FACS plots of pregated $CD3^+CD8^+$ T cells. Cells were isolated from SLOs on d3.5 and d6 from healthy B6 mice (blue) or allo-HCT recipients (red) and analyzed by flow cytometry for cell surface expression of α4β7, GRP15, CD162E and CD162P. **B, C, D** and **E** show individual values (% or MFI) of the respective markers on living $CD3^+CD8^+$ T cells. All values were displayed as mean ± SD (n = 1 healthy B6, n = 3 B6→BALB/c for each time point). Statistical significance was tested by unpaired t-test and indicated for significance as *, $P \leq 0.05$; **, $P \leq 0.01$; ***, $P \leq 0.001$.

12.1.3 Surface receptor profile of donor T cells in the PB of miHAg mismatch recipients

12.1.3.1 Onset of aGvHD in two miHAg mismatch allo-HCT mouse models

GvHD target organ infiltration depends on the appropriate expression of homing receptors on migrating cells (Wysocki et al., 2005). Therefore, we tested an extended panel of surface markers consisting of adhesion molecules, chemokine receptors, and activation markers to determine potential biomarkers that may specifically define alloreactive T cells in the PB. To this end, we compared two $CD4^+$ and $CD8^+$ T cell dependent miHAg mismatched allogeneic mouse models (B6→BALB/b and B10.D2→BALB/c, **Figure 13 A**) with syngeneic HCT recipients and healthy WT controls. Based on our previous results of donor T cell migration kinetics (Bäuerlein et al., 2013), we chose two peak time points during the early and later phase of T cell mobilization (days+6 and +15) and included day +21 (clinically apparent aGvHD onset after murine miHAg allo-HCT) as appropriate for a precise receptor analysis.

First, we analyzed whether miHAg B10.D2→BALB/c allo-HCT showed the same aGvHD kinetics as the previously reported B6→BALB/b model (Bäuerlein et al., 2013). Host conditioning regimen and transplantation procedure resulted in 20% – 30% weight loss during the first 8 days after allo-HCT in B10.D2→BALB/c miHAg mismatched recipients of BM and T cells. Mice recovered after 10 days and reached 80% – 90% of their initial body weight but could not recover completely. Weight remained at the same level until the end of the experiment. In contrast, weight loss of syngeneic B10.D2→B10.D2 recipients was rather mild during the first week after HCT (10%) compared to BM recipients (15% – 20%, **Figure 13 B**). Both groups recovered 10 days after HCT and reached their starting weight. In allo-HCT recipients, typical signs of aGvHD occurred around day+20. Symptoms included diarrhea, skin inflammation, and ruffled fur (**Figure 13 C**). Histopathological analysis confirmed aGvHD in the small and large bowel as well as the skin on day+25 after B10.D2→BALB/c allo-HCT (**Figure 13 D, E**). Increased tissue damage, T cell infiltration, and crypt apoptosis contributed to the significant aGvHD histological score in the large bowel whereas typical signs of aGvHD in the skin featured necrotic keratinocytes, inflammation, and basal vacuolization of the epidermis.

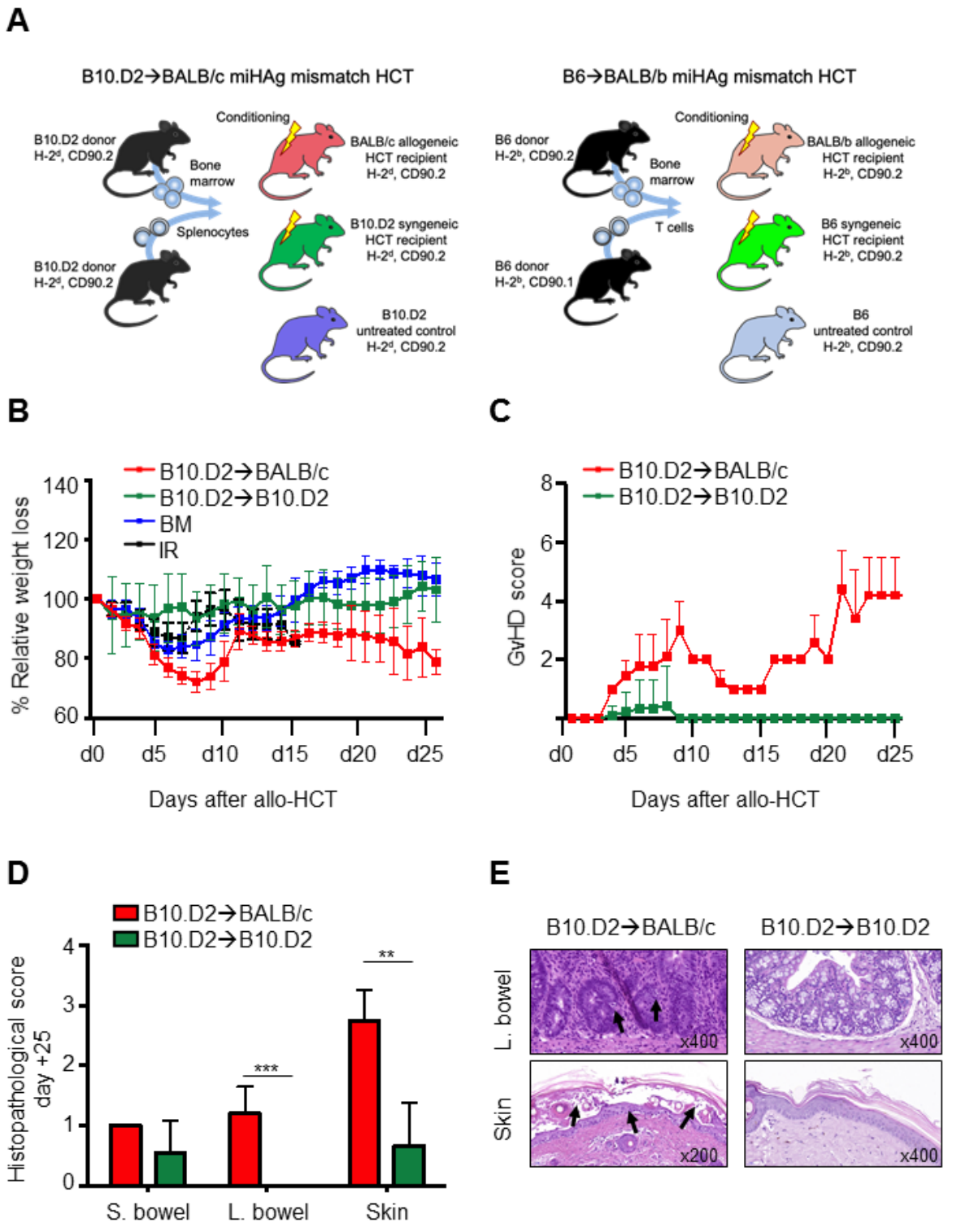

Figure 13: Murine MHC matched miHAg mismatched allo-HCT models to assess a biomarker panel on peripheral blood (PB) CD8⁺ T cells for aGvHD.
A Schematic overview of the two described miHAg mismatch allo-HCT and syngeneic HCT models**.** **B–E** Validation of aGvHD induction in the B10.D2→BALB/c miHAg mismatch allo-HCT model. **B** Weight loss relative to day 0 of HCT of the B10.D2→BALB/c model and the respective control groups. **C** Clinical scores during aGvHD progression of miHAg mismatch and syngeneic recipients. **D** Histopathological grading of the aGvHD target organs intestine and skin on day+25 after allo-HCT and **E** representative hematoxylin-eosin stains at indicated magnification. Values are displayed as means ± SD. MiHAg mismatch B10.D2→B10.D2 BM+T cells, n = 9; syngeneic B10.D2→B10.D2 BM+T cells, n = 9; BM only, n = 5; irradiation only, n = 5. T = T cells, BM = Bone Marrow, IR = Irradiation.

12.1.3.2 Alloreactive donor CD8$^+$ T cells upregulate homing molecules early after HCT

Next, we collected blood samples of the tail vein from allogeneic and syngeneic recipients on days+6, +15, and +21 for immune phenotyping of PB CD8$^+$ T cells and compared these to the respective untreated controls. PB CD8$^+$ T cells highly up-regulated the mucosal homing receptor $\alpha4\beta7$ integrin after miHAg mismatch allo-HCT (**Figure 14 A**, representative histograms) in both miHAg models. In the allogeneic B6→BALB/b model, $\alpha4\beta7^+$ CD8$^+$ T cell frequencies in the PB significantly exceeded those after syngeneic HCT at all time points and the expression peaked at day+15 (28.7 ± 3.9% vs. 8.1 ± 2.1%, P < 0.0001; < 1% $\alpha4\beta7^+$PB CD8$^+$ T cells in untreated controls, **Figure 14 B**). Similarly, PB CD8$^+$ T cells of B10.D2→BALB/c miHAg mismatch recipients expressed significantly higher levels of $\alpha4\beta7$ integrin compared to syngeneic controls at all measured time points and $\alpha4\beta7$ expression peaked on day+15 (42.72 ± 5.3% vs. 2.4 ± 0.8%, P = 0.0002, **Figure 14 C**). Next, we analyzed expression levels of the skin homing receptors CD162E and CD162P after allo-HCT. Notably, in B10.D2→BALB/c miHAg allo-HCT recipients, CD162E expression levels of alloreactive PB CD8$^+$ T cells exceeded significantly the levels found in syngeneic controls at all measured time points (e.g., 74.3 ± 11.2% vs. 28.1 ± 6.95% on day+6, P < 0.0001) (**Figure 14 A, C**). On day+6, in B6→BALB/b miHAg allo-HCT recipients, CD162E$^+$ CD8$^+$ T cell frequencies did not differ between allogeneic and syngeneic HCT recipients. However, thereafter, levels of CD162E$^+$ T cells after miHAg mismatch allo-HCT exceeded those found in syngeneic controls (20.5 ± 4.4% versus 8.5 ± 4.7% on day+15, P = 0.1). By day+21, CD162E expression levels almost equaled between both groups again. In contrast, in untreated controls less than 5% of PB CD8$^+$ T cells expressed CD162E under steady-state conditions. Additionally, PB CD8$^+$ T cells highly up-regulated CD162P in both miHAg allo-HCT models (**Figure 14 B, C**) compared to syngeneic controls. In B6→BALB/b miHAg allo-HCT recipients, 45.2 ± 4.4% of CD8$^+$ T cells expressed CD162P already on day+6 compared to 13.8 ± 6.8% of CD8$^+$ T cells in syngeneic controls (P = 0.01) and less than 10% of CD8$^+$ T cells in untreated controls. Already by day+6 in B10.D2→BALB/c allo-HCT, CD8$^+$CD162P$^+$ expression levels of allo-HCT recipients significantly exceeded those of syngeneic recipients (75.6 ± 17.4% vs 22.6 ± 11.4%; P = 0.0001). Furthermore, the lymphoid homing receptor CD62L significantly decreased on PB CD8$^+$ T cells after allo-HCT and remained significantly lower compared to syngeneic HCT at all analyzed time points (30.2 ± 9.6%

vs. 76.4 ± 4.4%, P = < 0.0001 on day+6 after B6→BALB/b allo-HCT and 41 ± 12.3% vs. 85.2 ± 5%, P = 0.0019 on day+6 after B10.D2→BALB/c allo-HCT, respectively). In syngeneic recipients, PB $CD8^+CD62L^+$ T cell frequencies were only slightly lower than those of untreated controls (75 to 95% $CD62L^+$).

To assess the activation status of PB $CD8^+$ T cells we investigated the expression of CD69 and CD25. Frequencies of PB $CD8^+CD69^+$ T cells differed significantly between the two groups only on day+15 (37.1 ± 11.8% in allogeneic B6→BALB/b vs. 18.9 ± 8.7% in syngeneic recipients, P = 0.0409; < 3% of circulating $CD8^+$ $CD69^+$ T cells in untreated controls) and +21 (**Figure 14 B**). After B10.D2→BALB/c allo-HCT, CD69 expression exceeded the levels measured on PB $CD8^+$ T cells of syngeneic controls on day+6 (8.3 ± 3.2 vs. 2.3 ± 1.1; P = 0.08).

PB $CD8^+$ T cells of B6→BALB/b allo-HCT recipients significantly up-regulated the activation marker CD25 compared to syngeneic controls on days+15 and day +21 (32.7 ± 10.5% $CD8^+CD25^+$ T cells in allogeneic vs. 15.03 ± 8.7% in syngeneic recipients, P = 0.03, **Figure 14 B**). Yet, no significant differences between allogeneic and syngeneic recipients were determined after B10.D2→BALB/c allo-HCT (**Figure 14 C**). Other markers such as CC-chemokine receptors (CCRs 2, 4, 5, 6, 7, 9) surprisingly never differed between allogeneic and syngeneic recipients (**Figure 15**). At day+6, PB $CD8^+$ T cells highly up-regulated all CCRs both in allogeneic B6→BALB/b recipients and in syngeneic B6→B6 controls compared to untreated animals. After day+6, CCR expression levels decreased similarly in allogeneic and syngeneic recipients. The differences in CCR expression levels did not reach statistical significance at any of the analyzed time points.

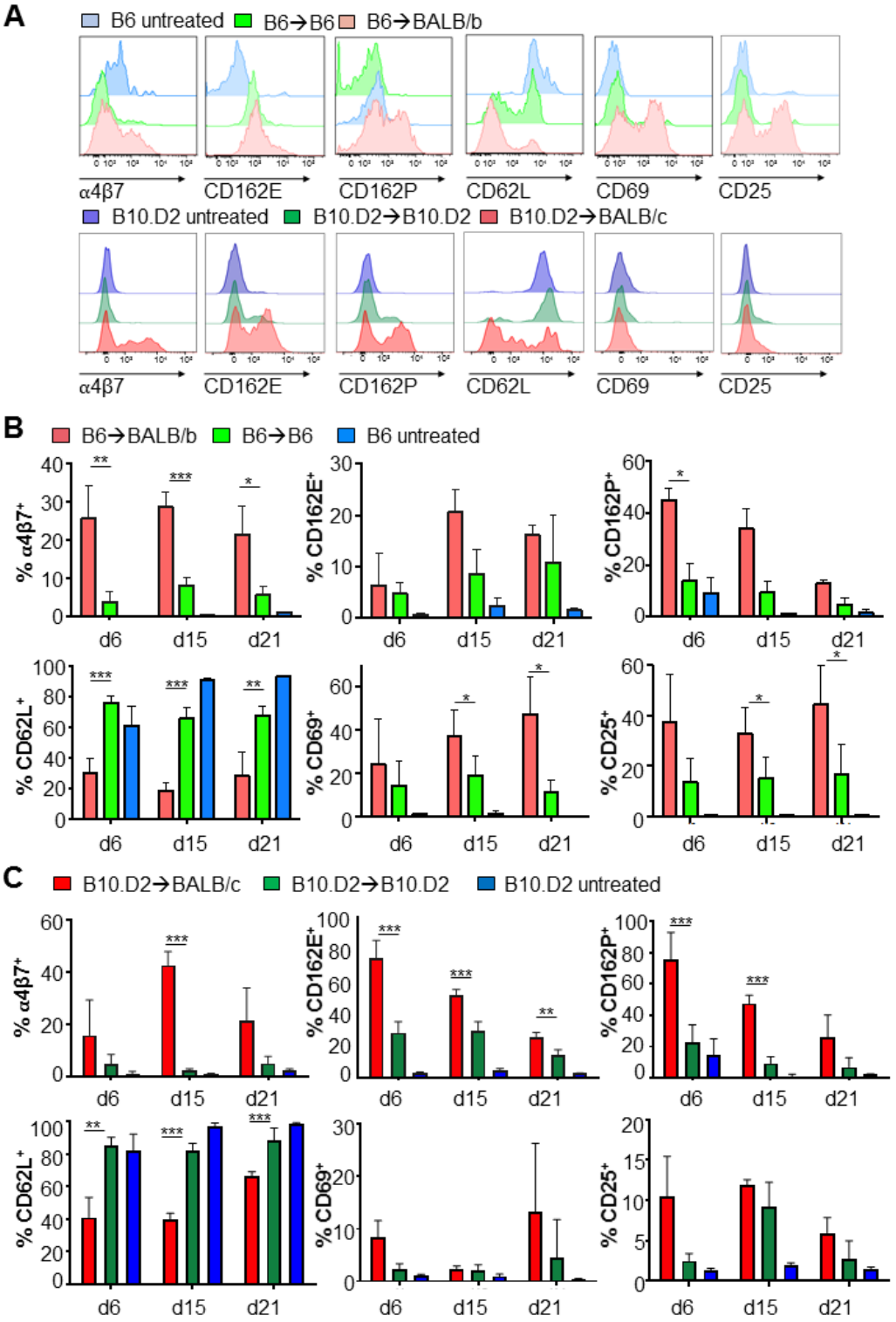

Figure 14: Allogeneic peripheral blood CD8⁺ T cells display a distinct surface marker profile before the onset of aGvHD.

A Representative histograms show surface receptor expression on PB CD8⁺ T cells on day +15 (upper row B6→BALB/B model, lower row B10.D2→BALB/c model) after allo-HCT compared to the respective expression levels of syngeneic and untreated healthy controls. **B, C** Summary of surface receptor expression on PB CD8⁺ T cells at indicated time points after HCT and untreated controls. Values are displayed as means ± SD. B6→BALB/b: n= 3 – 6 in each group, B10.D2→BALB/c: n = 5 – 9 in miHAg mismatch and syngeneic control group, untreated B10.D2 n = 4. Statistical significance between miHAg mismatch recipients and syngeneic controls was determined with a repeated ANOVA and posthoc analysis using Bonferroni correction of the significance level. *P ≤ 0.05; ** P ≤ 0.01; *** P ≤ 0.001.

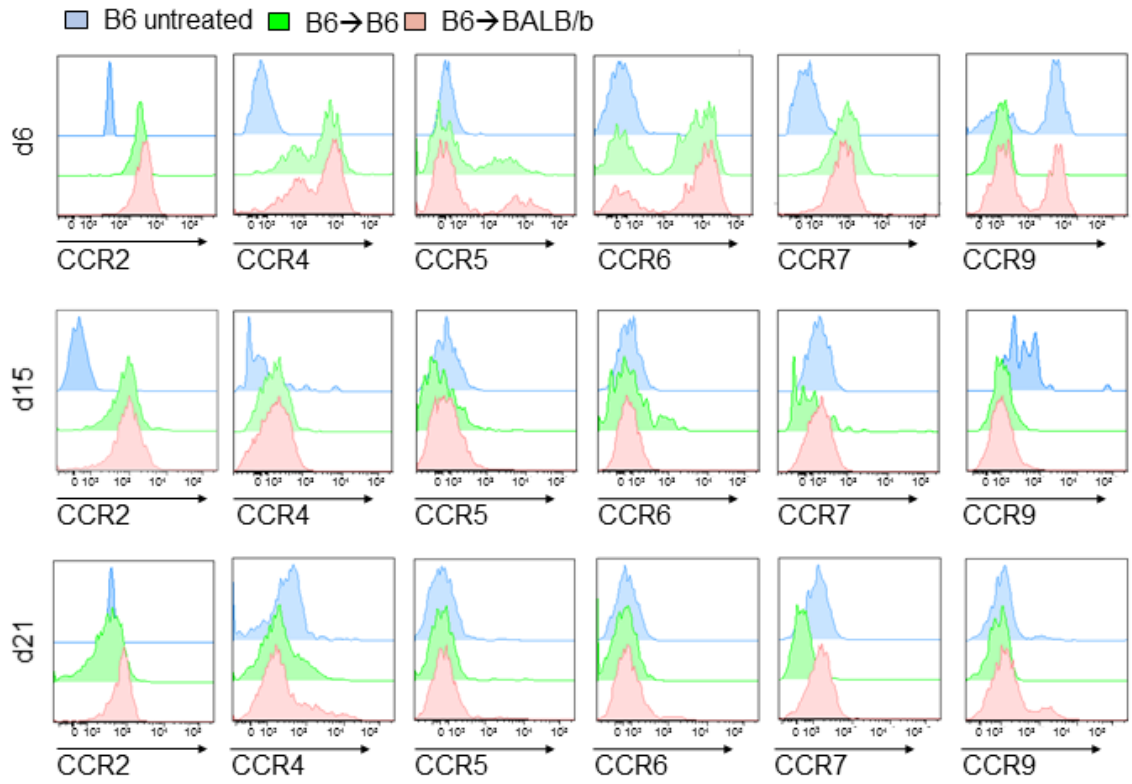

Figure 15: CC-Chemokine receptor expression profiles of donor T cells do not characterize CD8⁺ T cells in the peripheral blood.
Chemokine receptor expression levels on PB CD8⁺ T cells of B6→BALB/b miHAg mismatch and B6→B6 syngeneic recipients are shon in representative histograms (day+ 6, +15, +21 after HCT in comparison to untreated B6 controls) (n = 3 – 10).

12.1.3.3 Combined surface marker panel predicts aGvHD onset

Based on these results, we next asked whether the combination of T-cell surface markers can clearly discriminate allogeneic transplanted mice from syngeneic recipients and untreated controls (**Figure 16 A**). Our principle component analysis considered the four surface markers $\alpha4\beta7$ integrin, CD162E, CD162P, and CD62L as CD25, CD69, and CC-chemokine receptors were not exclusively expressed on alloreactive T-cells. To classify the animals based on their treatment, we applied an unsupervised K-means clustering on the percentage of CD8⁺ T cells with high expression levels of the four aforementioned surface markers for day+6 as an early GvHD prediction would be most beneficial. We compared the clustering based on four markers to a clustering based on the single marker $\alpha4\beta7$ integrin to investigate if the combination of several markers could enhance the predictive value (**Figure 16 B**). The first two principal component spaces (PC1 and PC2) predict the variance in the data. The clustering analysis based on $\alpha4\beta7$ integrin alone could unequivocally separate allogeneic from syngeneic recipients on day+15 but not on day+6. Determining the

accuracy score [= (number of true classified samples)/ (number of total test data)] for several marker combinations on day+6 showed that in both models the maximum prediction accuracy could be obtained with a minimum of three parameters (**Figure 16 C)**. Conclusively, our data suggest that the early upregulation of α4β7 integrin, CD162E, CD162P as well as low expression levels of CD62L on circulating PB $CD8^+$ T cells serve as strong predictor of aGvHD and that the combination of at least three markers increases the precision of our analysis.

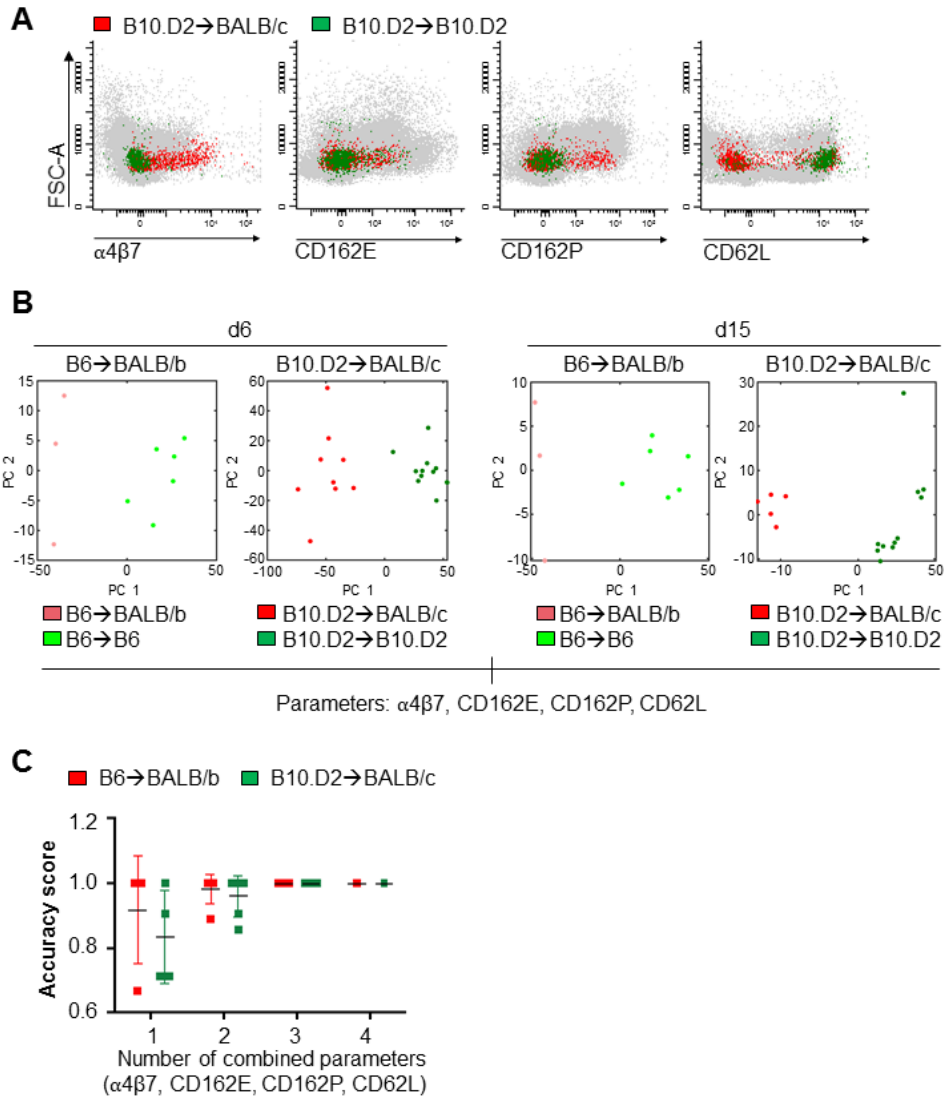

Figure 16: Combination of surface receptors defines alloreactive T cells in the PB of allo-HCT recipient.
A Representative FACS plots of PB samples on day+15 analyzed with Infinicyte Flow Cytometry Software. Overlay of allogeneic (red) vs. syngeneic (green) $CD3^+CD8^+$ T cells of total peripheral blood mononuclear cells (PBMC, in grey). **B** Principal component analysis based on four parameters and unsupervised K-means clustering of individual samples. Each data point represents one mouse. Red dots show allogeneic and green dots show syngeneic recipients of both models. Distances between data points represent the similarity. **C** Determination of accuracy score [= (number of true classified samples)/(number of total test data)] for the combination of parameters. Each point represents one possible marker combination.

12.2 Part II: Expression kinetics of immunomodulatory molecules on donor and host T cell populations

12.2.1 Imunmodulatory molecules are highly upregulated on activated T cells

The first part of this work revealed homing receptors on alloreactive T cells, such as $\alpha4\beta7$ integrin and CD162P, as two potential therapeutic targets. The overreaching goal of this project was the development of a novel therapeutic approach to selectively target alloreactive T cells without affecting immune reconstitution and the desired GvL effect. Therefore, an improved understanding of the immunobiology of highly activated T cells during aGvHD progression appeared highly relevant. In addition to T cell homing receptors we investigated receptors of the TNFR superfamily on alloreactive T cells on d3.5 and d6 after allo-HCT and compared their expression profile to T cells of healthy mice. The aim was to identify immunomodulatory molecules, which are differently expressed on alloreactive Tregs and Tcons. To this end we used the previously described MHC major mismatch aGvHD model (B6→BALB/c) (**Figure 7**, **Figure 9**, **Figure 10**). We isolated T cells from spleen on d3.5, a time point when most of the donor T cells are still located in the SLOs undergoing activation and proliferation. We selected d6 as second time point during the aGvHD effector phase and analyzed T cells from spleen and intestines. At this time point the first wave of T cells infiltrated already the target organs and intestinal aGvHD is already manifested.

We analyzed the expression levels of 4-1BB, CD27, GITR and TNFR2, which belong to the TNFR superfamily. Furthermore, we analyzed the expression of the immunomodulatory molecule PD1 and the co-stimulatory molecule ICOS. Since we were aiming to develop a highly selective therapeutic approach, we analyzed Tregs ($CD4^+Foxp3^+$) and Tcons ($CD4^+Foxp3^-$, $CD8^+Foxp3^-$) separately according to the gating strategy in **Figure 17 A**. Furthermore, representative histograms of the respective FMO controls were displayed in **Figure 17 B**. Representative FACS plots showing the gating and representative histograms of individual surface markers analyzed on d6 in the spleen are displayed in **Figure 18**. Histograms of healthy control mice (blue) were overlaid with histograms from alloreactive T cells (red). The frequency of positive cells for each marker on d6 was displayed in **Figure 22** and MFI values were calculated from the FACS measurements of both analyses and displayed as mean values ± SD (**Figure 19**).

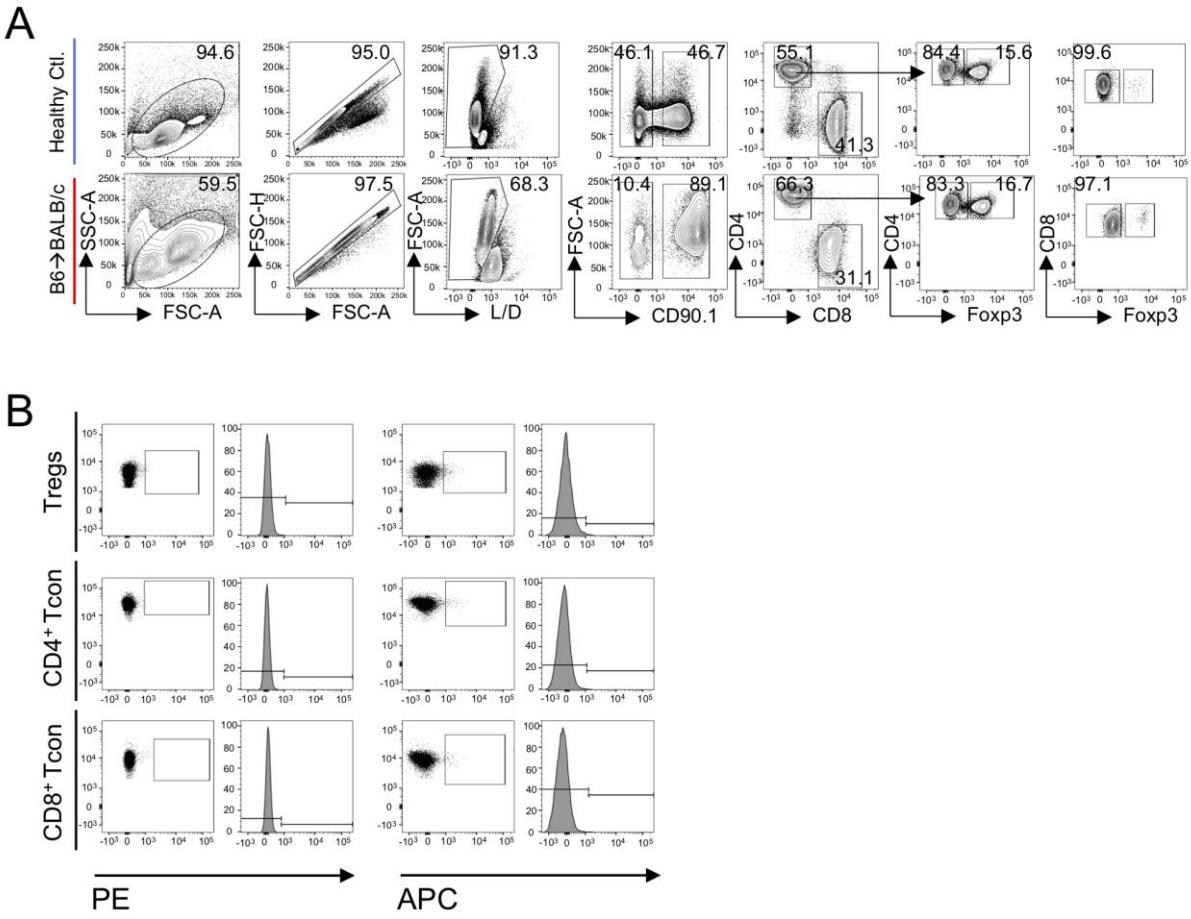

Figure 17: Gating strategy for splenic Tcons and Tregs.
Spleens were harvested on d6 after MHC major mismatch allo-HCT and T cells were analyzed by FACS for surface expression of TNFR superfamily members. **A** Representative gating strategy to identify distinct T cell subsets. T cells were pregated for living and CD90.1$^+$ (congenic marker). Tcon populations were selected according to the expression of CD4$^+$Foxp3$^-$ and CD8$^+$Foxp3$^-$. To gate on Tregs cells were intracellularly stained for Foxp3. **B** Representative histograms of FMO controls on pregated CD4$^+$Foxp3$^-$ and CD8$^+$Foxp3$^-$as well as CD4$^+$Foxp3$^+$ Tregs.

On d3.5 alloreactive CD8$^+$ Tcons upregulated 4-1BB 36-fold compared to CD8$^+$ Tcons from naïve mice (4-1BB MFI on alloreactive CD8$^+$ 2833 ± 268 vs. 77 ± 27 on naive CD8$^+$). CD27 expression levels were not changed significantly between naïve and recently activated T cell populations on this early time point after transplantation (**Figure 19**). The highest GITR expression levels were observed on Tregs and did not differe significantly between Tregs from healthy or transplanted mice (GITR MFI on healthy Tregs 15879 ± 1920 vs. alloreactive Tregs 16157 ± 2651). GITR expression levels on CD4$^+$ Tcons and CD8$^+$ Tcons were not changed significantly between healthy and alloreactive donor T cells on d3.5. Furthermore, TNFR2 expression was highly

induced on Tregs and $CD8^+$ Tcons on d3.5 after allo-HCT, and to a lesser degree also on $CD4^+$.

PD1 levels were were very similar between $CD4^+$ Tcons and Tregs on d3.5 after allo-HCT. However, a slightly increased PD1 expression was observed on $CD8^+$ T cells. ICOS expression was upregulated on Tregs and $CD4^+$ Tcons on this early time point after transplantation (**Figure 19**).

This data suggests that on d3.5 only few significant changes are taking place in alloreactive T cells. Our observation showed that 4-1BB and TNFR2 appeared to be strongly induced on alloreactive $CD8^+$ Tcons and Tregs. Furthermore, Tregs of healthy mice expressed higher levels of GITR, TNFR2, ICOS and CD27 under steady state compared to naïve Tcons (**Figure 19 A**).

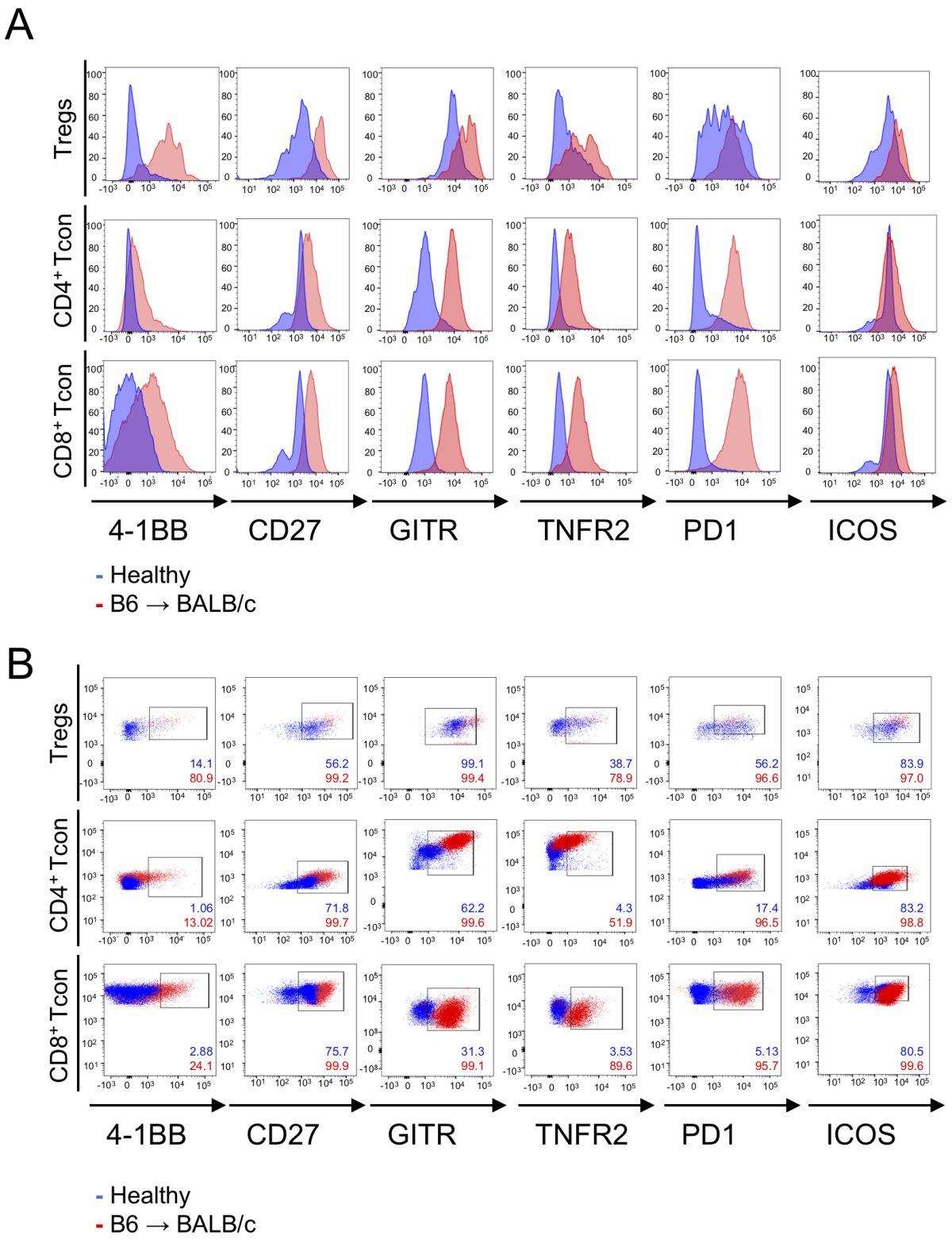

Figure 18: Alloreactive T cells upregulate ICOS, PD1 and receptors of the TNFR SF on d6 after allo-HCT.
Spleens were harvested on d6 after MHC major mismatch allo-HCT and T cells were analyzed by FACS for surface expression of TNFR superfamily members. **A** Representative histograms of pregated $CD4^+Foxp3^-$ and $CD8^+Foxp3^-$ Tcons as well as Tregs were overlaid for the respective marker (healthy, blue; MHC major mismatch B6→BALB/c, red). **B** Representative FACS Plots and gating strategy to determine the percentage of positive cells for individual surface markers.

On d6 after aGvHD induction, Tregs expressed 8-fold and 2.5-fold higher levels of 4-1BB compared to alloreactive $CD4^+$ and $CD8^+$, respectively (MFI values on alloreactive Tregs reached 3815 ± 681, whereas MFI values on alloreactive $CD4^+$ Tcons and $CD8^+$ Tcons were around 489 ± 83 and 1560 ± 261).

CD27 expression levels were highest on allogeneic Tregs (MFI 13778 ± 2299) compared to $CD4^+$ Tcons (MFI 3499 ± 2091) and $CD8^+$ Tcons (MFI 5005 ± 1200). Highest expressionof PD1 was observed on $CD8^+$ Tcons MFI 8179 ± 521 compared to 5546 ± 270 on $CD4^+$ and 5087 ± 350 on Tregs.

On d6 we observed a high infiltration of T cells into the intestine. Therefore, we asked if the phenotype of effector T cells in a target organ differs from T cells, which were still in the SLOs. The small intestine of healthy and allo-HCT recipients (on d6) were enzymatically digested and T cells isolated. In general, we could obtain only very low numbers of living T cells from allo-HCT recipients as seen in **Figure 20**. Especially Treg counts were very low in both group (less than 100 events per sample). However, all analyzed surface molecules (4-1BB, CD27, GITR, TNFR2, PD1 and ICOS) were highly expressed on donor T cells isolated from the small intestine. Furthermore, intestinal donor $CD4^+$ as wells $CD8^+$ Tcons expressed higher PD1 levels compared to Tregs (MFI values donor $CD4^+$ 2661 ± 565; donor $CD8^+$ 4259 ± 2420 and donor Tregs 771 ± 332).

To summarize, on d3.5 we observed only moderate changes in surface expression of immunomodulatory molecules on alloreactive T cells. However, by d6 alloreactive T cells in the spleen had a completely changed phenotype compared to healthy T cells. All analyzed immunomodulatory molecules were highly upregulated on alloreactive Tregs and to a lesser extend on Tcons. Only PD1 was stronger induced on recently activated donor $CD4^+$ as well as $CD8^+$ from spleen and intestine compared to Tregs from the same organ. Furthermore, alloreactive T cells in the intestine showed changes of expression levels of the tested immunomodulatory molecules when compared to healthy T cells from the intestine.

With this part of the work, we demonstrated that the phenotype of activated and naïve T cell populations is significantly different. This is of particular importance for the development of novel T cell subset-specific therapeutic approaches. However, previous reports have shown that host T cell populations persist after myeloablative irradiation (Anderson et al., 2004; Hirshfeld et al., 2006). Therefore, we did extensive

analysis on host Treg and Tcon numbers and analyzed if remaining cells expressed immunomodulatory makers to the same extend as donor T cells.

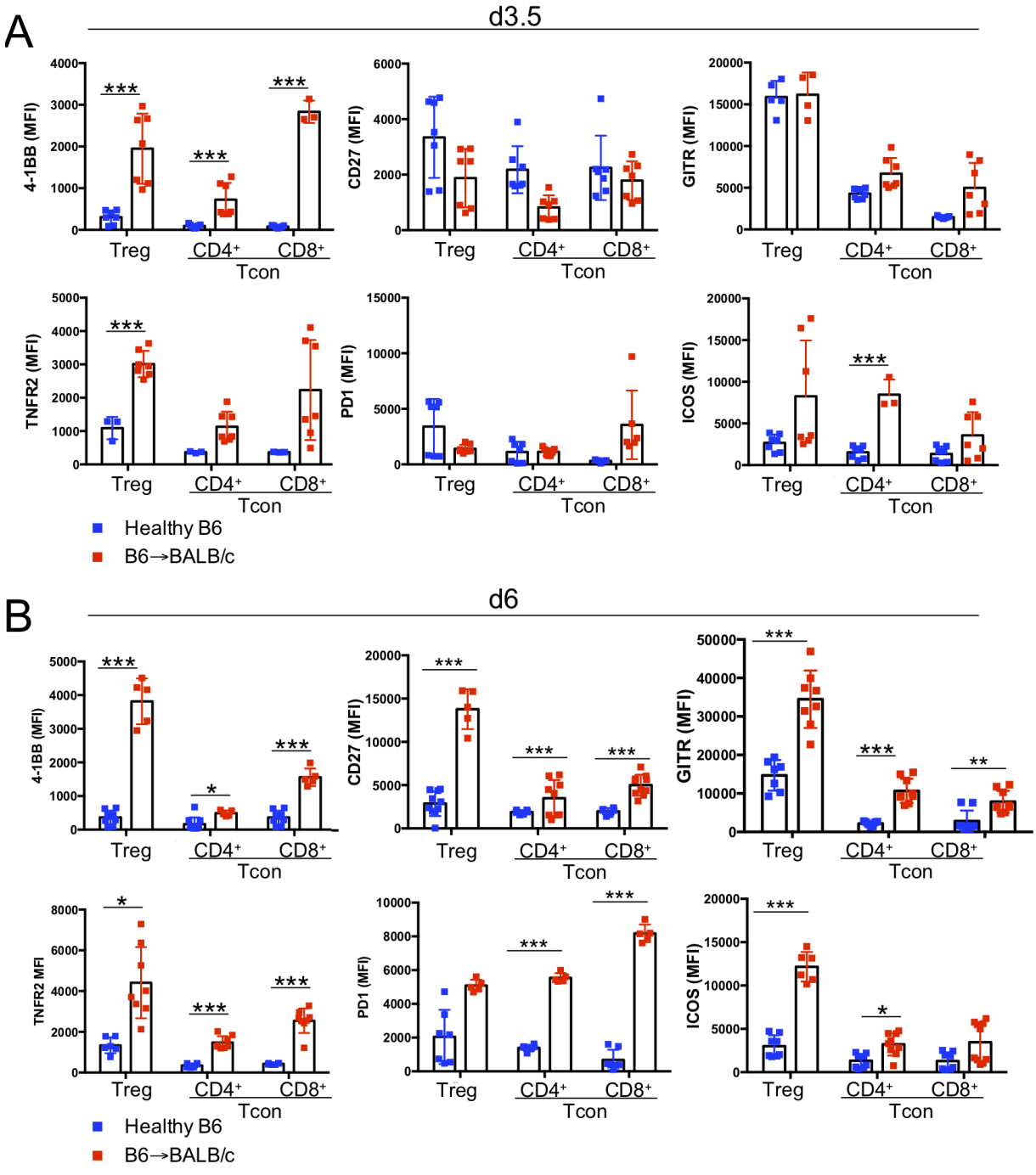

Figure 19: Induced expression of immunomodulatory molecules on splenic alloreactive T cells. Cells were isolated from the spleen of healthy B6 (blue) and allogeneic T cell recipients (B6 → BALB/c, red) after allo-HCT. Cells were pre-gated for living CD90.1$^+$ and T cell subsets were selected according to CD4$^+$Foxp3$^-$, CD8$^+$Foxp3$^-$ and CD4$^+$Foxp3$^+$ expression. Relative MFI values were displayed as mean ± SD on **A** d3.5 and **B** d6 after allo-HCT. n = 3-8 per group and time point. Statistical significance was determined by unpaired t-test (*, $P \leq 0.05$; **, $P \leq 0.01$; ***, $P \leq 0.001$)

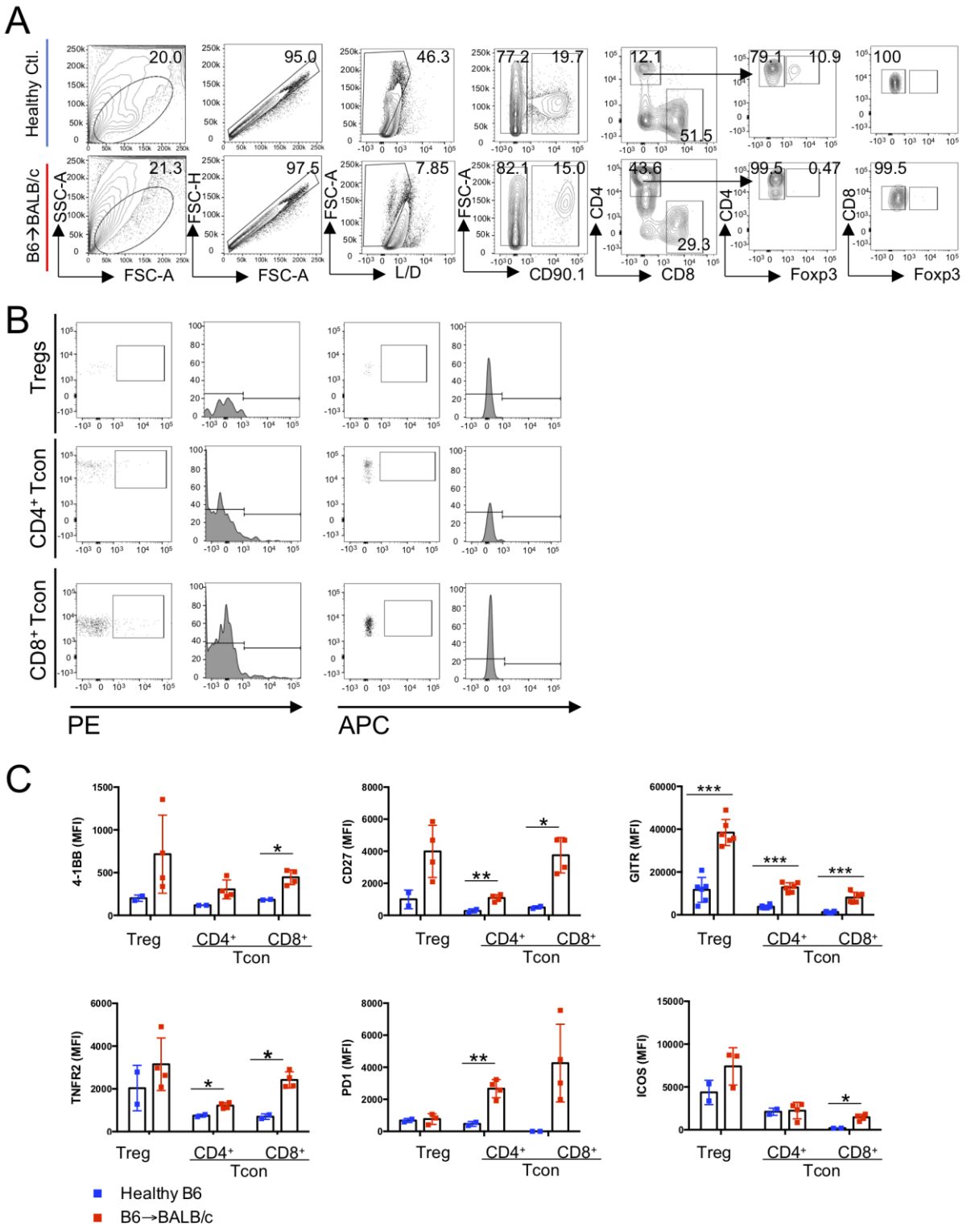

Figure 20: Allogeneic donor Tregs in the small intestines upregulate immunomodulatory molecules.

Cells were isolated from the small intestine of healthy mice (blue) and allogenic T cell recipients (B6→BALB/c, red) on d6 after allo-HCT. **A** Representative gating strategy for T cell subsets. T cells were pregated for living and CD90.1 (congenic marker). Tcon populations were selected according to the expression of $CD4^+Foxp3^-$ and $CD8^+Foxp3^-$. To gate on Tregs cells were intracellularly stained for Foxp3. **B** Representative histograms of FMO controls on pregated $CD4^+Foxp3^-$ and $CD8^+Foxp3^-$ Tcons as well as Tregs. **C** Relative MFI values displayed as mean ± SD. n = 2-4 per group and timepoint. Statistical significance was determined by unpaired t-test (*, P ≤ 0.05; **, P ≤ 0.01; ***, P ≤ 0.001).

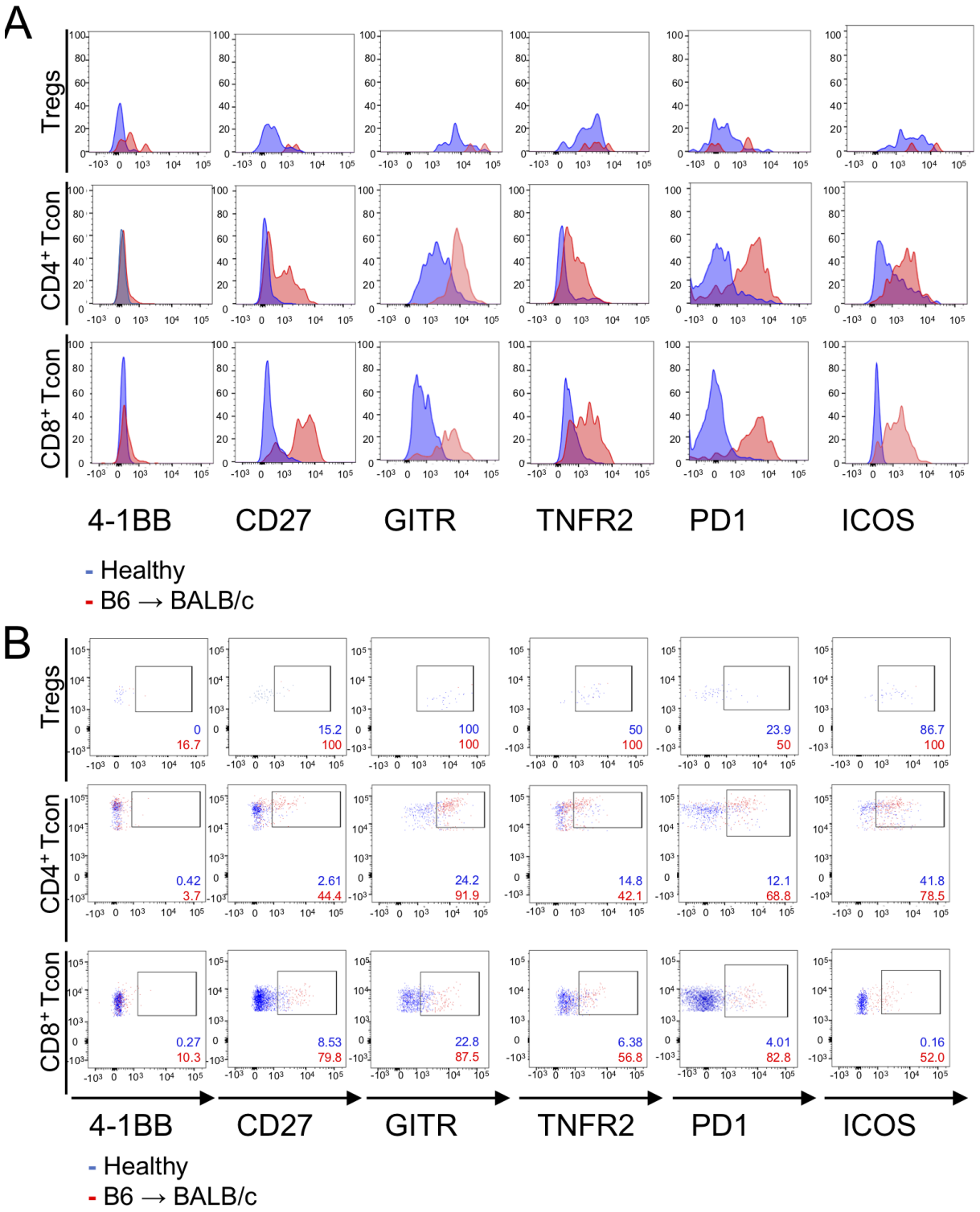

Figure 21 Alloreactive T cells upregulate ICOS, PD1 and receptors of the TNFR SF on d6 after allo-HCT in the small intestine.
Small intestines were obtained on d6 after MHC major mismatch allo-HCT and T cells were analyzed by FACS for surface expression of TNFR superfamily members. **A** Representative histograms of pregated $CD4^+Foxp3^-$ and $CD8^+Foxp3^-$ Tcons as well as Tregs were overlaid for the respective marker (healthy, blue; MHC major mismatch B6→BALB/c, red). **B** Representative FACS Plots and gating strategy to determine the percentage of positive cells for individual surface markers.

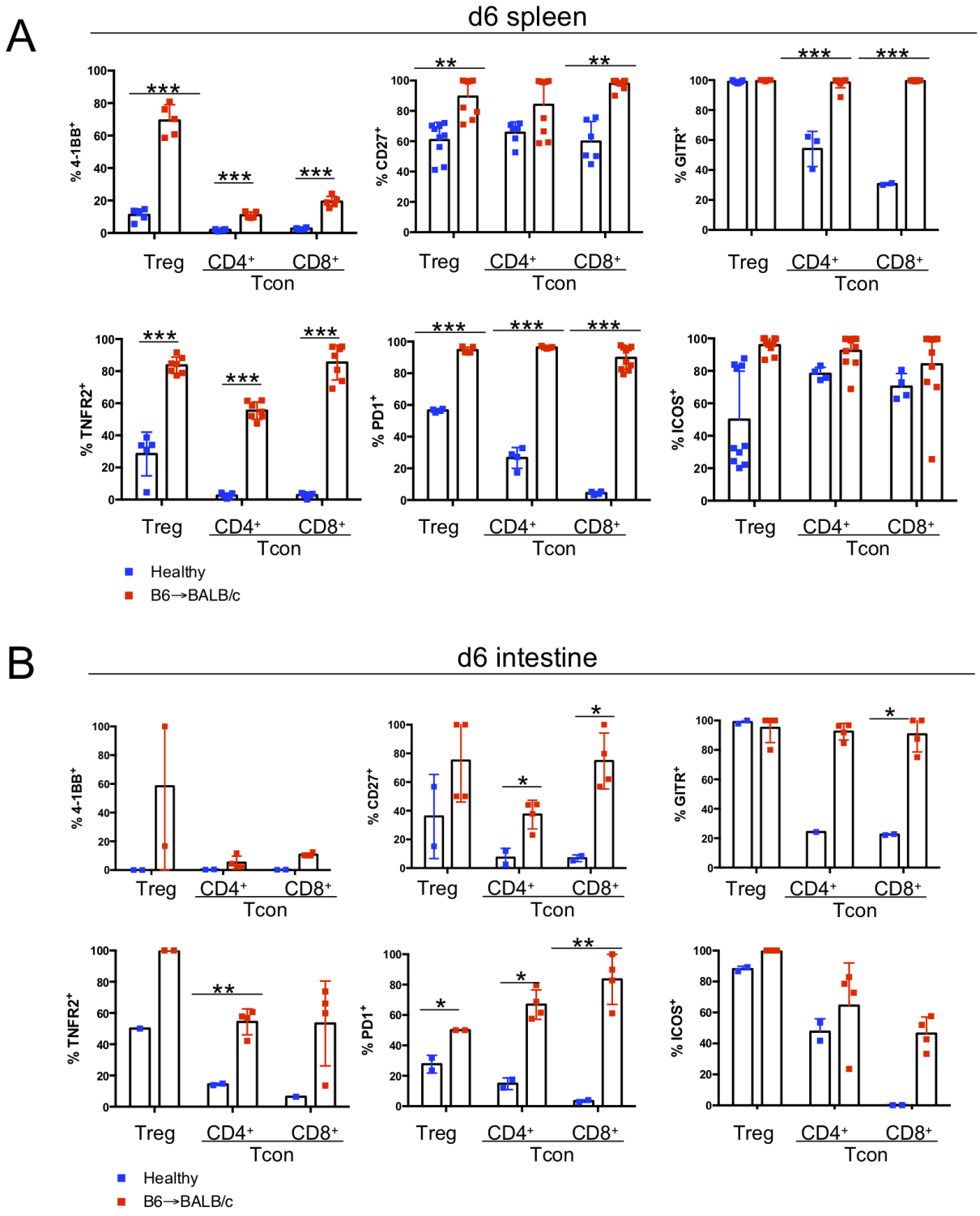

Figure 22: Increased frequency of alloreactive T cells expressing immunomodulatory molecules on d6 after allo-HCT in spleen and small intestine.
A Spleens and **B** small intestines were harvested on d6 after MHC major mismatch allo-HCT and T cells were analyzed by FACS for surface expression of ICOS, PD-1 and TNFR SF members. Tcon populations were selected according to the expression of $CD4^+Foxp3^-$ and $CD8^+Foxp3^-$. To gate on Tregs cells were intracellularly stained for Foxp3. Values were displayed as mean ± SD (n = 2-8 per group and time point). Statistical significance was determined by unpaired t-test (*, $P \leq 0.05$; **, $P \leq 0.01$; ***, $P \leq 0.001$).

12.2.2 Host T cells persist in spleen and intestine at least until d6 after myeloablative irradiation

To differentiate between donor and host lymphocytes we used a congenic mouse strain. All B6 donors expressed CD90.1, a variant of CD90 that can be used as a congenic marker. To analyze remaining host T cells in B6→BALB/c MHC major mismatch model we gated on $CD90.1^-$ donor cells. Earlier we showed by bioluminescence imaging that donor T cells expand in the SLOs and migrate to the intestine, lung and skin during the first week after transplantation (**Figure 10**). Since we were interested in finding unique marker profiles particularly on donor T cells, we first analyzed how many host T cells were remaining on d3.5 after irradiation (**Figure 23**). Host and donor ratios were shown as absolute cell counts and percentages and compared the absolut cell numbers of healthy controls. Data is displayed as mean ± SD (healthy n = 10, allogenic n = 20 per group, biological and technical replicates). The frequency of splenic Tregs in the healthy group was around 16.2 ± 0.7 % and Treg frequencies in the donor T cell compartment were higher compared to the host T cell compartment (donor 15.5 ± 5.2 % vs. host 11.2 ± 2.4 %). Absolute T cell counts of both Tcons and Tregs were much lower in transplanted mice compared to healthy controls, probably due to the conditioning regimen and the early time point of the analysis.

Next, we determined how donor and host compartments change from d3.5 (initiation phase) to d6 (the effector phase) after allo-HCT. At this time point we additionally analyzed the host and donor cell frequencies in the small intestines, since on d6 already large numbers of T cells infiltrated the intestinal tract (**Figure 10**). In general, donor cell frequencies and cell counts increased highly from d3.5 to d6 in the spleen. On d6 28.1 ± 26.1 % of host $CD4^+$ cells expressed $Foxp3^+$ compared to 3.56 ± 1.71 % of $Foxp3^+$ cells in the donor $CD4^+$ compartment of the intestine. Furthermore, high numbers of donor $CD4^+$ (22.4 ± 19.1 %) and $CD8^+$ (28.5 ± 10.9%) infiltrated the intestine 6 days after allo-HCT (**Figure 24**).

To sum up, our data indicates that especially host Tregs persisted after irradiation in the intestine and that more donor $CD8^+$ T cells infiltrated the intestine compared to $CD4^+$ T cells.

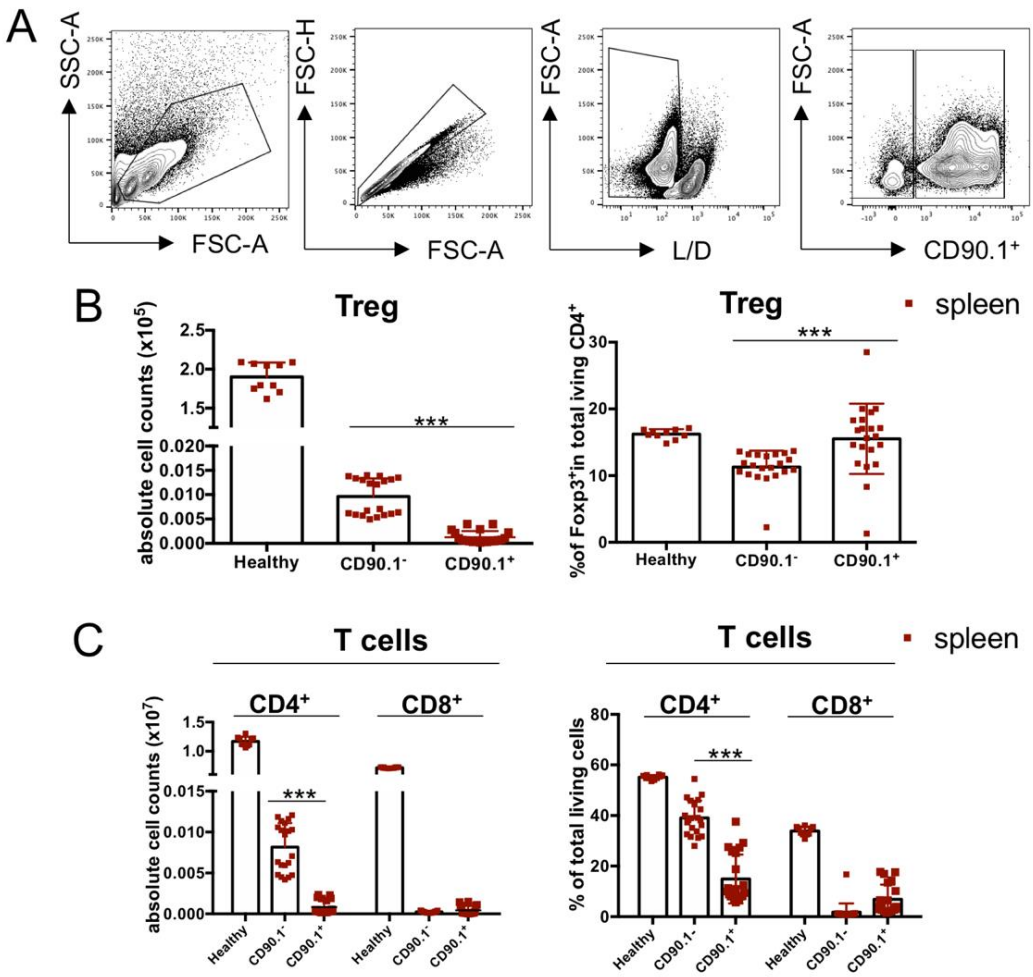

Figure 23: CD90.1$^-$ host T cell subsets persist in the spleen on d3.5 after irradiation.
T cells were isolated on d3.5 after allo-HCT from spleen. Healthy splenocytes were analyzed as control populations. All cells were pre-gated for living cells and CD90.1$^-$ for host cell compartment and CD90.1$^+$ for donor cell compartment, respectively. To identify T cell population CD90.1$^-$ and CD90.1$^+$ were subgated for CD4$^+$, CD8$^+$ and CD4$^+$Foxp3$^+$. Values were displayed as mean ± SD (n = 9-20 for allo-HCT recipients, biological and technical replicates). Statistical significance between both compartments was determined by unpaired t-test (*, $P \leq 0.05$; **, $P \leq 0.01$; ***, $P \leq 0.001$).

The aim of the study was to identify immunomodulatory molecules, which are selectively expressed on alloreactive donor T cells. Our analysis in **Figure 23** and **Figure 24** revealed that host cells persist after irraditation. Especially, Tregs seem to be irradiation resistant. To understand these observations more closely and to define distinct targets on alloreactive T cells we asked whether host cells express immunomodulatory molecules to the same extent as donor T cells. The relative MFI values of host and donor T cells in spleen and intestine were displayed in **Figure 25**. We found that host cells also express certain levels of the analyzed immunomodulatory molecules. However, the expression levels for all molecules were much lower on host cells compared to donor T cells on d6 after transplantation.

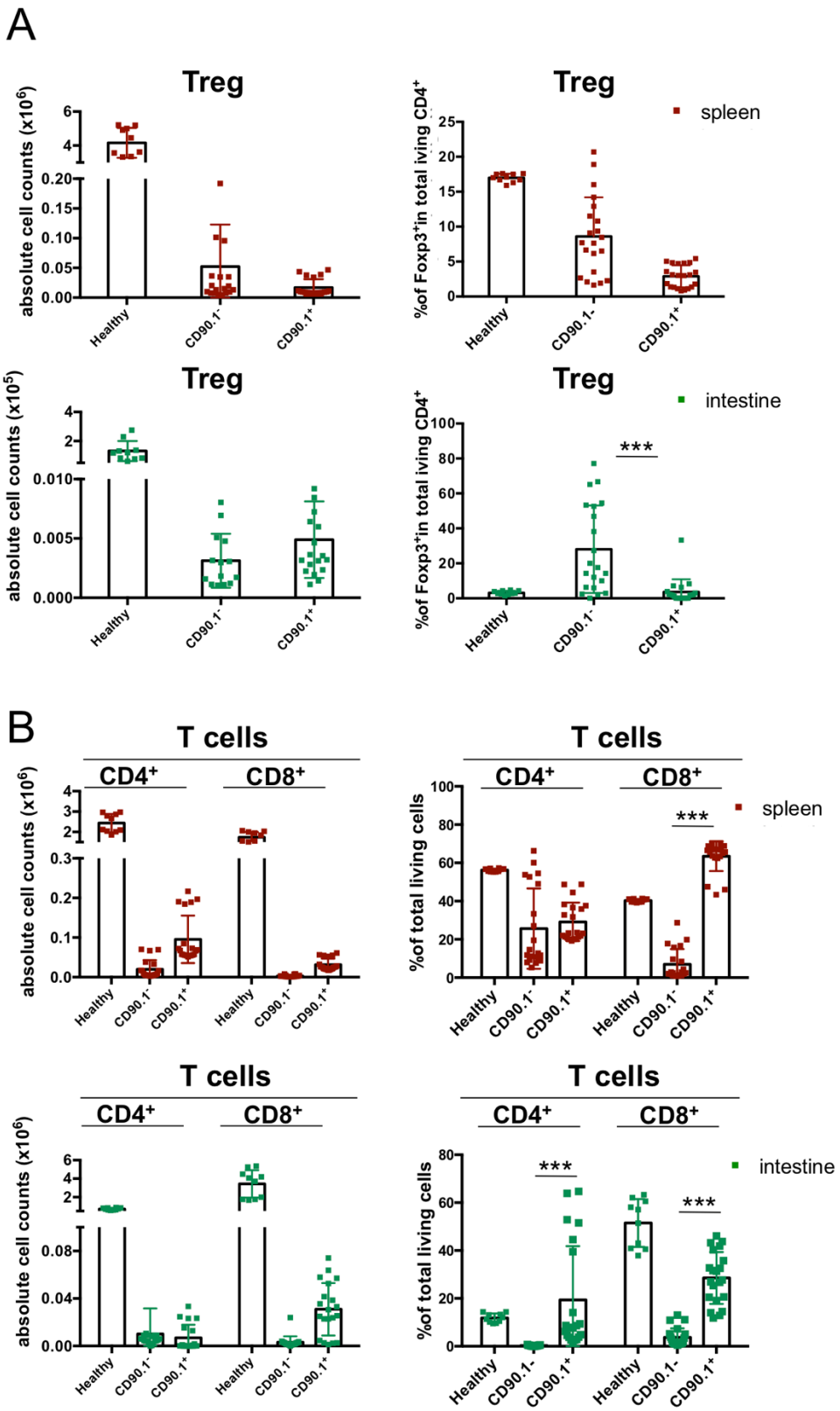

Figure 24: CD90.1$^-$ host Tregs persist in the intestine until d6 after allo-HCT.
T cells were isolated on d6 after allo-HCT from spleen (red) and small intestine (green). Healthy mice were analyzed as control group. All cells were pre-gated for living cells and CD90.1$^-$ for host cell compartment and CD90.1$^+$ for donor cell compartment, respectively. To identify T cell populations CD90.1$^-$ and CD90.1$^+$ were subgated for CD4$^+$, CD8$^+$ and CD4$^+$Foxp3$^+$. Values were displayed as mean ± SD (n = 9-20 for allo-HCT recipients, n= 10 for healthy, biological and technical replicates). Statistical significance between both compartments was determined by unpaired t-test (*, $P \leq 0.05$; **, $P \leq 0.01$; ***, $P \leq 0.001$).

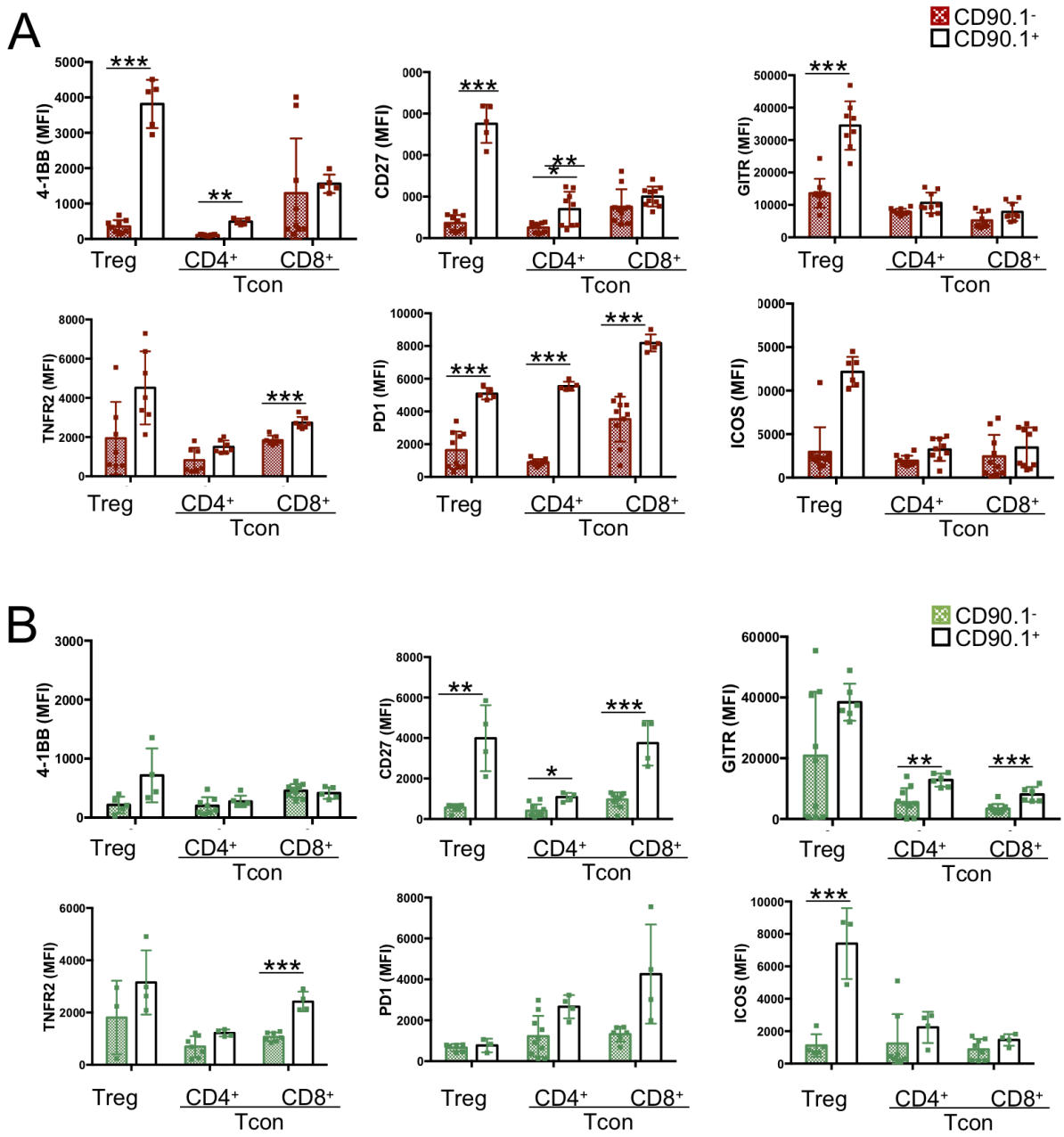

Figure 25: Expression of immunomodulatory molecules on host and donor cells.
T cells were isolated on d6 after allo-HCT from **A** spleen (red) and **B** small intestine (green). All cells were pre-gated for living cells and CD90.1$^-$ for host cell compartment and CD90.1$^+$ for donor cell compartment, respectively. To identify T cell population CD90.1$^-$ and CD90.1$^+$ were subgated for CD4$^+$Foxp3$^-$, CD8$^+$Foxp3$^-$ and CD4$^+$Foxp3$^+$. Values were displayed as mean ± SD (n = 3-9 for allo-HCT recipients). Statistical significance between both compartments were determined by unpaired t-test (*, $P \leq 0.05$; **, $P \leq 0.01$; ***, $P \leq 0.001$).

To summarize, numbers of alloreactive donor cells were still low on d3.5 after allo-HCT and increased significantly on d6 in the spleen. Furthermore, significant numbers of Tregs remained in the spleen and the intestine after irradiation and transplantation. This part of the work showed that immunomodulatory molecules are dynamically expressed on different T cell populations after allo-HCT. We could observe a tendency of higher expression of the analyzed molecules on d3.5 but results were more

significant on d6. This might be due to fewer cell numbers in SLOs on d3.5. For modulation of recently activated as well as naïve Tregs we found 4-1BB, CD27, GITR, TNFR2, PD1 and ICOS being unique and suitable Treg markers. Our observation also showed that almost all analyzed surface markers were strongly upregulated on inflammatory $CD4^+$ and $CD8^+$ after allo-HCT in spleen as well as in the small intestine.

12.3 Part III: Development of therapeutic (antibody) fusion proteins to selectively target alloreactive T cells

The previous parts of the thesis formed the basis for the development of novel strategies to target T cells, which will be the focus of the following chapter. Based on the previous observations, we selected α4β7 integrin and P-Selectin ligand (CD162P/P-Lig) as main target molecules on the surface of alloreactive T cells. Since the main goal of this project is to develop novel treatment strategies for selective targeting of alloreactive T cells, it was analyzed whether host cells also upregulated these two homing markers during aGvHD. The expression levels of α4β7 and CD162P/P-Selectin ligand on $CD4^+$ and $CD8^+$ of allo-HCT recipients (B6→BALB/c) compared to healthy B6 controls were analyzed by FACS and displayed as histogram (d6 analysis, one mouse per group, n = 3 B6→BALB/c; n = 3 healthy B6). This analysis revealed that alloreactive donor T cells strongly upregulate α4β7 and CD162P/P-Lig, whereas host cells expressed only low levels of these two molecules. From these results we concluded that these two surface homing receptors are selectively expressed on alloreactive T cells and might serve as potential target.

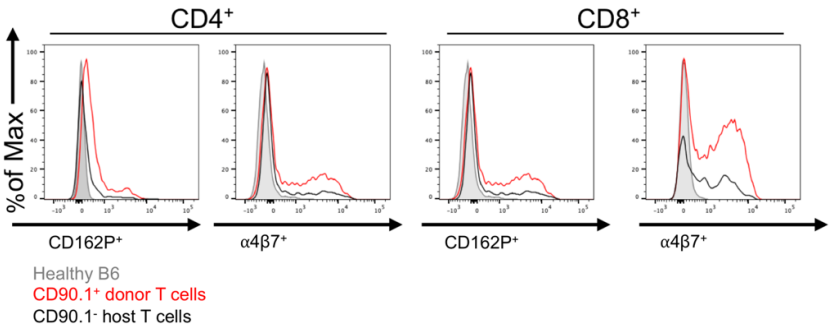

Figure 26: Few splenic host T cells express low levels of α4β7 integrin and CD162P (P-Lig). Representative histograms of donor $CD90.1^+$ vs. host $CD90.1^-$ $CD4^+$ and $CD8^+$ cells. Splenocytes were isolated on d6 after allo-HCT from MHC major mismatch recipients. Cells were pregated for live $CD90.1^+$ or $CD90.1^-$ populations and histograms display relative expression levels of α4β7 and CD162P (P-Lig) for one representative mouse for each group.

To target α4β7 we designed ligenad-based fusion proteins, where the sequence of the extracellular domain (ed) of murine (mu) MAdCAM-1 was used as a targeting domain.

MAdCAM-1 is the natural ligand of α4β7 integrin and expressed on intestinal endothelial cells (Erle et al., 1994). To target CD162P/P-Selectin ligand, we designed fusion proteins, where the extracellular domain (ed) of murine (mu) P-Selectin (CD162P) was used as targeting domain. P-Selectin is expressed on activated vascular endothelial cells and blood platelets and facilitate T cell entry into inflamed tissues such as the skin in aGvHD (Lu et al., 2010). These targeting domains were addiotionally fused to the extracellular FasL domain (Ankersmit et al., 2002), single-chain TNF80 (binds TNFR2/CD120b) (Grell et al., 1993) or PD1L (CD274, binds to PD1/CD279) (Zak et al., 2017), which served as effector domains. As a second approach, we developed antibody-based fusion proteins. The advantage of antibodies is high target affinity, increased serum half-life and the conformational stability. To target α4β7 integrin, we used the sequences of the murine, monoclonal α4β7-targeting antibody (clone DATK32). A schematic overview of the generated fusion proteins / antibody fusion proteins is displayed in **Figure 27**.

To analyze the binding properties of the recombinant fusion proteins, we additionally generated variants of these proteins with an additional *Gaussia princeps* luciferase (GpL) domain enabling easy and highly sensitive quantification of binding affinity.

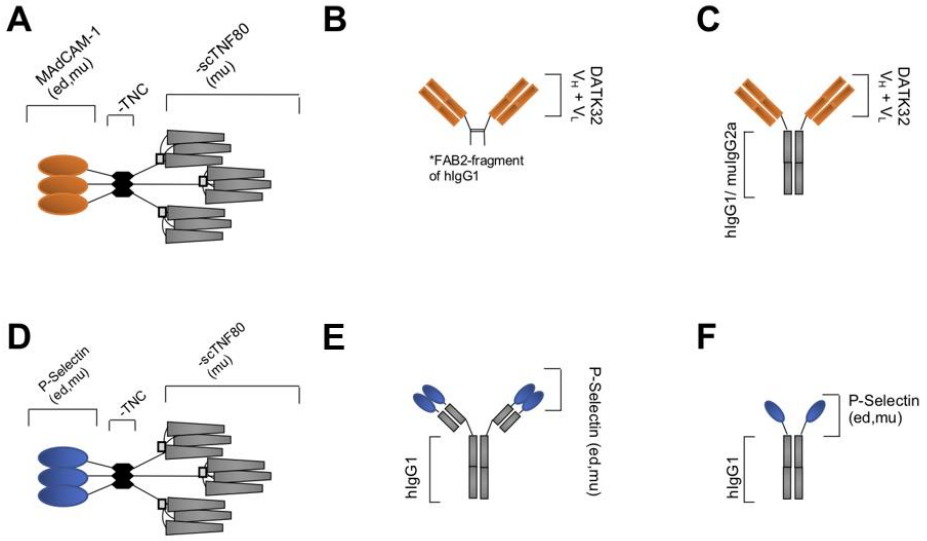

Figure 27: Summary of generated ligand- or antibody-based fusion proteins to selectively target alloreactive T cells.

Schemes of fusion proteins and antibodies which were generated during this work.

A Fusion protein containing a MAdCAM-1 domain to target α4β7 integrin, **B** FAB2 fragment of DATK32 antibody and **C** DATK32 antibody as humanized full-length antibody IgG1 and murine IgG2a. **D** Fusion protein containing the natural selectin receptor P-Selectin specific for P-Selectin Ligand, **E** hIgG1 antibody fusion protein where V_H and V_L were exchanged by P-Selectin ed domain, **F** ed domain of P-Selectin fused to a hIgG1 Fc. All recombinant proteins contain a FLAG-tag for simple protein detection and purification. ed = extracellular domain, mu = murine, h = human, DATK32 = variable domains of the monoclonal antibody DATK32 specific for α4β7, VH = variable heavy, VL = variable light, MAdCAM-1 = Mucosal adressin cell adhesion molecule 1

12.3.1 Production efficiency of recombinant (antibody) fusion proteins

For production of the recombinant (antibody) fusion proteins, HEK293T cells were transfected by polyethyleneimine (PEI) with the respective plasmid(s). The supernatant of the cells was harvested 5-7 days after transfection and proteins were detected by anti-FLAG western blot. The production efficiency was documented in **Table 5** and every transfection was repeated for a minimum of 3 times.

The majority of recombinant (antibody) fusion proteins were produced with a concentration between 2-7 μg/ml. The MAdCAM-1 fusion proteins (except for one) could not be produced at detectable levels.

Plasmid name	Conc. 1 (μg/ml)	Conc. 2 (μg/ml)	Conc. 3 (μg/ml)	Mean (μg/ml)
DATK32-V_H-FAB2-hIgG1 + DATK32-V_L-hIgG1	3,4	3,3	3,5	3,4
DATK32-V_H-hIgG1 + DATK32-V_L-hIgG1	1,5	3,5	2,6	2,5
DATK32-V_H-FAB2-hIgG1 + DATK32-V_L-hIgG1	3,5	3,4	3,4	3,4
DATK32-V_H-FAB2-hIgG1 + DATK32-V_L-hIgG1-GpL(w/o)	2,6	2,5	3,2	2,5
DATK32-V_H-muIgG2a + DATK32-V_L(h)	2,7	1,4	1,6	1,9
MAdCAM-1-F-FasL(h)	-	-	-	-
MAdCAM-1-F-FasL(mu)	-	-	-	-
MAdCAM-1-F-PD1L(mu)	-	-	-	-
MAdCAM-1-F-scTNF80(mu)	-	-	-	-
MAdCAM-1-F-TNC-FasL(h)	-	-	-	-
MAdCAM-1-F-TNC-FasL(mu)	2,5	2,1	1,3	1,9
MAdCAM-1-F-TNC-GpL(w/o)	-	-	-	-
MAdCAM-1-F-TNC-PD1L(mu)	-	-	-	-
MAdCAM-1-F-TNC-scTNF80(mu)	-	-	-	-
MAdCAM-1F-GpL(w/o)	-	-	-	-
P-Selectin-F-FasL(h)	5,1			-
P-Selectin-F-FasL(mu)	2,2	3,4	2,8	2,8
P-Selectin-F-GpL(w/o)	2,3	1,9	2,0	2,1
P-Selectin-F-PD1L(mu)	3,2			
P-Selectin-F-scTNF80(mu)	5,0	5,4	4,5	4,9
P-Selectin-F-TNC-FasL(mu)	4,0	13,0	4,5	7,2
P-Selectin-F-TNC-GpL(w/o)	2,0	1,9	2,1	2,0
P-Selectin-F-TNC-PD1L(mu)	5,0	1,3	2,0	2,8
P-Selectin-F-TNC-scTNF80(mu)	3,0	5,3	2,0	3,4
P-Selectin(ed)-2xF-Fc-GpL(w/o)	7,1	4,9	5,8	5,9
P-Selectin(ed)-V_H-hIgG1 + P-Selectin(ed)-V_L-hIgG1	3,4	2,9	3,1	3,1
P-Selectin(ed)-V_H-hIgG1 + P-Selectin(ed)-V_L-hIgG1-GpL	3,0	3,4	2,9	3,1
PD1L-F-GpL	3,4	3,2	1,9	2,8

Table 5: Production efficiency of (antibody) fusion proteins.
HEK293T cells were transiently transfected with PEI and 12 μg plasmid DNA overnight. Cells were harvested 5-7 days after transfection and protein concentration in the supernatant was determined by anti-FLAG western blot. To determine the protein concentration a FLAG-tagged protein standard was added to the same gel.

12.3.2 Functionality of effector domains

Fusion proteins with the P-Selectin ectodomain as targeting domain did not show specific binding affinity to CD162P/P-Selectin ligand expressing Wehi-3 cells. Nevertheless, we analyzed whether the effector domains of these P-Selectin fusion proteins were functional. To this end, CHX-sensitized HT1080 cells were challenged with the various constructs in the presence and absence of the anti-FLAG antibody M2 and cell viability was determined after 24 hours. The P-Selectin(ed, mu)-FLAG fusion proteins without TNC could not induce cell death in HT1080 cells, whereas the positive control FLAG-FasL(h) was able to induce apoptosis in a concentration dependent manner (**Figure 28**). However, P-Selectin(ed, mu)-FLAG-TNC-FasL(mu) induced apoptosis in HT1080 cells in a concentration dependent manner upon crosslinking with M2. The apoptosis induction efficiency was similar to the positive control FLAG-FasL(h). These results emphasize that the trimerizing TNC-domain in the murine FasL constructs is necessary to stabilize the trimeric state of the soluble murine FasL molecules, which is required for its functionality (Berg et al., 2007).

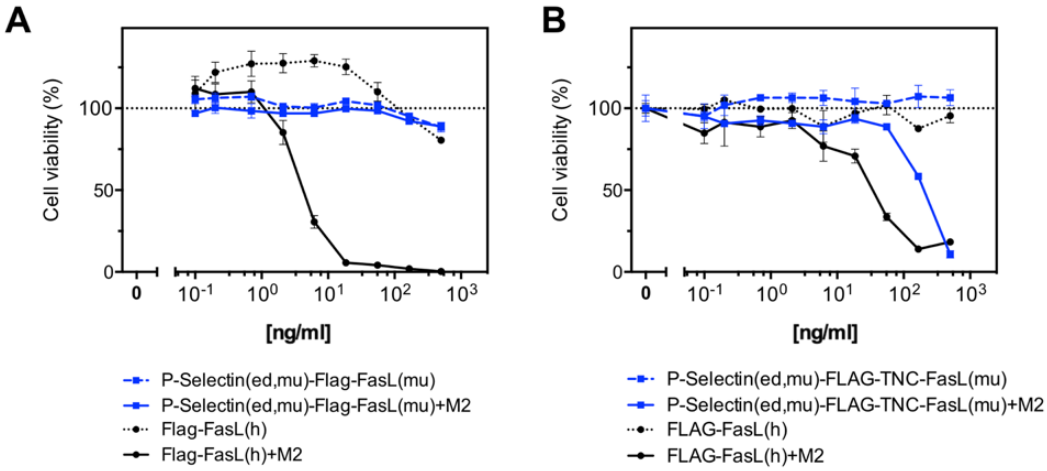

Figure 28: P-Selectin-FasL(mu) fusion proteins require a TNC domain to induce apoptosis. HT1080 (Fas-expressing human cell line) cells were sensitized with CHX and stimulated with P-Selectin-FasL fusion proteins **A** with and **B** without TNC-domain. As positive control for apoptosis induction a FLAG-FasL(h) fusion protein was used. Wells were incubated with and without an M2 antibody, which is required for crosslinking. After stimulation, supernatants were discarded and dead cells were determined by crystal violet staining. Values were represented as mean ± SD (n = 3, technical replicates).

Next, we analyzed if recombinant P-Selectin proteins fused to murine scTNF80-domain were able to signal via TNFR2. We stimulated HT1080-Bcl2 cells, which were stably transfected with TNFR2, with the respective fusion proteins in a concentration dependent manner. HT1080-Bcl2 cells without TNFR2 expression served as negative controls in this assay set up. After 24 hours, supernatants of all conditions were

harvested and IL-6 secretion was determined by ELISA. IL-6 secretion serves as read out for the activation of the NFκB signaling pathway upon TNFR2 stimulation.

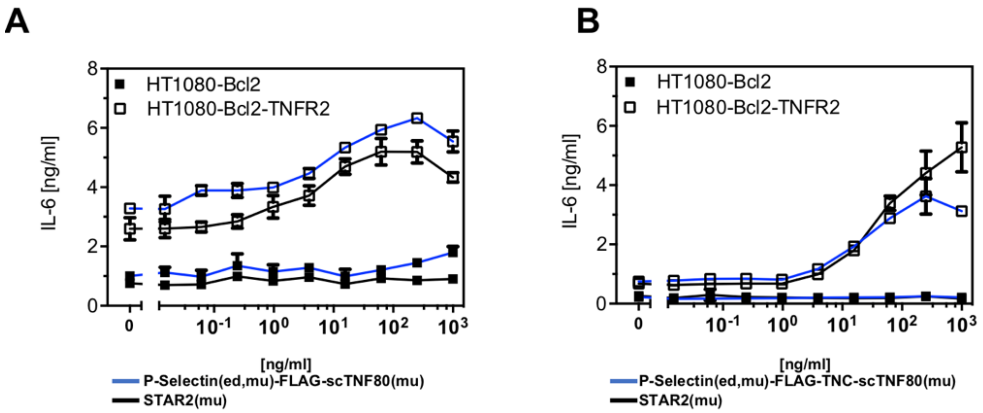

Figure 29: P-Selectin-scTNF80 fusion proteins can activate NFκB pathway.
HT1080-Bcl2 cells (with and without TNFR2 expression) were co-incubated with P-Selectin-scTNF80 fusion protein variants. **A** Representative analysis for TNFR2 stimulation by P-Selectin fused to TNC-scTNF80. **B** Representative analysis for TNFR2 stimulation by P-Selectin fused to scTNF80. A selective agonist of TNFR2 was used (STAR2) as positive control for NFκB activation and IL-6 secretion. Cell supernatants were harvested 24 h after stimulation and analyzed by ELISA for IL-6. Values were represented as mean ± SD (n = 3, technical replicates).

The data showed that P-Selectin(ed, mu)-scTNF80 variants -with and without TNC-domain- induced the same level of IL-6 secretion as the positive control STAR2 (Selective Agonist of TNFR2) (**Figure 29**). In contrast to the murine FasL fusion proteins, where a TNC domain was needed to ensure functionality of the effector domain, the murine scTNF80 domain could induce signaling without the TNC domain. As described earlier, most of the ligand-based fusion proteins could not be produced at all or only in very low concentration. Furthermore, tested P-Selectin(mu, ed) fusion proteins did not show any binding to CD162P/PSelectin ligand expressing Wehi-3 cells. Therefore, antibody-based fusion proteins were developed for further studies.

12.3.3 Binding study of antibody-based fusion proteins

Binding affinity of the antibody-based fusion proteins were studied by help of recombinant variants, which were genetically fused with a *Gaussia princeps* luciferase domain (Kums et al., 2017). Every binding study was performed for minimum of three times and one representative experiment is displayed in **Figure 30** and **Figure 31**. We observed that all tested antibody-based fusion proteins showed high binding affinity to their target. Furthermore, we observed differential binding affinities based on the format of the antibody structure.

For P-Lig targeting antibody fusion proteins the binding affinity of a full-length antibody was higher compared to the Fc-fusion protein (KD 16 nM vs. 61 nM), which might be explained by the increased number of targeting domains (4 vs. 2) as depicted in **Figure 30**.

The highest binding affinity of the α4β7-targeting antibody formats were observed with the full length hIgG1 (KD 4 nM), which was followed by the FAB2-fragment (KD 10 nM). The muIgG2a isotype showed the lowest affinity in this comparison (KD 29 nM).

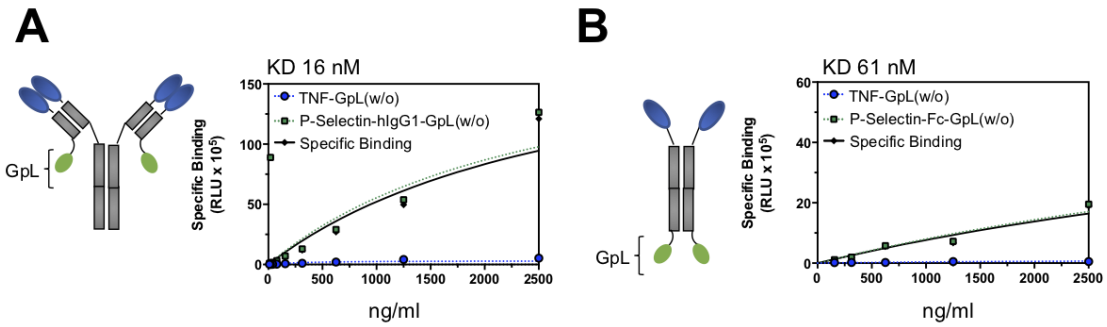

Figure 30: P-Selectin antibody-based fusion proteins show specific binding to P-Lig⁺ cells.
A P-Selectin-hIgG1 (V_H & V_L) full length antibody variant and **B** extracellular P-Selectin domain fused to human IgG1-Fc part were analyzed for their specific binding affinities. Both fusion antibody plasmids encoded the *Gaussia princeps* luciferase (GpL) enabling cellular binding studies. The fusion antibodies were co-incubated for 30 min with P-Lig expressing Wehi-3 cells. Cells were washed 10 times with ice cold PBS to remove unbound antibodies. Background binding was determined by using unspecific GpL-fusion protein (TNF-GpL). Specific binding was determined by subtracting unspecific signals (RLU) from the specific signals obtained from the respective P-Selectin-GpL variants. Figures show one representative experiment. Binding studies were repeated more than 3 times.

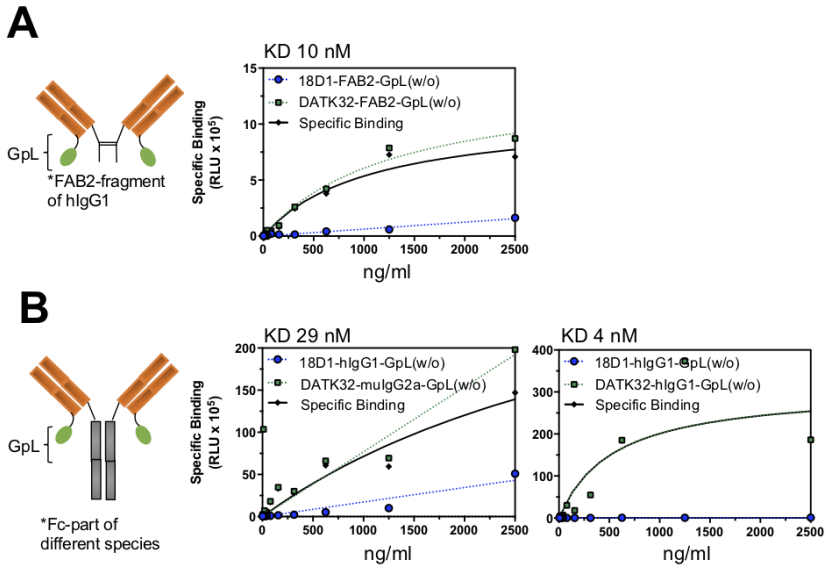

Figure 31: DATK32 antibody-based fusion proteins show specific binding to α4β7⁺ cells.
A DATK32 (V_H & V_L) FAB2 antibody and **B** DATK32 (V_H & V_L) full length antibody (muIgG2a / hIgG1) were analyzed for their specific binding affinities. All fusion antibody plasmids encoded the *Gaussia princeps* luciferase (GpL) enabling cellular binding studies. The fusion antibodies were co-incubated for 30 min with TK1 cells, which expressed α4β7⁺ integrin. Cells were washed 10 times with ice cold PBS to remove unbound antibodies. Background binding was determined by using an unspecific GpL-fusion antibody of the same antibody format as the corresponding DATK32 antibodies. Specific binding was determined by subtracting unspecific signals (RLU) from the specific signals obtained with DATK32-GpL variants. Figures show one representative experiment. Binding studies were repeated more than 3 times.

12.4 Part IV: Modulation of alloreactive T cells via NFATc1 SUMOylation

Calcineurin inhibitors like Cyclosporin A (Cs A) and Tacrolimus are used for HCT patients to control alloreactive reactions after transplantation. Calcineurin is an important phosphatase downstream of the TCR signaling complex and its inhibition leads to decreased T cell activation. One major target of calcineurin are NFAT transcription factors, which are indirectly inhibited by calcineurin inhibitors as well. It is well known that calcineurin inhibitors are highly immunosuppressive and interfere with the desirable GvL effect mediated by donor T cells. Here, we asked if a selective modulation of alloreactive T cells can be achieved by targeting specific NFAT family members.

12.4.1 NFATc1/ΔS T cell recipients show reduced aGvHD symptoms

To study the effects of averted NFATc1 SUMOylation in alloreactive T cells, we used a MHC major mismatch mouse model (**Figure 7**). We irradiated BALB/c recipients with 8 Gy and reconstituted with 1.2 x 10^6 T cells derived from WT or NFATc1/ΔS donors together with 5 x 10^6 BM cells. Mice which received NFATc1/ΔS T cells showed better survival after allo-HCT compared to WT T cell recipients (**Figure 32**). During the first week after transplantation all mice lost around 20-25 % of weight. Both, WT and NFATc1/ΔS recipients recovered between d10-d14. Nevertheless, all WT mice succumbed to severe GvHD symptoms around d20. In contrast, 50 % of NFATc1/ΔS recipients survived until d30 after allo-HCT although never reaching 100 % of their body weight again. The BM group recovered quickly after 1 week and regained 100 % of their body weight and IR controls died from myeloablative irradiation around d10 confirming that 8 Gy TBI was lethal (**Figure 32**).

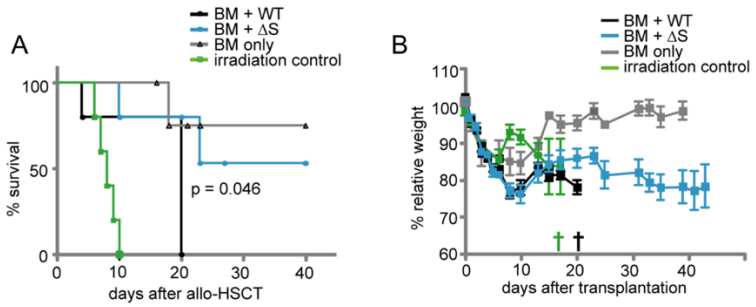

Figure 32: GvHD survival and weight loss of WT and NFATc1/ΔS T cell recipients.
BALB/c (MHC major mismatch) recipient mice were irradiated with 8 Gy and injected i.v. with 1.2 x 10^6 / 3 x 10^5 enriched T cells (from WT or NFATc1/ΔS donors) together with 5 x1 0^6 BM cells from the same B6 species. As experimental control, some BALB/c mice only received 5 x 10^6 BM cells derived from B6 donors (BM). Additional BALB/c mice were only irradiated and not reconstituted with BM (IR). **A** show the percentage survival of individual groups and **B** represents the weight loss relative to d0.

12.4.2 NFATc1/ΔS T cells show reduced proliferation and target organ infiltration

During the first week after allo-HCT we monitored T cell proliferation by *in vivo* bioluminescence imaging as seen in **Figure 33**. T cells of NFATc1/ΔS donors showed less *in vivo* proliferation and migratory behavior compared to WT T cell recipients. By quantifying the emitted photons/sec, we observed less alloreactive T cell proliferation, which was significantly lower on d4 and d5 in NFATc1/ΔS T cell recipients.

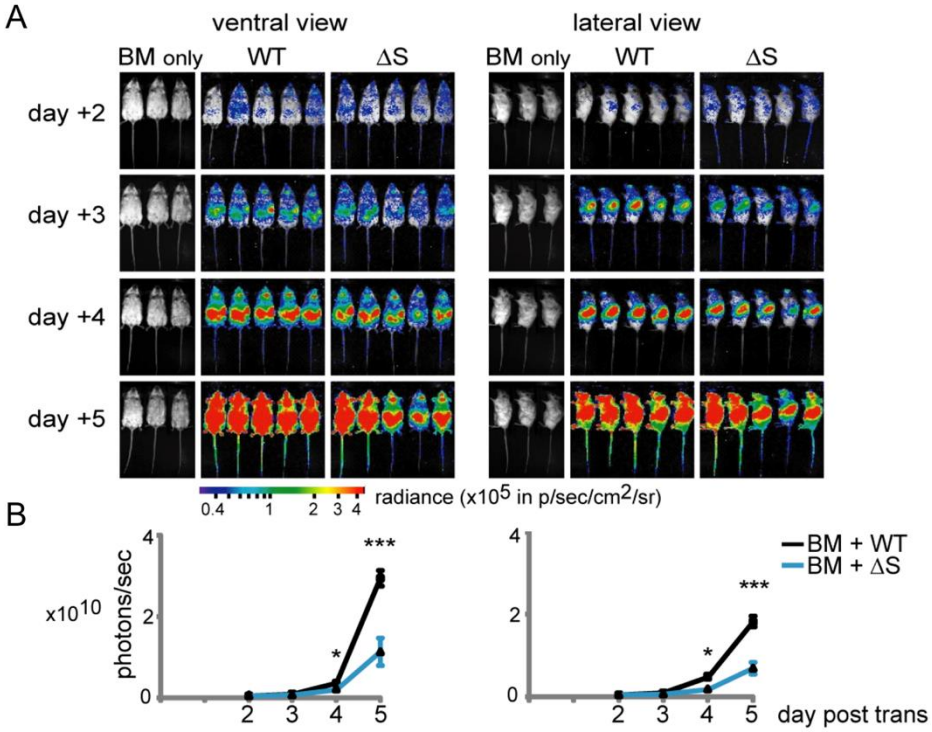

Figure 33: NFATc1/ΔS T cell show reduced in vivo proliferation after allo-HCT.
BALB/c recipients were irradiated with 8 Gy and transplanted with 1.2 x 10^6 T cells from WT or NFATc1/ΔS donors together with 5 x 10^6 BM cells. **A** Representative images of allo-HCT recipients as ventral and lateral view. All transplanted CD90.1 donor T cells expressed the enzyme luciferase. Signals were measured 10 min after i.p. injection of D-Luciferin. **B** for quantitative analysis the emitted photons per second were analyzed. Values displayed as mean ± SD. n = 8 per group and time point, statistical significance was determined by unpaired t-test (*, $P \leq 0.05$; **, $P \leq 0.01$; ***, $P \leq 0.001$).

To provide more detailed information about target infiltration and migratory behavior of alloreactive T cells, we harvested organs on d6 after allo-HCT for *ex vivo* bioluminescence imaging. After quantifying the emitted photons/sec we observed that especially the infiltration of the GI tract was significantly reduced in mice, which received NFATc1/ΔS T cells compared to WT T cell recipients. Furthermore, isolated $CD4^+$ T cells on d6 after allo-HCT showed reduced expression of the gut homing molecule $\alpha4\beta7$ integrin, which could be a reason for the reduced intestinal infiltration (**Figure 34**).

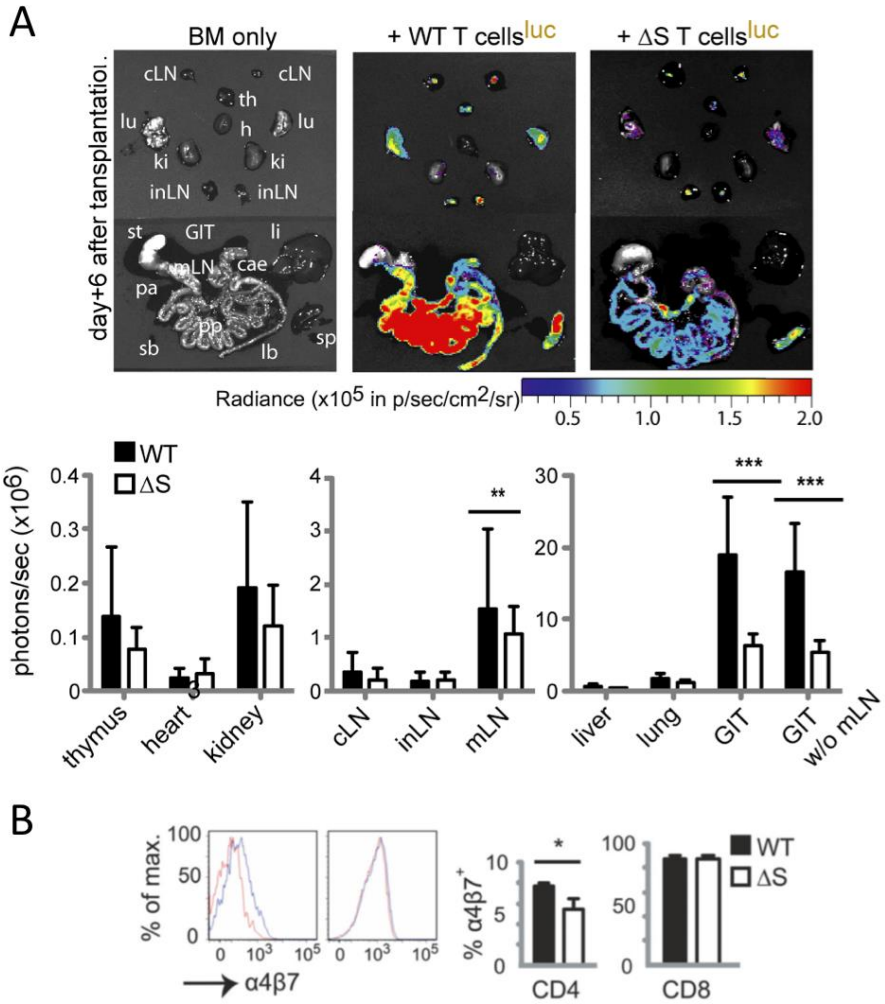

Figure 34: Less target organ infiltration in NFATc1/ΔS T cell recipients.
A To resolve T cell distribution in particular organs mice were sacrificed 10 min after i.p. injection of D-Luciferin and organs were imaged within 3-5 min *ex vivo*. For quantitative analysis, emitted photons/sec were calculated. **B** Frequency of $\alpha4\beta7^+$ donor T cells in the spleen were determined by FACS analysis. Values displayed as mean ± SD. n = 8 per group, statistical significance was determined by unpaired t-test (*, $P \leq 0.05$; **, $P \leq 0.01$; ***, $P \leq 0.001$).

12.4.3 Higher Treg frequencies in NFATc1/ΔS T cell recipients

Further analysis was performed to detect the frequencies of - presumably protective - Tregs in both WT and NFATc1/ΔS T cell recipients. We compared Tcon and Treg frequencies on d6 after allo-HCT to get more insights into the cellular mechanism of reduced alloreactivity of NFATc1/ΔS T cells. $CD4^+$ and $CD8^+$ ratios were similar between WT and NFATc1/ΔS T cell recipients. However, Treg frequencies differed between both recipient groups. We pregated cells for $CD90.1^+CD4^+$ and analyzed the frequency of $CD25^+Foxp3^+$ cells. We found higher Treg frequencies in both mLN (WT 1.8 ±0.5 % vs. NFATc1/ΔS 3.8 ± 1.1 %) and spleen (WT 2.3 ± 1.1 % vs. NFATc1/ΔS 5.9 ± 2.0 %) of NFATc1/ΔS T cell recipients (**Figure 35**).

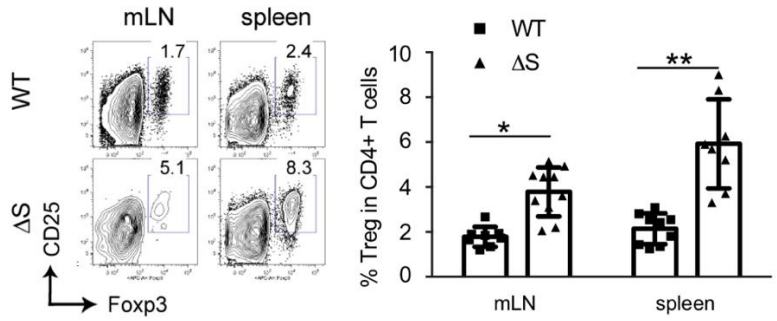

Figure 35: NFATc1/ΔS T cell recipients show higher Treg frequencies on d6 after allo-HCT. Spleen and mLN were isolated on d6 after allo-HCT and cell suspensions prepared for FACS staining. To determine the frequency of donor Tregs, cells were stained for surface CD25 and intracellular Foxp3 expression. Donor $CD4^+$ T cells were gated for $CD25^+Foxp3^+$ to determine Treg frequencies. Values displayed as mean ± SD. n = 8 per group, statistical significance was determined by unpaired t-test (*, $P \leq 0.05$; **, $P \leq 0.01$; ***, $P \leq 0.001$).

To get more insights in early changes of $CD4^+$ T cells, we isolated $CD4^+$ of both WT and NFATc1/ΔS T cell recipients on d4 after allo-HCT from the spleen and performed RNAseq assay. We selected d4 for RNASeq analysis, since on this time point most of donor T cells were still located in the SLOs. Thus, d4 was a suitable time point to analyze early transcriptional changes before aGvHD manifestation.

12.4.4 NFATc1/ΔS T cells show reduced effector phenotype

Living $CD90.1^+CD4^+$ T cells of both WT and NFATc1/ΔS T cell recipients were enriched by flow cytometry and directly collected into RNA lysis buffer. The transcriptional changes on this early time point were moderate, however our screening revealed lower RNA levels of inflammatory cytokines (TNF-α and IFN-γ) in NFATc1/ΔS T cell recipients. This was also reflected in the serum of these mice on d5 and d6 during the cytokine storm after allo-HCT (**Figure 36 B)**. RNA levels of pro-survival factors Bcl2A1 were increased in NFATc1/ΔS T cells, suggesting a overall better survival of NFATc1/ΔS T cells. To confirm the reduced inflammatory signature of the $CD4^+$ cells we analyzed the cells for intracellular cytokine levels on d6 after allo-HCT (**Figure 36**). We found a significant decrease of intracellular TNF-α and IFN-γ levels in *ex vivo* restimulated $CD4^+$ T cells from NFATc1/ΔS T cell recipients compared to WT controls. Whereas, no differences in $CD4^+IL\text{-}2^+$ frequencies could be detected between both groups. Furthermore, levels of anti-inflammatory IL-10 cytokine did not differ between WT and NFATc1/ΔS recipients (**Figure 36 B**).

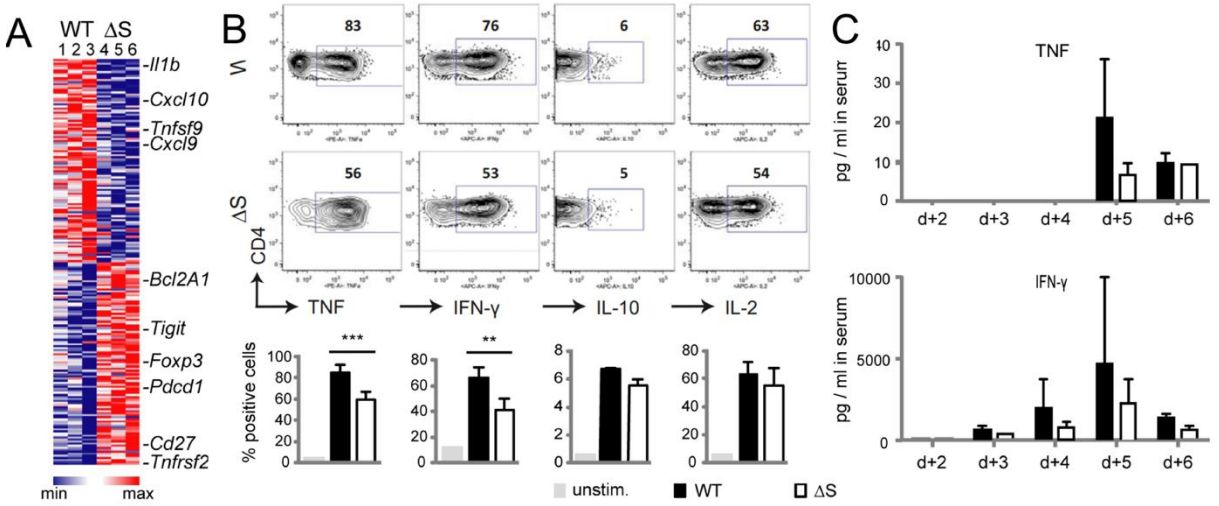

Figure 36: CD4⁺ of NFATc1/ΔS T cells display a reduced inflammatory signature.
A CD4⁺ from spleen of WT and NFATc1/ΔS recipients were FACS sorted (purity of living CD90.1⁺CD4⁺ lied around 95-98%) and RNAseq assay was performed (n = 3 per group). **B** Isolated CD4⁺ cells were re-stimulated *in vitro* with TPA/Ionomycin for 5 h and analyzed for intracellular cytokine levels by FACS. **C** Serum of WT and NFATc1/ΔS T cell recipients was collected during aGvHD progression and analyzed for cytokine levels. Values were displayed as mean ± SD. n = 5-8 per group and statistical significance was determined by unpaired t-test (*, $P \leq 0.05$; **, $P \leq 0.01$; ***, $P \leq 0.001$).

To summarize, this part has shown decreased effector function and alloreactivity in CD4⁺ T cells of NFATc1/ΔS T cell recipients compared to WT controls, which could be an explanation for the reduced aGvHD score and better survival of NFATc1/ΔS T cell recipients.

12.4.5 Protective effect of reduced alloreactivity lies within NFATc1/ΔS Tcons which support Tregs

To analyze if Tregs or Tcons mediate the protective effect during the course of aGvHD, we used WT or NFATc1/ΔS donor mice, which were crossed with C57BL/6-Tg(Foxp3-DTR/EGFP). The depletion of Foxp3-expressing cells in these mice were achieved by treatment with Diphtheria Toxin (DTx). Therefore, transplanted splenic donor T cells of these mice contained no Tregs and allowed to study if WT and NFATc1/ΔS Tcons have the same potential to induce pTregs. For this purpose, we transplanted 1.2×10^6 enriched Tcons (both CD4⁺ and CD8⁺, depleted of Foxp3⁺-expressing cells) into irradiated BALB/c recipients (MHC major mismatch). As observed previously, Tcons of NFATc1/ΔS origin showed significantly reduced proliferation and target organ infiltration (**Figure 37**).

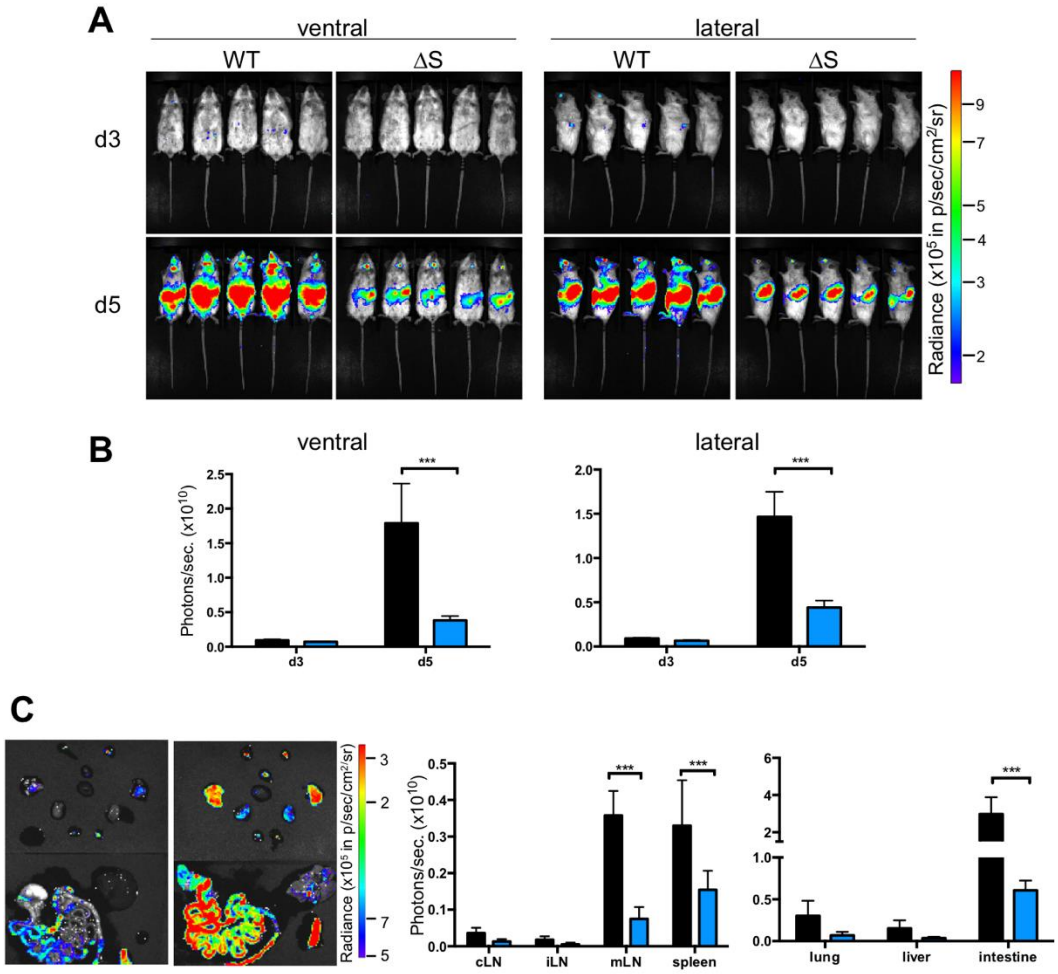

Figure 37: NFATc1/ΔS Tcon show reduced proliferation *in vivo.*
A, B WT and NFATc1/ΔS Tcon donors were treated with DTx two days before transplantation to deplete DEREG expressing Tregs. 1.2 x 10^6 T cons together with 5 x 10^6 BM cells were i.v. injected into irradiated BALB/c recipients and Tcon proliferation was measured on several days after allo-HCT. **C** Mice were sacrificed 10 min after i.p. injection of D-Luciferin and organs were imaged within 3-5 min after isolation for *ex vivo* bioluminescence. For quantitative analysis, emitted photons/sec were determined and values were displayed as mean ± SD. n = 5 per group, statistical significance was determined by unpaired t-test (*, $P \leq 0.05$; **, $P \leq 0.01$; ***, $P \leq 0.001$).

Cells of DEREG donor mice expressed GFP under the control of the regulatory elements of Foxp3, which enabled the quantification of GFP^+ pTregs in this experimental setting. Six days after allo-HCT with Treg-depleted Tcons only 0.32 ± 0.05 % of $CD4^+Foxp3\text{-}Gfp^+$ T cells in WT and 0.63 ± 0.12 % in NFATc1/ΔS recipients were detectable in the spleen. Thus, the potential of Tcons to differentiate into pTregs under these inflammatory conditions, was very low in both groups, although intracellular IL-2 levels were clearly detectable and with 21.5 ± 3.3 % (compared to 14.0 ± 3.8 % in WT) higher in NFATc1/ΔS Tcon.

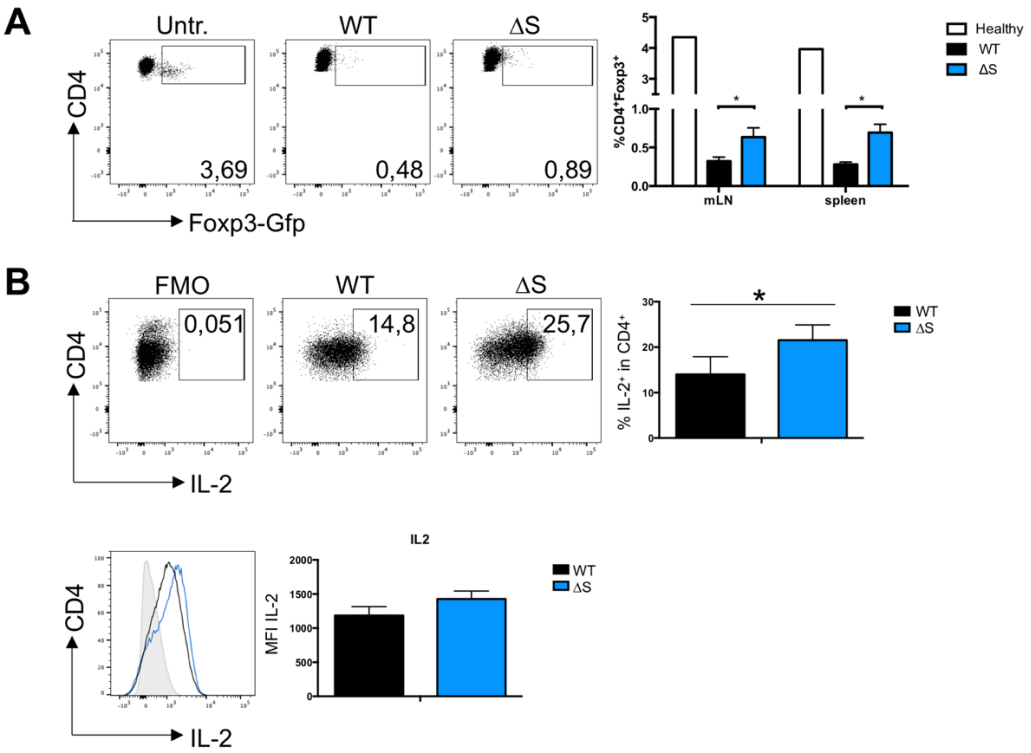

Figure 38: IL-2 and peripheral Treg induction in Tcon recipients.
A CD4⁺ cells were isolated from spleen and mLN and analyzed for Foxp3-GFP expression. **B** CD4⁺ cells were *ex vivo* stimulated with TPA/Ionomycin for 5 h and analyzed for intracellular IL-2 levels. Values were displayed as mean ± SD. n = 5 per WT/ ΔS group; n = 1 healthy DEREG, statistical significance was determined by unpaired t-test (*, $P \leq 0.05$; **, $P \leq 0.01$; ***, $P \leq 0.001$).

A surplus in IL-2 does not only support conversion into pTregs but ensures survival and proliferation of tTregs. Consequently, we evaluated if the less severe induction of aGvHD by NFATc1/ΔS T cells can attribute to Tcon and/ or Tregs. To distinguish between the effect of either one, we transferred WT vs. NFATc1/ΔS Tcons together with WT or NFATc1/ΔS Tregs into irradiated BALB/c mice. Of note, in this particular experimental setting only Tcons were expressing the enzyme luciferase, whereas Tregs were not detectable by bioluminescence (**Figure 39**).

According to the absolute emitted photons/sec, mice which received WT Tcons together with NFATc1/ΔS Tregs, demonstrated reduced bioluminescence signals compared to mice, which received both T cell types from WT mice (especially in the *ex vivo* analysis on d6). When additionally comparing WT Tcon with NFATc1/ΔS Tcon it was obvious that NFATc1/ΔS Tcons proliferated less *in vivo*, no matter if WT or NFATc1/ΔS Tregs were present (**Figure 39**). *Ex vivo* imaging revealed reduced organ infiltration in all mice, which received NFATc1/ΔS Tcons, indicating that the Tcons of NFATc1/ΔS donors might be more important for the protective effect during aGvHD. Nevertheless, underscoring the impact of the intrinsic positive effect of the avoidance

of NFATc1 SUMOylation in Tregs themselves, the lowest bioluminescence signals on d6 were observed in mice that had received Tcons as well as Tregs from NFATc1/ΔS donors.

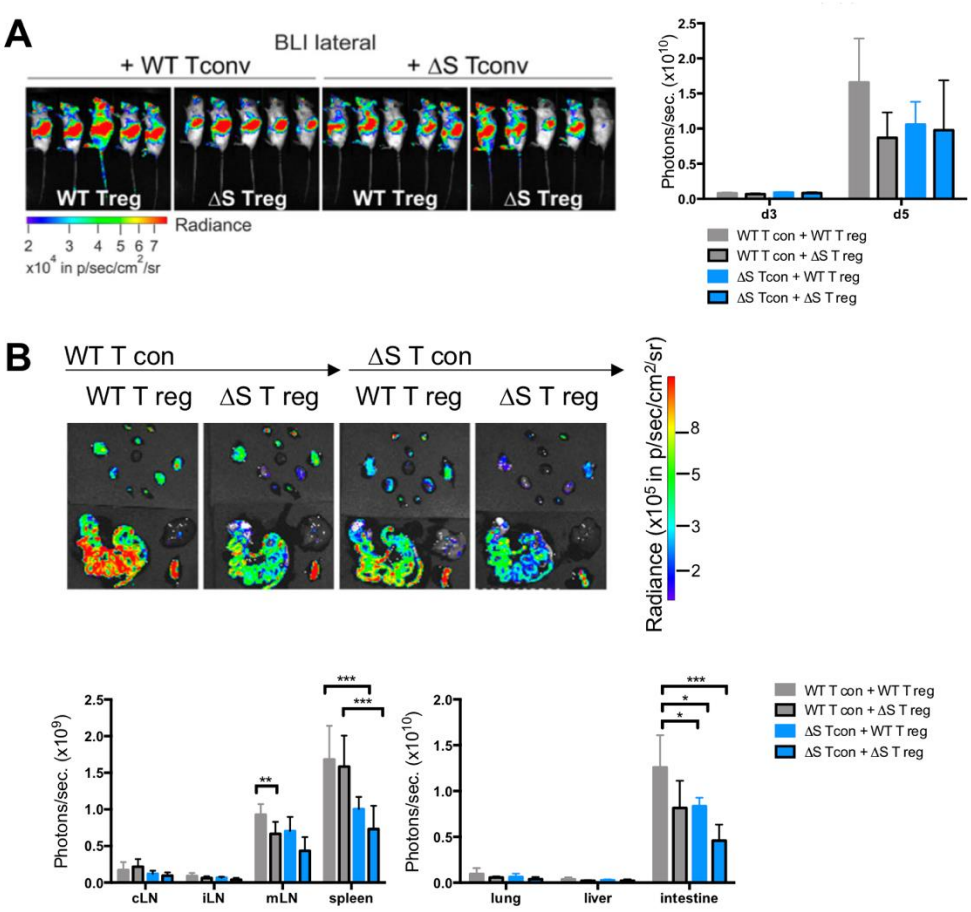

Figure 39: Suppressive capacity of WT vs. NFAT/ΔS Tregs during aGvHD.
WT and NFATc1/ΔS Tcon donors were treated with DTx two days before transplantation to deplete DEREG expressing Tregs. 1.2 x 10^6 Tcons (Treg-depleted) were co-transplanted with 0.6 x 10^6 Tregs of the respective donor. All recipients additionally received 5 x 10^6 BM cells of allogeneic donors. **A** Analysis of *in vivo* proliferation on d3 and d5 **B** *Ex vivo* analysis of target organ infiltration on d6 after allo-HCT. Values displayed as mean ± SD. n = 5 per group, statistical significance was determined by unpaired t-test (*, $P \leq 0.05$; **, $P \leq 0.01$; ***, $P \leq 0.001$).

To determine Treg frequencies in this experimental set up, we isolated splenocytes on d6 and analyzed the $CD4^+$ population by FACS for the frequency of $CD25^+Foxp3^+$ Tregs. As seen in **Figure 40**, highest frequency of Tregs was found in mice, which received NFATc1/ΔS Tcons and Tregs (7.7 ± 3.7 % in spleen). On the contrary, the lowest frequency was found in mice which received Tcons and Tregs from WT donors (1.9 ± 0.7 % in spleen). Interestingly, only in the presence of NFATc1/ΔS Tregs the frequencies of IL-2^+ $CD4^+$ NFAT ΔS Tcons were significantly increased compared to WT Tcon (**Figure 40**).

Furthermore, the IL-2 frequencies were increased significantly in NFATc1/ΔS Tcon and Treg recipients (10.1 ± 2.4 % vs. 2.3 ± 0.1 % in WT Tcon + WT Treg).

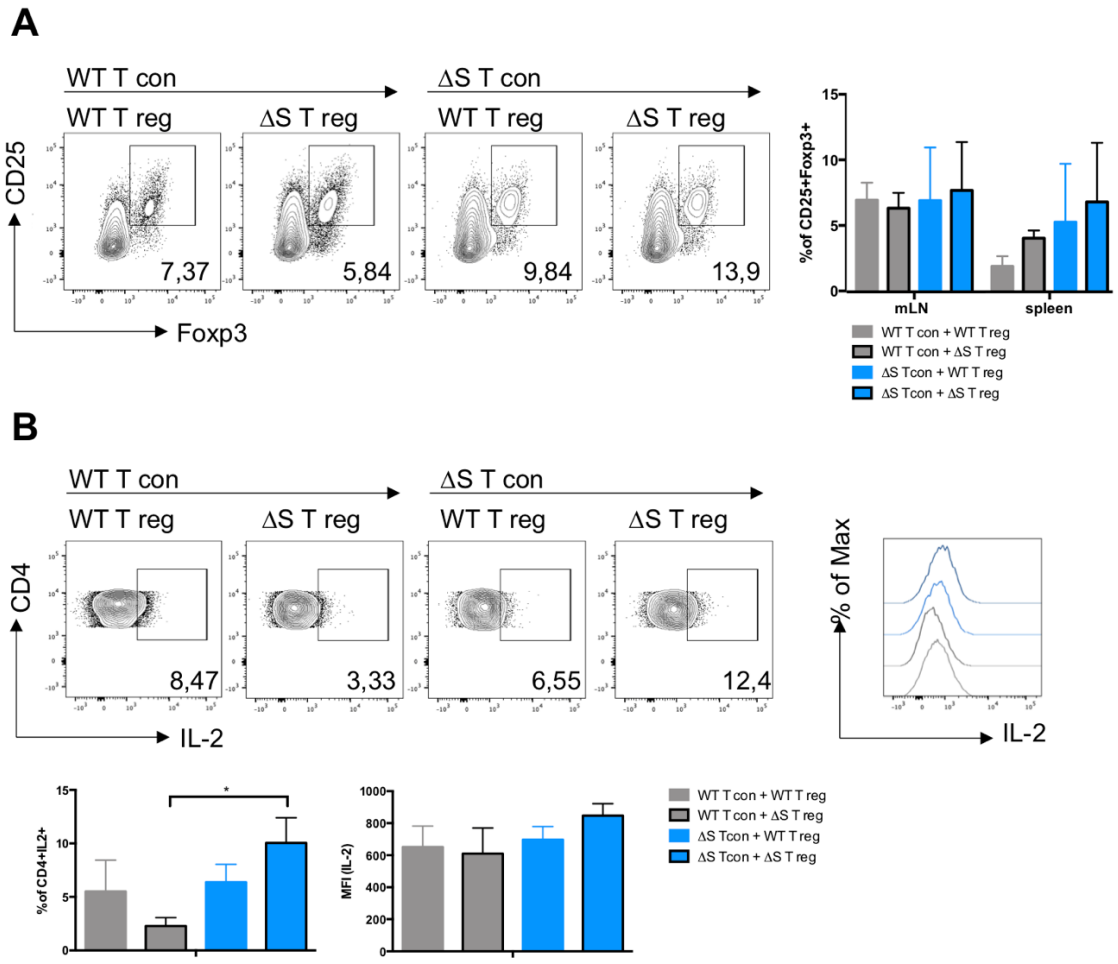

Figure 40: Treg and IL-2 frequencies increase in presence of NFATc1/ΔS Tcon.
A $CD4^+$ cells were isolated from spleen and mLN and analyzed for intracellular Foxp3 levels. Representative FACS plots of mLN showing percentage of $CD25^+Foxp3^+$ cells. **B** $CD4^+$ cells were *ex vivo* stimulated with TPA/Ionomycin for 5 h and analyzed for intracellular IL-2 levels. Values displayed as mean ± SD. n = 5 per group, statistical significance was determined by unpaired t-test (*, $P \leq 0.05$; **, $P \leq 0.01$; ***, $P \leq 0.001$).

To sum up, we have shown here that averted NFATc1 SUMOylation can reduce the pathogenicity of alloreactive T cells, which was confirmed by reduced *in vivo* and *ex vivo* proliferation of donor T cells. Furthermore, effector function of NFATc1/ΔS Tcons was significantly reduced compared to WT T cells on d6 after allo-HCT. The protective effect lies most probably within the Tcon population, although Tregs appeared to suppress better, when NFATc1 SUMOylation was prevented intrinsically in Tregs.

13 Discussion

Allogeneic hematopoietic cell transplantation (allo-HCT) is a curative treatment for many malignant and non-malignant hematological diseases. Number of HCTs performed worldwide are constantly increasing and allo-HCT still remains one of the most effective anti-tumor therapies (Gratwohl et al., 2015). Although, Graft-versus-Leukemia (GvL) effects are highly beneficial, the success of this therapy is limited due to a highly inflammatory reaction, which is named acute Graft-versus-Host Disease (aGvHD). This complication is caused by hyperactivated T cells, which induce massive tissue damage and inflammation in aGvHD target organs skin, liver and intestine. This work focused on several aspects of aGvHD pathophysiology and especially on alloreactive T cells.

13.1 Part I: Development of a predictive marker panel for aGvHD

In this study, we present a combinatorial panel of $\alpha4\beta7$ integrin, CD162E, CD162P and CD62L as predictive markers to unequivocally identify alloreactive $CD8^+$ T cells in the PB of murine allo-HCT recipients. Benefiting from insights into donor T cell migration kinetics in the PB early after HCT (Bäuerlein et al., 2013), we analyzed the dynamic changes of surface markers on donor $CD8^+$ T cells after miHAg mismatch allo-HCT. Combination of these markers proved superior to single markers at early time points after allo-HCT allowing a reliable prediction for early time points. In preparation for a prospective clinical study we hypothesized whether the measurement of several homing markers together would enhance the predictive value of our proposed blood test. Examining if the combination of chemokine receptors, homing and activation markers could give more defined insights into T cell homing to specific aGvHD target tissues we confirmed in two independent miHAg allo-HCT models that the expression of $\alpha4\beta7$ integrin, CD162E, CD62P and lack of CD62L on PB $CD8^+$ T cells preceded the onset of aGvHD. Conversely, we could exclude an extended panel of surface receptors (several chemokine receptors, CD69 and CD25) as these did not turn out as reliable predictors.

Our analysis in two independent murine models of aGvHD, confirmed previous studies in mice showing that alloreactive $CD8^+$ donor T cells highly up-regulate α4β7 integrin at early time points after HCT (Beilhack et al., 2008; Petrovic et al., 2004; Waldman et al., 2006). In patients, upregulation of α4β7 integrin on conventional T cells or reduction

of α4β7$^+$ Tregs correlated with intestinal aGvHD manifestation. Accordingly, α4β7 integrin also proved as a relevant therapeutic target for the treatment of intestinal inflammation. Vedolizumab, a monoclonal antibody against α4β7, is approved for ulcerative colitis and under current investigation for the prophylactic treatment of aGvHD (NCT03657160, ClinicalTrials.gov). Furthermore, the frequency of α4β7$^+$ T cells in the PB of colitis ulcerosa patients before Vedolizumab treatment could predict treatment outcome (Fuchs et al., 2017). Therefore, α4β7 integrin appears not only as an attractive diagnostic and prognostic biomarker for intestinal aGvHD but may also be predictive for treatment outcomes.

In both murine miHAg allo-HCT models, allogeneic PB CD8$^+$ T cells upregulated the skin homing receptors CD162E and CD162P. Both mouse surface molecules, or the corresponding human skin homing receptor CLA, respectively, are strongly associated with aGvHD initiation (Ali et al., 2012; Asaduzzaman et al., 2009), even if redundancy with other homing pathways have been observed (Eom et al., 2005). Patients suffering from aGvHD showed higher levels of circulating CLA$^+$ T cells compared to patients who did not develop aGvHD (Khandelwal et al., 2017).

The lymphoid homing receptor CD62L is expressed on naïve, central memory T cells but also T cells with a stem-cell like memory phenotype (Gattinoni et al., 2012). Enhanced mobilization of CD8$^+$CD44^{hi}CD62L^{low} effector T cells paralleled with decreased circulating CD62L$^+$ naïve T cell numbers appeared as strong indicator days and even weeks before aGvHD onset.

In our unbiased clustering analysis, α4β7 integrin alone could not robustly separate allogeneic from syngeneic recipients on d6 after allo-HCT – two weeks before clinical aGvHD onset, whereas the combination of surface marker detection deemed highly reliable (α4β7, CD162E/CD162P (CLA) and CD62L). Based on these results, we postulate that this combined four marker panel may prove valuable for an early prediction of aGvHD.

First and foremost, the obtained results are based on HCT mouse models with several shortcomings when compared to allo-HCT in human patients (Zeiser et al., 2016). First, both miHAg allo-HCT mouse models and syngeneic controls relied on a myeloablative irradiation only-based conditioning regimen, whereas in patients a variety of conditioning protocols are used. Second, genetic uniformity of donors and recipients utilizing inbred mouse strains were in contrast to the enormous genetic heterogeneity in patients who also vary in their clinical history, age, underlying diseases and previous

medications. Third, mice were housed in homogenous specific pathogen-free microbial conditions. Fourth, mice did not receive any immunosuppressive GvHD prophylaxis, e.g. it has been reported that steroids can have an impact on expression levels of homing receptors (Bouazzaoui et al., 2011). Fifth, only µl of blood samples could be obtained from mice resulting in very low acquired cell numbers. Especially at the earliest time point after HCT, detection of a few hundred cells with flow cytometry was clearly at the limit of detection. Sixth, due to the highly controlled experimental settings, time to the onset of clinically apparent aGvHD could be standardized in the mouse models, which is not the case and highly individual in patients and can vary from days to several months after allo-HCT. Seventh, by design of our study, allo-HCT recipients did not suffer from malignant diseases or succumbed to infections. Biomarkers for the beneficial Graft-versus-Leukemia effect and the efficient combat of opportunistic infections still need to be defined. However, all these limitations make clear that the advantage of the reductionist approach employing miHAg GvHD mouse models had the advantage to evaluate the reproducibility of candidate biomarkers. By utilizing one miHAg allo-HCT model for a discovery set of biomarkers and the second miHAg allo-HCT model for validation helped to identify a basket of biomarkers while ruling out a range of preconceived candidates that now await to be rigorously tested in patients.

In contrast to the analyzed integrin and selectin family members, none of the tested CC-chemokine receptors could give more insights into T cell homing to different tissues or GvHD onset. This may be partially explained by their dynamic regulation, vulnerability to loss of expression and artifacts upon *ex vivo* cell manipulation and redundant expression of CCRs (Munoz et al., 2012). Yet, inflammation after conditioning appears to trigger CCR and endothelial ligand expression (Chakraverty et al., 2006; Eyrich et al., 2005), consistent with our observed CCR up-regulation in both allogeneic and syngeneic recipients. Of note, over time CCR expression decreased, suggesting that host conditioning upregulated CCRs on CD8 T cells independent of the allogeneic or syngeneic setting. Nevertheless, CCRs still hold the potential as therapeutic targets. Reshef et al. reported the beneficial effects of CCR5 blockade, which resulted in reduced aGvHD in phase I/II clinical trials (Reshef et al., 2012, 2019). These effects were consistent with previously published results in murine models (Murai et al., 1999, 2003).

Unbiased clustering analysis revealed a four $CD8^+$ T cell surface marker panel (α4β7, CD162E/CD162P (CLA)) T cells in two independent miHAg allo-HCT models. This

suggests that flow cytometric analysis of PB T cells in patients undergoing allo-HCT could predict aGvHD before patients become symptomatic. Based on these results, we recommend to prospectively test the combination of the aforementioned surface molecules in allo-HCT patients at early time points. Cytotoxic $CD8^+$ effector T cells are key players in aGvHD pathophysiology. Thus, it appears attractive to design GvHD prophylaxis protocols based on the detection of circulating alloreactive T cells, even before they can exert their tissue destructive force. As time to onset of GvHD markedly varies between patients, it will be important to design a prospective clinical trial based on a calendar-driven collection to standardize data acquisition plus an event-driven sample collection. Second, as efficient homing of immune effector cells is a prerequisite to combat infections and to exert the desired GvL effect, a vigorous prospective study will require a relatively large sample size and meticulous clinical and laboratory documentation to discern aGvHD causing alloimmune responses from these scenarios. Furthermore, it will be interesting to compare and cross-validate the proposed 4 surface flow cytometric biomarker panel with currently investigated serum and urine biomarkers.

Finally, we propose that the identified four T cell surface marker panel may be suited to isolate circulating $CD8^+$ T cells from the PB of patients undergoing allo-HCT for more refined single-cell RNAseq and proteomic analysis. This may provide a reasonable strategy for deeper analysis and discovery of new biomarkers and targets for treatment interventions.

13.2 Part II: Expression kinetics of immunomodulatory surface molecules during aGvHD

The tumor necrosis factor superfamily (TNFR SF) is a family of proteins expressed on the surface of many cells and is involved in the regulation of cell proliferation, survival, differentiation and apoptosis (Aggarwal, 2003). The family members can be ligands as well as receptors and can act either as agonists or antagonists. Both, ligands and receptors are expressed on a variety of immune cells like B cells, T cells, NK cells, monocytes and DCs. Ligand binding to the receptors can induce apoptosis (TNFR1 or CD95L) or proliferation (such as CD27, CD40, OX40, 4-1BB). Recent research has demonstrated that TNFR SF members control the immune response on multiple levels (Wajant, 2013, 2016). Of particular importance for this work is the expression of TNFR SF members on Tcons and Tregs and we asked whether the expression levels are

spatio-temporally regulated during the progression of aGvHD and evaluated if these receptors might have a potential as therapeutic drug targets to selectively modulate subsets of T cells.

Tumor necrosis factor (TNF) is secreted by a variety of cells and mediates cellular responses via TNR1 and TNFR2 (Papadakis et al., 2000). TNFR2 is expressed on immune cells (especially Tregs) and soluble or membrane bound ligands can mediate the activation of the classical NFKB pathway via TNFR2 (Rothe et al., 1995). In line with this observation, successful therapeutic approaches to selectively expand Tregs via TNFR2 activation were developed during the last years. A recent publication of our group showed that Treg expansion by a selective agonist prior to allo-HCT could reduce post-transplant mortality in a murine model of aGvHD (Chopra et al., 2016). Consistent with these findings, our data confirmed high TNFR2 expression on naive Tregs. Additionally, a strong upregulation of TNFR2 was observed on alloreactive $CD4^+$ and $CD8^+$ Tcons on d6 after allo-HCT. Therefore, the differentiation of alloreactive Tcons and Tregs based on TNFR2 expression levels will probably be insufficient for a Tcon targeting approach by therapeutic antibodies.

CD27 is expressed on several T cell subsets and binds CD70 on APCs (Hintzen et al., 1993). It functions a co-stimulatory molecule and its expression is induced rapidly after activation to promote cell survival and proliferation. Previous reports have demonstrated the important role of CD27-CD70 interaction during aGvHD. Blockade of CD70 during aGvHD increased T cell activation and showed that CD70 binding to CD27 suppresses T cell responses in a murine allo-HCT model (Leigh et al., 2017). In this murine allo-HCT model, CD70 expressing host cells inhibited T cell proliferation and therefore reduced alloreactivity. Therefore, host-derived CD70 binding to CD27 on donor T cells seems to be a negative regulator of alloreactive T cell responses. Our findings revealed, that CD27 is highly upregulated on alloreactive Tcons as well as Tregs after allo-HCT. Of note, Tregs derived from naïve mice showed already high levels of CD27 before transplantation. Based on these observation, agonistic antibodies against CD27 might be a suitable approach for selective Treg expansion prior to transplantation.

4-1BB (CD137, TNFRSF9) was highly expressed on naive Tregs and almost no expression levels were detecte on naive Tcons. In general, its expression is highly induced upon T cell activation mediating co-stimulatory signals into T cells (Wen et al., 2002). Similiarly, we observed a rapid induction of 4-1BB expression on Tcons on d6

after allo-HCT. Kim et al. demonstrated in a model of chronic GvHD (cGvHD) that the injection of an agonistic monoclonal antibody against 4-1BB reduced $CD4^+$ T cells and cutaneous GvHD symptoms in murine allo-HCT recipients (Kim et al., 2007). Moreover, they have shown that early injection of anti-4-1BB (during the acute phase of GvHD) leads to higher mortality due to hyperactivation of T cells. Based on these observations, 4-1BB targeting might be an appropriate approach for chronic inflammatory conditions rather than for aGvHD.

GITR is expressed on Tregs and upregulated upon activation on Tcons, where it functions as a costimulatory molecule (van Olffen et al., 2009). We have observed higher GITR expression on Tregs than on Tcons derived from healthy mice. However, activated Tcons – isolated on d3.5 and d6 from HCT recipients – showed increased GITR expression levels but could not reach the expression levels of Tregs. Based on these findings, GITR expression reliably identifies Tregs in healthy and inflammatory conditions and the selective agonism of GITR by therapeutic antibodies might serve as another promising approach to expand Tregs prior to HCT.

Recent reports showed that strong or chronic activation of costimulatory pathways can reduce autoimmune diseases and GvHD (Yu et al., 2004). The underlying anti-inflammatory effect of these approaches was based on the depletion of alloantigen-activated donor T cells. Our results demonstrated that 4-1BB, CD27, GITR and TNFR2 are highly expressed on Tregs before and until d6 after allo-HCT. However, alloreactive Tcons significantly upregulated these surface molecules during aGvHD progression. Therefore, the discrimination of Tcons vs. Tregs during an ongoing inflammatory reaction based on these markers will probably be insufficient. To selectively deplete Tcons during aGvHD progression we propose to use targeting moieties against 4-1BB, CD27, TNFR2 and PD1 and to study if hyperactivation of Tcons leads to selective T cell depletion/anergy induction. This approach might be more difficult to achieve, however other groups have shown that it is feasible (Yu et al., 2004).

With this part of the work we got more insights into dynamic changes in immunomodulatory surface marker expression levels on host vs. donor Tcons and Tregs. Based on the findings, we propose to use agonistic antibodies against GITR, CD27, 4-1BB to induce Treg proliferation before allo-HCT. In general, this work revealed significant changes and dynamic expression of immunomodulatory molecules and the potential to use many of these molecules to expand Tregs or modulate

alloreactive Tcons and further research needs to be done in order to exploit their potential.

13.3 Part III: Development of therapeutic (antibody) fusion proteins to selectively target alloreactive T cells

Antibody fusion proteins exhibit an enormous potential for clinical applications. In general, therapeutic fusion proteins are created by fusion of DNA fragments encoding different proteins or protein domains. During this work we validated $\alpha4\beta7$ and CD162P/P-Lig as alloreactive T cell markers. Research from other groups has already demonstrated the importance of both homing molecules during aGvHD progression. For example, the transplantation of $\alpha4\beta7$ ko donor T cells prevented T cell infiltration into the intestine of murine HCT recipients (Petrovic et al., 2004; Waldman et al., 2006) emphasizing the important function of $\alpha4\beta7$ for aGvHD manifestation. Based on these preclinical data a humanized monoclonal antibody against $\alpha4\beta7$, Vedolizumab, was developed and is currently in several clinical trials for the treatment of inflammatory disorders such as Crohn's Disease and GI GvHD. However, preliminary results suggest a highly immunosuppressive effect of Vedolizumab resulting in severe side effects and infectious complications. Based on these data, we aimed to develop therapeutic antibody fusion proteins by recombinant DNA technology against $\alpha4\beta7$ and CD162P/P-Lig to evaluate novel strategies for selective T cell modulation after allo-HCT. Major goal of this part of the work was the development of bispecific and bifunctional ligand-based or antibody-based fusion proteins with one targeting and one effector domain.

The ligand-based fusion proteins contained the extracellular domain of murine MAdCAM-1 or P-Selectin to target $\alpha4\beta7$ or CD162P/P-Lig, respectively. In general, MAdCAM-1 fusion proteins were not produced by transfected HEK293T cells at all. Whereas almost all P-Selectin fusion proteins were produced in relatively high amounts (3-5 μg). The production of the proteins was performed by PEI transfection of HEK293T cells. However, to exclude technical problems such as insufficient delivery of plasmids into the cytosol, we also tried the transfection of the plasmids by electroporation. Even electroporated MAdCAM-1 plasmids were not translated and secreted in detectable levels. We assume some difficulties in correct translation, post-translational modifications and protein folding after transfection with these plasmids, which resulted in poor production efficiency. Based on these results, we decided to

proceed with the development of antibody-based fusion proteins rather than with ligand-based fusion proteins.

For targeting $\alpha4\beta7$ the V_H and V_L sequences of a monoclonal antibody (clone DATK32, murine) were used and full length antibodies as well as FAB2 fragments were generated. The advantage of an full length antibody is the high serum half-life (around 10-21 days) (Booth et al., 2018). Whereas, FAB2 fragments have a serum half-life of 7-20 hours but due to the smaller size an increased tissue penetration (Davé et al., 2016). Almost all developed antibody-based variants against $\alpha4\beta7$ showed improved production efficiency.

To target CD162P/P-Lig the V_H and V_L of an hIgG1 antibody were exchanged with the extracellular domain of murine P-Selectin. In a second approach, we fused the extracellular domain of P-Selectin via linkers directly to the Fc domain of human IgG1. The antibody-based variants showed much higher binding affinity to their target compared to the fusion proteins. The antibody-based variants contain in total 4 binding sites for CD162P/P-Lig, whereas the ligand-based fusion proteins had only 2 binding sites, which might be an explanation for the poor binding affinity of ligand-based fusion proteins.

Based on our data and extensive surface marker profiling on Tcons vs. Tregs, we assume that the expression of an intestinal/skin homing receptor together with an immunomodulatory molecule exclusively identifies alloreactive T cells in allo-HCT recipients. Therefore, future work will focus on the development of bifunctional and bispecific antibody-based fusion proteins for the selective modulation of Treg/Tcon subsets prior/during HCT. These antibodies will contain a T cell recognition domain (e.g. against $\alpha4\beta7$ or CD162P/P-Lig) and an effector domain (e.g. against PD1, TNFR2 or other immunomodulatory molecules). Consequently, these bifunctional antibodies would induce apoptosis or anergy in alloreactive T cells, which are specifically homing to the target organs skin or intestine. Another approach would be to selectively expand skin- or gut-homing Tregs by agonistic antibodies. Depending on the selected strategy, the timing of the therapeutic intervention during aGvHD progression will be very crucial to selectively modulate either Tregs or Tcons. Another perspective is the evaluation of other molecules and their differential expression kinetics during aGvHD. Alahmari et al. reported that the blockade of $\alpha4\beta1$ is more effective than $\alpha4\beta7$ in order to prevent aGvHD in a fully MHC mismatched murine allo-HCT model (Alahmari et al., 2016; Zundler et al., 2017). Furthermore, antibodies with strong affinity to activating FcγR

might be an alternative approach for the depletion of alloreactive T cells. This approach has shown high potential for specific Treg depletion within the tumor microenvironment (Dahan et al., 2015). In general, binding of an antibody to an activatory FcγR induces activation of macrophages and DCs (Nimmerjahn et al., 2015, 2006). Since aGvHD is a highly inflammatory disease this approach would need careful investigation and might be a possible treatment option for cGvHD rather than for aGvHD.

13.4 Part IV: Modulation of alloreactive T cells via NFAT SUMOylation

NFAT transcription factors regulate important cellular processes in T cells like activation, survival and anergy induction. NFAT proteins are activated downstream of TCR signaling and regulated by the phosphatase calcineurin. Calcineurin activation is calcium- and calmodulin-dependent and leads to the dephosphorylation of NFAT proteins after positive TCR engagement. NFAT transcription factors are then translocated into the nucleus and bind response elements within the regulatory elements of genes for IL-2, TNF-α, IFN-γ, IL-4 and IL-5. Calcineurin inhibitors are a class of potent immunosuppressive agents, which are clinically used for the prevention and treatment of inflammatory conditions such as aGvHD. These inhibitors strongly reduce alloreactive T cell responses but also cause severe side effects and diminish the desirable GvL effect. Therefore, we asked if direct modulation of NFAT molecules could decrease the alloreactivity of T cells while allowing immune reconstitution and GvL. Previous work has reported that Tcons lacking the NFAT family members, NFATc1 and/or NFATc2 cause less aGvHD due to decreased effector function. Quite the reverse, the frequency of Tregs seemed even enriched (Vaeth et al., 2015). Consistently, the desirable GvL effect was maintained.

A sensitive regulator of NFATc1 activity is the post-translational modification by SUMO (Small Ubiquitin-related MOdifier) (Johnson, 2004). Previous data revealed the importance of the C-terminal-specific SUMO consensus sites K702 and K914 (Nayak et al., 2009). To investigate the role of NFATc1 SUMOylation *in vivo*, we generated a mouse strain, where the critical lysines within the consensus motifs for SUMOylation were changed to arginine in the NFATc1/C-specifc C-terminus. Therefore, NFATc1/C SUMOylation was prevented in all cells including T cells derived from these mice. All former data demonstrated that averted SUMOylation of NFATc1/C leads to higher IL-2 levels due to better accessibility of the *Il2* promotor (Nayak et al., 2009). First

challenges of NFATc1/ΔS mice under chronic inflammatory conditions revealed an anti-inflammatory phenotype and increased tTreg frequencies due to higher IL-2 levels. During this work it was shown that averted SUMOylation of NFATc1/C could significantly reduce alloreactivity of donor T cells during MHC major mismatch aGvHD on multiple levels. Mice which received NFATc1/ΔS T cells showed significantly less *in vivo* proliferation and had reduced target organ infiltration compared to WT T cells. Confirming our previous studies showing that NFAT proteins are key regulators in T cell signaling and effector function (Vaeth et al., 2015).

Nayak et al. showed previously in *in vitro* experiments that averted NFATc1 SUMOylation leads to a reduction of effector cytokines and in increase in IL-2 production. In line with this result, we we have observed a significant decrease in inflammatory cytokine production such as TNF-α and IFN-γ in alloreactive T cells derived from NFATc1/ΔS mice. Surprisingly, we could not detect higher IL-2 levels in NFATc1/ΔS recipients during aGvHD progression. Nevertheless, higher Treg frequencies were observed in NFATc1/ΔS T cell recipients compared to WT T cell recipients. Tregs are essential to control acute immune responses by downregulation of Tcons via several immunosuppressive mechanisms (Sakaguchi et al., 2009). Consistent with the presented data, it has been reported that mice deficient in one or more NFAT family members have functional Tregs (Bopp et al., 2005). Based on previous findings we assumed to detect higher IL-2 levels in alloreactive T cells derived from NFATc1/ΔS donors. To our surprise, we could not observe this effect NFATc1/ΔS T cell recipients. One explanation for this might be the induced Blimp-1 expression upon IL-2 signaling. It was shown by others that Blimp-1 can act as direct repressor of IL-2 (Martins et al., 2008). Indeed, we found a strong induction of Blimp-1 in NFATc1/ΔS donor T cells and assume that the heightened IL-2 levels expressed by non-SUMOylated NFATc1 induces Blimp-1, which then negatively feeds back on IL-2 expression. With this, the initial plus in IL-2 would direct the immune response to a less inflammatory, at the same time preventing an uncontrolled expansion of alloreactive Tcon by a timely restriction of elevated IL-2 production.

Equally important, levels of IFN-γ and TNF-α were significantly reduced after allo-HCT in mice, which received NFATc1/ΔS T cells. Consistent with the presented data, it has been shown by others that Blimp-1 represses IFN-γ expression directly and via *Tbx21* (encoding T-bet) inhibition (Cimmino et al., 2008).

Since IL-2 – together with TGF-β - supports the conversion of naïve $CD4^+$ T cells into pTregs and since we observed a higher frequency of $Foxp3^+$ Tregs, we studied the pTreg induction during aGvHD. We transplanted WT and NFATc1/ΔS Tcons from C57BL/6-Tg(Foxp3-DTR/EGFP) mice. These T cell donors were treated by DTx before isolation of T cells in order to deplete DTR-expressing $Foxp3^+$ Tregs. In this Treg-depleted setting, we could indeed observe higher IL-2 frequencies in Tcons derived from NFATc1/ΔS mice. However, the induction of pTregs in both WT and ΔS recipients were below 1%. Of note, the Treg frequencies were determined 6 days after allo-HCT and the time for pTreg induction might have been too short. Furthermore, pTregs are predominantly induced on mucosal sites for which reason we might have missed their presence with the analysis of splenic Tregs (Schmitt et al., 2013).

Conclusively, the obtained results point towards a possible novel therapeutic approach to selectively reduce alloreactivity of Tcons while maintaining Treg function. The therapeutic effect of averted NFATc1 SUMOylation in T cells is very comparable to low dose IL-2 administration for treatment of inflammatory diseases (Tahvildari et al., 2019). However, low dose IL-2 administration in a preclinical aGvHD mouse model not only led to higher Treg frequencies but expanded inflammatory Tcons to the same extend resulting in higher aGvHD severity (Hirakawa et al., 2016; Pérol et al., 2014). Therefore, we propose the modulation of the NFATc1/C SUMOylation pathway as novel strategy to selectively modulate inflammatory immune responses. One possible approach might be the development of small molecules against the NFATc1/C terminus leading to reduced accessibility by the SUMOylation machinery. Alternatively, genetic engineering of T cells – for example by the revolutionizing new technique CRISPR/Cas9 – prior to transplantation, would transiently equip the incoming immune system with less pro-inflammatory T cells, predicted to still confer the GvL effect. As shown here, this approach would at least moderately modify the immune reaction by favoring Treg expansion and inhibition of Th1 effector function via molecular mechanisms such as the negative feedback loop of Blimp1.

14 Conclusion and Perspective

Studies in two independent miHAg mismatch models revealed the identification of alloreactive T cells in the PB of murine HCT recipients by a combinatorial T cell surface marker panel. Alloreactive $CD8^+$ T cells were identified by high levels of $\alpha4\beta7$, CD162E/CD162P and low levels of CD62L. The combination of these markers reliably predicted allo-HCT outcomes before aGvHD symptoms occurred. Furthermore, we excluded a panel of other surface markers, which could not reliably predict allo-HCT outcomes. These promising findings in murine models await to be further validated in allo-HCT patients in order to proof the predictive value of the developed test.

Preclinical data and clinical trials have shown that the blockade of homing pathways for T cells can enormously modulate inflammatory responses. During this work it was shown that antibody-based fusion proteins were superior to ligand-based fusion proteins for targeting the homing receptors $\alpha4\beta7$ and CD162P/P-Selectin ligand. It was proofed that antibody-based formats showed higher affinity to their target structure and better production efficiency compared to the ligand-based fusion protein variants. These identified antibody formats can be further extended by additional effector domains, which would enable the selective modulation of skin or gut homing Tcons or Tregs during aGvHD. Possible immunological targets on alloreactive Tcons vs. Tregs were evaluated in this thesis and promising candidates such as GITR, 4-1BB, CD27, TNFR2 and PD1 were identified.

Calcineurin inhibitors are strong immunosuppressive agents used for the treatment of aGvHD. Although highly effective, these molecules can cause severe side effects and inhibit the desirable GvL effect. It was demonstrated here, that the modification of NFATc1 SUMOylation pathway could reduce alloreactivity while maintaining the protective properties of Tregs. Thus, this pathway might be a novel treatment strategy for the modulation of alloreactive T cells after or even before transplantation, which might be achieved by development of small molecules against the C-terminus of NFATc1/C. Furthermore, it might be worth considering the exchange of arginine to lysin in the C-terminus of NFATc1 by CRISPR/Cas9, which would lead to selective posttranslational regulation of NFATc1/C activity only in donor T cells.

Conclusively, the work of this thesis revealed several novel strategies that await now to be adopted for the modulation of alloreactive T cells after allo-HCT.

15 Bibliography

Abbas, A., Lichtman, A., & Pillai, S. (2017). *Cellular and Molecular Immunology* (9th ed.).

Abu Zaid, M., Wu, J., Wu, C., Logan, B. R., Yu, J., Cutler, C., Antin, J. H., Paczesny, S., & Choi, S. W. (2017). Plasma biomarkers of risk for death in a multicenter phase 3 trial with uniform transplant characteristics post-allogeneic HCT. *Blood*, *129*(2), 162–170.

Afkarian, M., Sedy, J. R., Yang, J., Jacobson, N. G., Cereb, N., Yang, S. Y., Murphy, T. L., & Murphy, K. M. (2002). T-bet is a STATI-induced regulator for IL-12R expression in naïve CD4+T cells. *Nature Immunology*, *3*(6), 549–557.

Aggarwal, B. B. (2003). Signalling pathways of the TNF superfamily: A double-edged sword. *Nature Reviews Immunology*, *3*(9), 745–756.

Alahmari, B., Choi, J., Cooper, M. L., Vij, K. R., Ritchey, J., Wang, B., & DiPersio, J. F. (2016). Selective Inhibition of α4β1 Integrin (VLA-4) Mitigates GvHD. *Blood ASH Publications*, *128*(22), 3344.

Ali, N., Flutter, B., Sanchez Rodriguez, R., Sharif-Paghaleh, E., Barber, L. D., Lombardi, G., & Nestle, F. O. (2012). Xenogeneic Graft-versus-Host-Disease in NOD-scid IL-2Rγnull Mice Display a T-Effector Memory Phenotype. *PLoS ONE*, *7*(8), 1–10.

Anderson, B. E., McNiff, J., Matte, C., Athanasiadis, I., Shlomchik, W. D., & Shlomchik, M. J. (2004). Recipient CD4+ T cells that survive irradiation regulate chronic graft-versus-host disease. *Blood*, *104*(5), 1565–1573.

Ankersmit, H. J., Moser, B., Zuckermann, A., Roth, G., Taghavi, S., Brunner, M., Wolner, E., & Boltz-Nitulescu, G. (2002). Activation-induced T cell death, and aberrant T cell activation via TNFR1 and CD95-CD95 ligand pathway in stable cardiac transplant recipients. *Clinical and Experimental Immunology*, *128*(1), 175–180. https://doi.org/10.1046/j.1365-2249.2002.01836.x

Artis, D., Humphreys, N. E., Porten, C. S., Wagner, N., Müller, W., McDermott, J. R., Grencis, R. K., & Eise, K. J. (2000). β7 integrin-deficient mice: Delayed leukocyte recruitment and attenuated protective immunity in the small intestine during enteric helminth infection. *European Journal of Immunology*, *30*(6), 1656–1664.

Asaduzzaman, M., Mihaescu, A., Wang, Y., Sato, T., & Thorlacius, H. (2009). P-Selectin and P-Selectin Glycoprotein Ligand 1 Mediate Rolling of Activated CD8+ T Cells in Inflamed Colonic Venules. *Journal of Investigative Medicine*, *57*(7), 765–768.

Aziz, M. D., Shah, J., Kapoor, U., Dimopoulos, C., Anand, S., Augustine, A., Ayuk, F., Chaudhry, M., Chen, Y.-B., Choe, H. K., Etra, A., Gergoudis, S., Hartwell, M. J., Hexner, E. O., Hogan, W. J., Kitko, C. L., Kowalyk, S., Kröger, N., Merli, P., … Levine, J. E. (2020). Disease risk and GVHD biomarkers can stratify patients for risk of relapse and nonrelapse mortality post hematopoietic cell transplant. *Leukemia*.

Ball, L. M., & Egeler, R. M. (2008). Acute GvHD: Pathogenesis and classification. *Bone Marrow Transplantation*, *41*, 58–64.

Barry, M., & Bleackley, R. C. (2002). Cytotoxic T lymphocytes: all roads lead to death. *Nature Reviews. Immunology*, *2*(6), 401–409.

Bäuerlein, C. A., Riedel, S. S., Baker, J., Brede, C., Garrote, A. L. J., Chopra, M., Ritz, M., Beilhack, G. F., Schulz, S., Zeiser, R., Schlegel, P. G., Einsele, H., Negrin, R. S., & Beilhack, A. (2013). A diagnostic window for the treatment of acute graft-versus-host disease prior to visible clinical symptoms in a murine

model. *BMC Medicine*, *11*(1).
Beilhack, A., Schulz, S., Baker, J., Beilhack, G. F., Nishimura, R., Baker, E. M., Landan, G., Herman, E. I., Butcher, E. C., Contag, C. H., & Negrin, R. S. (2008). Prevention of acute graft-versus-host disease by blocking T-cell entry to secondary lymphoid organs. *Blood*, *111*(5), 2919–2928.
Beilhack, A., Schulz, S., Baker, J., Beilhack, G. F., Wieland, C. B., Herman, I., Baker, E. M., Cao, Y., Contag, C. H., Negrin, R. S., Dc, W., & Herman, E. I. (2005). In vivo analyses of early events in acute graft-versus-host disease reveal sequential infiltration of T-cell subsets. *Blood*, *106*(3), 1113–1122.
Berger, M., Signorino, E., Muraro, M., Quarello, P., Biasin, E., Nesi, F., Vassalo, E., & Fagioli, F. (2013). Monitoring of TNFR1, IL-2Rα, HGF, CCL8, IL-8 and IL-12p70 following HSCT and their role as GVHD biomarkers in paediatric patients. *Bone Marrow Transplant*, *48*, 1230–1236.
Berke, G. (1995). The CTL's kiss of death. *Cell*, *81*(1), 9–12.
Berlin, C., Berg, E. L., Briskin, M. J., Andrew, D. P., Kilshaw, P. J., Holzmann, B., Weissman, I. L., Hamann, A., & Butcher, E. C. (1993). α4β7 integrin mediates lymphocyte binding to the mucosal vascular addressin MAdCAM-1. *Cell*, *74*(1), 185–195.
Blazar, B. R., Kwon, B. S., Panoskaltsis-Mortari, A., Kwak, K. B., Peschon, J. J., & Taylor, P. A. (2001). Ligation of 4-1BB (CDw137) regulates graft-versus-host disease, graft-versus-leukemia, and graft rejection in allogeneic bone marrow transplant recipients. *Journal of Immunology*, *166*(5), 3174–3183.
Booth, B. J., Ramakrishnan, B., Narayan, K., Wollacott, A. M., Babcock, G. J., Shriver, Z., & Viswanathan, K. (2018). Extending human IgG half-life using structure-guided design. *MAbs*, *10*(7), 1098–1110.
Bopp, T., Palmetshofer, A., Serfling, E., Heib, V., Schmitt, S., Richter, C., Klein, M., Schild, H., Schmitt, E., & Stassen, M. (2005). NFATc2 and NFATc3 transcription factors play a crucial role in suppression of CD4+ T lymphocytes by CD4+ CD25+ regulatory T cells. *The Journal of Experimental Medicine*, *201*(2), 181–187.
Bouazzaoui, A., Spacenko, E., & Mueller, G. (2011). Steroid treatment alters adhesion molecule and chemokine expression in experimental acute graft-vs.-host disease of the intestinal tract. *Experimental Hematology*, *39*(2), 238–241.
Brodie, S. J., Sasseville, V. G., Reimann, K. A., Simon, M. A., Brodie, S. J., Sasseville, V. C., Reimann, K. A., Simon, M. A., Sehgal, P. K., & Ringler, D. J. (2010). This information is current as of April 7, 2010. *Journal Of Immunology*.
Budde, H., Papert, S., Maas, J., Reichardt, H., Wulf, G., Hasenkamo, J., Riggert, J., & Legler, T. (2017). Prediction of graft-versus-host disease: a biomarker panel based on lymphocytes and cytokines. *Ann Hematol.*, *96*(7), 1127–1133.
Chakraverty, R., Côté, D., Buchli, J., Cotter, P., Hsu, R., Zhao, G., Sachs, T., Pitsillides, C. M., Bronson, R., Means, T., Lin, C., & Sykes, M. (2006). An inflammatory checkpoint regulates recruitment of graft-versus-host reactive T cells to peripheral tissues. *The Journal of Experimental Medicine*, *203*(8), 2021–2031.
Chao, N. J. (2004). Minors Come of Age: Minor Histocompatibility Antigens and Graft-Versus-Host Disease. *Biology of Blood and Marrow Transplantation*, *10*(4), 215–223.
Choi, S. W., Kitko, C. L., Braun, T., Paczesny, S., Yanik, G., Mineishi, S., Krijanovski, O., Jones, D., Whitfield, J., Cooke, K., Hutchinson, R. J., Ferrara, J. L. M., & Levine, J. E. (2008). Change in plasma tumor necrosis factor receptor 1 levels in the first week after myeloablative allogeneic transplantation correlates with

severity and incidence of GVHD and survival. *Blood*, *112*(4), 1539–1542.
Choo, S. (2007). The HLA System: Genetics, Immunology, Clinical Testing, and Clinical Implications. *Yonsei Medical Journal*, *48*(1), 11–23.
Chopra, M., Biehl, M., Steinfatt, T., Brandl, A., Kums, J., Amich, J., Vaeth, M., Kuen, J., Holtappels, R., Podlech, J., Mottok, A., Kraus, S., Jordán-Garrote, A.-L., Bäuerlein, C. A., Brede, C., Ribechini, E., Fick, A., Seher, A., Polz, J., … Beilhack, A. (2016). Exogenous TNFR2 activation protects from acute GvHD via host T reg cell expansion. *The Journal of Experimental Medicine*, jem.20151563.
Cimmino, L., Martins, G., Liao, J., Magnusdottir, E., Grunig, G., Perez, R., & Calame, K. (2008). Blimp-1 Attenuates Th1 Differentiation by Repression of ifng, tbx21, and bcl6 Gene Expression. *J Immunol*, *181*(4), 2338–2347.
Connor, E., Eppihimer, M., Morise, Z., Granger, D., & Grisham, M. (1999). Expression of mucosal addressin cell adhesion molecule-1 (MAdCAM-1) in acute and chronic inflammation. *J Leukoc Biol*, *65*(3), 349–355.
Cooke, K., Kobzik, L., Martin, T., Brewer, J., Delmonte, J. J., & Crawford, J. et al. (1996). An experimental model of idiopathic pneumonia syndrome after bone marrow transplantation: 1. The roles of minor H antigens and endotoxin. *Blood*, *88*(8), 3230–3239.
Copelan, E. A. (2006). Hematopoietic Stem-Cell Transplantation. *New England Journal of Medicine*, *354*(17), 1813–1826.
Curotto de Lafaille, M. A., & Lafaille, J. J. (2009). Natural and Adaptive Foxp3+ Regulatory T Cells: More of the Same or a Division of Labor? *Immunity*, *30*(5), 626–635.
Dahan, R., Sega, E., Engelhardt, J., Selby, M., Korman, A. J., & Ravetch, J. V. (2015). FcγRs Modulate the Anti-tumor Activity of Antibodies Targeting the PD-1/PD-L1 Axis. *Cancer Cell*, *28*(3), 285–295.
Danylesko, I., Bukauskas, A., Paulson, M., Peceliunas, V., Gedde-Dahl d.y, T., Shimoni, A., Shouval, R., Griskevicius, L., Floisand, Y., & Nagler, A. (2019). Anti-α4β7 integrin monoclonal antibody (vedolizumab) for the treatment of steroid-resistant severe intestinal acute graft-versus-host disease. *Bone Marrow Transplantation*, *54*(7), 987–993.
Davé, E., Adams, R., Zaccheo, O., Carrington, B., Compson, J. E., Dugdale, S., Airey, M., Malcolm, S., Hailu, H., Wild, G., Turner, A., Heads, J., Sarkar, K., Ventom, A., Marshall, D., Jairaj, M., Kopotsha, T., Christodoulou, L., Zamacona, M., … Humphreys, D. P. (2016). Fab-dsFv: A bispecific antibody format with extended serum half-life through albumin binding. *MAbs*, *8*(7), 1319–1335.
Doe, W. F. (1989). The intestinal immune system. *Gut*, *30*(12), 1679–1685.
Elgert, K. (2009). Antibody Structure and Function. *John Wiley & Sons*, *2*.
Eom, H., Rubio, M., Means, T., Luster, A., & Sykes, M. (2005). T-cell P/E-selectin ligand α(1,3)fucosylation is not required for graft-vs-host disease induction. *Experimental Hematology*, *33*(12), 1564–1573.
Erle, D. J., Briskin, M. J., Butcher, E. C., Garcia-Pardo, A., Erle, D. J., Bri, M. J., Butcher, E. C., Garcia-Pardo, A., & Tidswell, M. (1994). Lazarovits and M Tidswell Expression and Function of the MAdCAM-1 Receptor, lntegrin a4P7, on Human Leukocytes'. *J Immunol*, *153*, 517–528.
Eyrich, M., Burger, G., Marquardt, K., Budach, W., Schilbach, K., Niethammer, D., & Schlegel, P. G. (2005). Sequential expression of adhesion and costimulatory molecules in graft-versus-host disease target organs after murine bone marrow transplantation across minor histocompatibility antigen barriers. *Biology of Blood and Marrow Transplantation*, *11*(5), 371–382.
Ferrara, J., Levine, J., Reddy, P., & Holler, E. (2009). Graft-versus-host disease. *The*

Lancet, *373*(9674), 1550–1561.
Ferrara, J., Levy, R., & Chao, N. (1999). Pathophysiologic mechanisms of acute graft-vs.-host disease. *Biology of Blood and Marrow Transplantation*, *5*(6), 347–356.
Fløisand, Y., Lazarevic, V. L., Maertens, J., Mattsson, J., Shah, N. N., Zachée, P., Taylor, A., Akbari, M., Quadri, S., Parfionovas, A., & Chen, Y. Bin. (2019). Safety and Effectiveness of Vedolizumab in Patients with Steroid-Refractory Gastrointestinal Acute Graft-versus-Host Disease: A Retrospective Record Review. *Biology of Blood and Marrow Transplantation*, *25*(4), 720–727.
Fu, H., Ward, E. J., & Marelli-Berg, F. M. (2016). Mechanisms of T cell organotropism. *Cellular and Molecular Life Sciences*, *73*(16), 3009–3033.
Fuchs, F., Schillinger, D., Atreya, R., Hirschmann, S., Fischer, S., Neufert, C., Atreya, I., Neurath, M. F., & Zundler, S. (2017). Clinical response to vedolizumab in ulcerative colitis patients is associated with changes in integrin expression profiles. *Frontiers in Immunology*, *8*(764), 1–12.
Fuchs, S., Sawas, N., Staedler, N., Schubert, D. A., D'Andrea, A., Zeiser, R., Piali, L., Hruz, P., & Frei, A. P. (2019). High-dimensional single-cell proteomics analysis identifies immune checkpoint signatures and therapeutic targets in ulcerative colitis. *European Journal of Immunology*, *49*(3), 462–475.
Fukatsu, K., Lundberg, A., Hanna, M., Wu, Y., Wilcox, H., Granger, D., Gaber, A., & Kudsk, K. (2000). Increased expression of intestinal P-selectin and pulmonary E-selectin during intravenous total parenteral nutrition. *Arch Surg*, *135*(10), 1177–1182.
Gattinoni, L., Lugli, E., Ji, Y., Pos, Z., Paulos, C. M., Quigley, M. F., Almeida, J. R., Gostick, E., Yu, Z., Carpenito, C., Wang, E., Douek, D. C., Price, D. A., June, C. H., Marincola, F. M., Roederer, M., & Restifo, N. P. (2012). A human memory T-cell subset with stem cell-like properties. *Nature Medicine*, *17*(10), 1290–1297.
Germain, R. N. (2002). T-cell development and the CD4–CD8 lineage decision. *Nature Reviews Immunology*, *2*(5), 309–322.
Ghimire, S., Weber, D., Mavin, E., Wang, X. N., Dickinson, A. M., & Holler, E. (2017). Pathophysiology of GvHD and other HSCT-related major complications. *Frontiers in Immunology*, *8*(79), 1–11.
Gorfu, G., Rivera-Nieves, J., & Ley, K. (2009). Role of β 7 integrins in intestinal lymphocyte homing and retention. *Current Molecular Medicine*, *9*(7), 836–850.
Gratwohl, A., Pasquini, M., Aljurf, M., Atsuta, Y., Baldomero, H., Foeken, L., Gratwohl, M., Gluckman, E., Greinix, H., Horowitz, M., Iida, M., Lipton, J., Madrigal, A., Mohty, M., Noel, L., Novitzky, N., Nunez, J., Oudshoorn, M., Passweg, J., … Frauendorfer, K. (2015). One million haemopoietic stem-cell transplants: a retrospective observational study. *Lancet Haematol*, *2*(3), e91-100.
Greinix, H., Loddenkemper, C., Pavletic, S., Holler, E., Socié, G., Lawitschka, A., Halter, J., & Wolff, D. (2011). Diagnosis and Staging of Chronic Graft-versus-HostDisease in the Clinical Practice. *American Society for Blood and Marrow Transplantation*, *17*, 167–175.
Grell, M., Scheurich, P., Meager, A., & Pfizenmaier, K. (1993). TR60 and TR80 tumor necrosis factor (TNF)-receptors can independently mediate cytolysis. *Lymphokine and Cytokine Research*, *12*(3), 143–148.
Habtezion, A., Nguyen, L., Hadeiba, H., & Butcher, E. (2015). No TitleLeukocyte Trafficking to the Small Intestine and Colon. *Gastroenterology*, *150*(2), 340–354.
Hammerschmidt, S. I., Ahrendt, M., Bode, U., Wahl, B., Kremmer, E., Förster, R., & Pabst, O. (2008). Stromal mesenteric lymph node cells are essential for the

generation of gut-homing T cells in vivo. *The Journal of Experimental Medicine*, *205*(11), 2483–2490.
Harrington, L. E., Hatton, R. D., Mangan, P. R., Turner, H., Murphy, T. L., Murphy, K. M., & Weaver, C. T. (2005). Interleukin 17-producing CD4+ effector T cells develop via a lineage distinct from the T helper type 1 and 2 lineages. *Nature Immunology*, *6*(11), 1123–1132.
Hartwell, M. J., Özbek, U., Holler, E., Renteria, A. S., Major-Monfried, H., Reddy, P., Aziz, M., Hogan, W. J., Ayuk, F., Efebera, Y. A., Hexner, E. O., Bunworasate, U., Qayed, M., Ordemann, R., Wölfl, M., Mielke, S., Pawarode, A., Chen, Y. Bin, Devine, S., … Ferrara, J. L. (2018). An early-biomarker algorithm predicts lethal graft-versus-host disease and survival. *JCI Insight*, *3*(16), 1–9.
Hintzen, R. Q., de Jong, R., Lens, S. M., Brouwer, M., Baars, P., & van Lier, R. A. (1993). Regulation of CD27 expression on subsets of mature T-lymphocytes. *Journal of Immunology*, *151*(5), 2426–2435.
Hirakawa, M., Matos, T., Liu, H., Koreth, J., Kim, H. T., Paul, N. E., Murase, K., Whangbo, J., Alho, A. C., Nikiforow, S., Cutler, C., Ho, V. T., Armand, P., Alyea, E. P., Antin, J. H., Blazar, B. R., Lacerda, J. F., Soiffer, R. J., & Ritz, J. (2016). Low-dose IL-2 selectively activates subsets of CD4+ Tregs and NK cell. *JCI Insight*, *1*(18), 1–18.
Hirshfeld, E., Weiss, L., Kasir, J., Zeira, M., Slavin, S., & Shapira, M. (2006). Post transplant persistence of host cells augments the intensity of acute graft-versus-host disease and level of donor chimerism, an explanation for graft-versus-host disease and rapid displacement of host cells seen following non-myeloablative stem cell . *Bone Marrow Transplant.*, *38*(5), 359–364.
Hogan, W. J., & Storb, R. (2004). Use of cyclosporine in hematopoietic cell transplantation. *Transplantation Proceedings*, *36*, 367–371.
Hori, S., Nomura, T., & Sakaguchi, S. (2003). *Control of Regulatory T Cell Development by the Transcription Factor Foxp3*. *299*, 1057–1062.
Jacobsohn, D. A., & Vogelsang, G. B. (2007). Acute graft versus host disease. *Orphanet Journal of Rare Diseases*, *2*(1), 1–9.
Jenq, R. R., & van den Brink, M. R. M. (2010). Allogeneic haematopoietic stem cell transplantation: individualized stem cell and immune therapy of cancer. *Nature Reviews Cancer*, *10*(3), 212–221.
Johnson, E. S. (2004). Protein Modification by SUMO. *Annual Review of Biochemistry*, *73*(1), 355–382.
Jondal, M., Schirmbeck, R., & Reimann, J. (1996). MHC class I-restricted CTL responses to exogenous antigens. *Immunity*, *5*(4), 295–302.
Kaufmann, S. H. E. (2014). *Basiswissen Immunologie*. Springer Berlin Heidelberg.
Khandelwal, P., Chaturvedi, V., Owsley, E., Davies, S. M., & Marsh, R. A. (2017). CD38 Bright CD8+ TEM Cells Detected Prior to Acute Gvhd are Activated, Cytotoxic, Proliferating, Trafficking Cells Which are Not Viral Specific. *Biology of Blood and Marrow Transplantation*, *23*(3), 137.
Kim, J., Kim, H. J., Park, K., Kim, J., Choi, H.-J., Yagita, H., Nam, S. H., Cho, H. R., & Kwon, B. (2007). Costimulatory molecule-targeted immunotherapy of cutaneous graft-versus-host disease. *Blood*, *110*(2), 776–782.
Koch, U., & Radtke, F. (2011). Mechanisms of T Cell Development and Transformation. *Annual Review of Cell and Developmental Biology*, *27*(1), 539–562.
Korngold, R., & Sprent, J. (1980). Negative selection of T cells causing lethal graft-versus-host disease across minor histocompatibility barriers. Role of the H-2 complex. *The Journal of Experimental Medicine*, *151*(5), 1114–1124.

Kröger, N., & Zander, A. (2011). Allogene Stammzelltherapie-Grundlagen, Indikationen und Perspektiven. *UNI-MED Verlag*, *3*.
Kums, J., Nelke, J., Rüth, B., Schäfer, V., Siegmund, D., & Wajant, H. (2017). Quantitative analysis of cell surface antigen-antibody interaction using Gaussia princeps luciferase antibody fusion proteins. *MAbs2*, *3*, 506–520.
Léger, C. S., & Nevill, T. J. (2004). Hematopoietic stem cell transplantation: a primer for the primary care physician. *CMAJ : Canadian Medical Association Journal = Journal de l'Association Medicale Canadienne*, *170*(10), 1569–1577.
Leigh, N. D., O'Neill, R. E., Du, W., Chen, C., Qiu, J., Ashwell, J. D., McCarthy, P. L., Chen, G. L., & Cao, X. (2017). Host-Derived CD70 Suppresses Murine Graft-versus-Host Disease by Limiting Donor T Cell Expansion and Effector Function. *The Journal of Immunology*, *199*(1), 336–347.
Li, Q. J., Baker, M., Li, W., Tsalik, E. L., He, Y. W., Woods, C. W., Wang, Y., Li, Z., Xiao, B., Guo, J., Palmer, S. M., Corbet, K., & Chao, N. J. (2013). Plasma microRNA signature as a noninvasive biomarker for acute graft-versus-host disease. *Blood*, *122*(19), 3365–3375.
Lu, S. X., Holland, A. M., Na, I.-K., Terwey, T. H., Alpdogan, O., Bautista, J. L., Smith, O. M., Suh, D., King, C., Kochman, A., Hubbard, V. M., Rao, U. K., Yim, N., Liu, C., Laga, A. C., Murphy, G., Jenq, R. R., Zakrzewski, J. L., Penack, O., … van den Brink, M. R. M. (2010). Absence of P-Selectin in Recipients of Allogeneic Bone Marrow Transplantation Ameliorates Experimental Graft-versus-Host Disease. *The Journal of Immunology*, *185*(3), 1912–1919.
Luckheeram, R. V., Zhou, R., Verma, A. D., & Xia, B. (2012). CD4 +T cells: Differentiation and functions. *Clinical and Developmental Immunology*, *2012*.
Major-Monfried, H., Renteria, A. S., Pawarode, A., Reddy, P., Ayuk, F., Holler, E., Efebera, Y. A., Hogan, W. J., Wölfl, M., Qayed, M., Hexner, E. O., Wudhikarn, K., Ordemann, R., Young, R., Shah, J., Hartwell, M. J., Chaudhry, M. S., Aziz, M., Etra, A., … Levine, J. E. (2018). MAGIC biomarkers predict long-term outcomes for steroid-resistant acute GVHD. *Blood*, *131*(25), 2846–2855.
Martin, P., Schoch, G., Fisher, L., Byers, V., Anasetti, C., & Appelbaum, F. et al. (1990). A retrospective analysis of therapy for acute graft-versus-host disease: initial treatment. *Blood*, *76*(8), 1464–1472.
Martins, G. a, Cimmino, L., Liao, J., Magnusdottir, E., & Calame, K. (2008). Blimp-1 directly represses Il2 and the Il2 activator Fos, attenuating T cell proliferation and survival. *Journal of Experimental Medicine*, *205*(9), 1959–1965.
Mason, K. L., Huffnagle, G. B., Noverr, M. C., & Kao, J. Y. (2008). Overview ofGut Immunology. *Advances in Experimental Medicine and Biology*, *635*.
Mathewson, N., Jenq, R., Mathew, A., Koenigsknecht, M., Hanash, A., & Toubai, T. (2016). Gut microbiome-derived metabolites modulate intestinal epithelial cell damage and mitigate graft-versus-host disease. *Nature Immunology*, *17*(5), 505–513.
Moller, J., Skirhoj, P., Hoiby, N., & Peterson, F. (1982). Protection against graft versus host disease by gut sterilization? *Experimental Haematology*, *10*(101).
Moore, K. L. (1998). Structure and Function of P-Selectin Glycoprotein Ligand-1. *Leukemia & Lymphoma*, *29*(1–2), 1–15.
Munoz, L., Holgado, B., Martinez, A., Rodriguez-Frade, J., & Mellado, M. (2012). Chemokine receptor oligomerization: a further step toward chemokine function. *Immunology Letters*, *145*(1–2), 23–29.
Murai, M., Yoneyama, H., Ezaki, T., Suematsu, M., Terashima, Y., Harada, A., Hamada, H., Asakura, H., Ishikawa, H., & Matsushima, K. (2003). Peyer's patch is the essential site in initiating murine acute and lethal graft-versus-host

reaction. *Nature Immunology*, *4*(2), 154–160.
Murai, M., Yoneyama, H., Harada, A., Yi, Z., Vestergaard, C., Guo, B., Suzuki, K., Asakura, H., & Matsushima, K. (1999). Active participation of CCR5+CD8+ T lymphocytes in the pathogenesis of liver injury in graft-versus-host disease. *Journal of Clinical Investigation*, *104*(1), 49–57.
Nayak, A., Glöckner-Pagel, J., Vaeth, M., Schumann, J. E., Buttmann, M., Bopp, T., Schmitt, E., Serfling, E., & Berberich-Siebelt, F. (2009). Sumoylation of the transcription factor NFATc1 leads to its subnuclear relocalization and interleukin-2 repression by histone deacetylase. *Journal of Biological Chemistry*, *284*(16), 10935–10946.
Nguyen, L., Pan, J., Dinh, T., Hadeiba, H., O'Hara, E., Ebtikar, A., Hertweck, A., Gökmen, M., Jenner, R., Butcher, E., & Habtezion, A. (2015). Role and species-specific expression of colon T cell homing receptor GPR15 in colitis. *Nature Immunology*, *16*(2), 207–213.
Nimmerjahn, F., Gordan, S., & Lux, A. (2015). FcγR dependent mechanisms of cytotoxic, agonistic, and neutralizing antibody activities. In *Trends in Immunology*.
Nimmerjahn, F., & Ravetch, J. V. (2006). Fcγ receptors: Old friends and new family members. *Immunity*, *24*, 19–28.
O' Shea, J., & Paul, W. (2010). Commitment and Plasticity of Helper. *Science*, *327*, 1098–1102.
O'Shea, J. J., Steward-Tharp, S. M., Laurence, A., Watford, W. T., Wei, L., Adamson, A. S., & Fan, S. (2009). Signal transduction and Th17 cell differentiation. *Microbes and Infection*, *11*(5), 599–611.
Omer, A. K., Weisdorf, D., Lazaryan, A., Shanley, R., Blazar, B., MacMillian, M. L., Brunstein, C., Bejanyan, N., & Arora, M. (2016). Late Acute Graft Versus Host Disease After Allogeneic Hematopoietic Stem Cell Transplantation. *Biology of Blood and Marrow Transplantation*, *22*(5), 879–833.
Ottinger, H., Ferencik, S., & Beelen, D. et al. (2003). Hematopoietic stem cell transplantation: contrasting the outcome of transplantations from HLA-identical siblings, partially HLA- mismatched related donors, and HLA-matched unrelated donors. *Blood*, *102*(3), 1131–1137.
Paczesny, S., Krijanovski, O. I., Braun, T. M., Choi, S. W., Clouthier, S. G., Kuick, R., Misek, D. E., Cooke, K. R., Kitko, C. L., Weyand, A., Bickley, D., Jones, D., Whitfield, J., Reddy, P., Levine, J. E., Hanash, S. M., & Ferrara, J. L. M. (2009). A biomarker panel for acute graft-versus-host disease. *Blood*, *113*(2), 273–278.
Pandiyan, P., Zheng, L., Ishihara, S., Reed, J., & Lenardo, M. J. (2007). CD4+CD25+Foxp3+ regulatory T cells induce cytokine deprivation–mediated apoptosis of effector CD4+ T cells. *Nature Immunology*, *8*(12), 1353–1362.
Papadakis, K. A., & Targan, S. R. (2000). Tumor necrosis factor: Biology and therapeutic inhibitors. *Gastroenterology*, *119*(4), 1148–1157.
Peled, J., Jenq, R., Holler, E., & van den Brink, M. (2016). Role of gut flora after bone marrow transplantation. *Nature Microbiology*, *1*(16036).
Pérol, L., Martin, G. H., Maury, S., Cohen, J. L., & Piaggio, E. (2014). Potential limitations of IL-2 administration for the treatment of experimental acute graft-versus-host disease. *Immunology Letters*, *162*(2), 173–184.
Petrovic, A., Alpdogan, O., Willis, L. M., Eng, J. M., Greenberg, A. S., Kappel, B. J., Liu, C., Murphy, G. J., Heller, G., & Van Den Brink, M. R. M. (2004). LPAM (α4β7 integrin) is an important homing integrin on alloreactive T cells in the development of intestinal graft-versus-host disease. *Blood*, *103*(4), 1542–1547.
Ponta, H., Sherman, L., & Herrlich, P. (2003). CD44: from adhesion molecules to

signalling regulators. *Nature Reviews Molecular Cell Biology*, *4*(1), 33–45.
Reshef, R., Ganetsky, A., Acosta, E. P., Blauser, R., Crisalli, L., McGraw, J., Frey, N. V., Hexner, E. O., Hoxie, J. A., Loren, A. W., Luger, S. M., Mangan, J., Stadtmauer, E. A., Mick, R., Vonderheide, R. H., & Porter, D. L. (2019). Extended CCR5 Blockade for Graft-versus-Host Disease Prophylaxis Improves Outcomes of Reduced-Intensity Unrelated Donor Hematopoietic Cell Transplantation: A Phase II Clinical Trial. *Biology of Blood and Marrow Transplantation*, *25*(3), 515–521.
Reshef, R., Luger, S., & Hexner, E. et al. (2012). Blockade of lymphocyte chemotaxis in visceral graft-versus-host disease. *New England Journal of Medicine*, *367*(2), 135–145.
Rivera-Nieves, J., Gorfu, G., & Ley, K. (2008). Leukocyte adhesion molecules in animal models of inflammatory bowel disease. *Inflammatory Bowel Diseases*, *14*(12), 1715–1735.
Rothe, M., Pan, M. G., Henzel, W. J., Ayres, T. M., & V. Goeddel, D. (1995). The TNFR2-TRAF signaling complex contains two novel proteins related to baculoviral inhibitor of apoptosis proteins. *Cell*, *83*(7), 1243–1252.
Rothermel, B. A., Vega, R. B., & Williams, R. S. (2003). The role of modulatory calcineurin-interacting proteins in calcineurin signaling. *Trends in Cardiovascular Medicine*, *13*(1), 15–21.
Roux, K. H., Strelets, L., & Michaelsen, T. E. (2018). *Flexibility of human IgG subclasses*.
Sakaguchi, S., Wing, K., Onishi, Y., Prieto-Martin, P., & Yamaguchi, T. (2009). Regulatory T cells: How do they suppress immune responses? *International Immunology*, *21*(10), 1105–1111.
Saliba, R., Sarantopoulos, S., Kitko, C., Pawarode, A., Goldstein, S., Magenau, J., Alousi, A., Churai, T., Justman, H., Paczesny, S., Reddy, P., & Couriel, D. (2018). B-cell activating factor (BAFF) plasma level at the time of chronic GvHD diagnosis is a potential predictor of non-relapse mortality. *Bone Marrow Transplant.*, *52*(7).
Sallusto, F., Lenig, D., Forster, R., Lipp, M., & Lanzavecchia, A. (1999). Two subsets of memory T lymphocytes with distinct homing potentials and effector functions. *Nature*, *401*, 708–712.
Sancho, D., Gomez, M., & Sanchez-Madrid, F. (2005). CD69 is an immunoregulatory molecule induced following activation. *Trends Immunol.*, *25*(3), 136–140.
Scheffold, A., Murphy, K. M., & Höfer, T. (2007). Competition for cytokines: T(reg) cells take all. *Nature Immunology*, *8*(12), 1285–1287.
Schmitt, E. G., & Williams, C. B. (2013). Generation and Function of Induced Regulatory T Cells. *Frontiers in Immunology*, *4*(152).
Schneider, P., Thome, M., Burns, K., Bodmer, J. L., Hofmann, K., Kataoka, T., Holler, N., & Tschopp, J. (1997). TRAIL receptors 1 (DR4) and 2 (DR5) signal FADD-dependent apoptosis and activate NF-κB. *Immunity*, *7*(6), 831–836.
Schroeder, & DiPersio, J. (2011). Mouse models of graft-versus-host disease: advances and limitations. *Disease Models & Mechanisms*, *4*(3), 318–333.
Schroeder, H., & Cavacini, L. (2009). Structure and function of immunoglobulins. Relation to allergy. *New York State Journal of Medicine*.
Serfling, E., Berberich-Siebelt, F., & Avots, A. (2007). NFAT in lymphocytes: a factor for all events? *Science STKE*, *2007*(398), 42.
Serfling, E., Berberich-Siebelt, F., Chuvpilo, S., Jankevics, E., Klein-Hessling, S., Twardzik, T., & Avots, A. (2000). The role of NF-AT transcription factors in T cell activation and differentiation. *Biochimica et Biophysica Acta*, *1498*(1), 1–18.

Shlomchik, W., Couzens, M., Tang, C., McNiff, J., Robert, M., & Liu, J. (1999). Prevention of graft versus host disease by inactivation of host antigen-presenting cells. *Science*, *285*(5426), 412–415.

Shresta, S., Pham, C. T., Thomas, D. A., Graubert, T. A., & Ley, T. J. (1998). How do cytotoxic lymphocytes kill their targets? *Current Opinion in Immunology*, *10*(5), 581–587.

Singh, A. K., & McGuirk, J. P. (2016). Allogeneic stem cell transplantation: A historical and scientific overview. *Cancer Research*, *76*(22), 6445–6451.

Socié, G., & Blazar, B. (2009). Acute graft-versus-host disease: from the bench to the bedside. *Blood*, *114*(20), 4327–4336.

Stefanich, E. G., Danilenko, D. M., Wang, H., O'Byrne, S., Erickson, R., Gelzleichter, T., Hiraragi, H., Chiu, H., Ivelja, S., Jeet, S., Gadkari, S., Hwang, O., Fuh, F., Looney, C., Howell, K., Albert, V., Balazs, M., Refino, C., Fong, S., … Williams, M. (2011). A humanized monoclonal antibody targeting the β7 integrin selectively blocks intestinal homing of T lymphocytes. *British Journal of Pharmacology*, *162*, 1855–1870.

Strob, R., Prentice, R., & Buckner, C. et al. (1983). Graft– versus–host disease and survival in patients with aplastic anemia treated by marrow grafts from HLA-identical siblings: beneficial effect of a protective environment. *N Eng J Med*, *308*(302).

Sureda, A., Bader, P., Cesaro, S., Dreger, P., Duarte, R. F., Dufour, C., Falkenburg, J. H. F., Farge-Bancel, D., Gennery, A., Kröger, N., Lanza, F., Marsh, J. C., Nagler, A., Peters, C., Velardi, A., Mohty, M., & Madrigal, A. (2015). Indications for allo- and auto-SCT for haematological diseases, solid tumours and immune disorders: Current practice in Europe, 2015. *Bone Marrow Transplantation*, *50*(8), 1037–1056.

Szmeja, Z. (2008). Recenzja podręcznika pt. „CT Teaching Manual. A Systematic Approach to CT Reading". *Otolaryngologia Polska*, *62*(1), 117.

Tahvildari, M., & Dana, R. (2019). Low-Dose IL-2 Therapy in Transplantation, Autoimmunity, and Inflammatory Diseases. *J Immunol*, *1*(203), 11.

Taur, Y., Jenq, R., Ubeda, C., van den Brink, M., & Pamer, E. (2015). Role of intestinal microbiota in transplantation outcomes. *Best Practice & Research Clinical Haematology*, *28*(2), 155–161.

Teshima, T., Reddy, P., & Zeiser, R. (2016). Acute Graft-versus-Host Disease: Novel Biological Insights. *Biology of Blood and Marrow Transplantation*, *22*(1), 11–16.

Turpeinen, H., Ojala, P., Ojala, K., Miettinen, M., Volin, L., & Partanen, J. (2013). Minor histocompatibility antigens as determinants for graft-versus-host disease after allogeneic haematopoietic stem cell transplantation. *International Journal of Immunogenetics*, *40*(6), 495–501.

Vaeth, M., Bäuerlein, C. A., Pusch, T., Findeis, J., Chopra, M., Mottok, A., Rosenwald, A., Beilhack, A., & Berberich-Siebelt, F. (2015). Selective NFAT targeting in T cells ameliorates GvHD while maintaining antitumor activity. *Proceedings of the National Academy of Sciences of the United States of America*, *112*(4), 1125–1130.

van Bekkum, D., Roodenburg, J., Heidt, P., & van der Waaij, D. (1974). Mitigation of secondary disease of allogeneic mouse radiation chimeras by modification of the intestinal microflora. *J Natl Cancer Inst.*, *52*, 401.

van Olffen, R. W., Koning, N., van Gisbergen, K. P. J. M., Wensveen, F. M., Hoek, R. M., Boon, L., Hamann, J., van Lier, R. A. W., & Nolte, M. A. (2009). GITR Triggering Induces Expansion of Both Effector and Regulatory CD4 + T Cells In Vivo. *The Journal of Immunology*, *182*(12), 7490–7500.

Vander Lugt, M. T., Braun, T. M., Hanash, S., Ritz, J., Ho, V. T., Antin, J. H., Zhang, Q., Wong, C., Wang, H., Chin, A., Gomez, A., Harris, A. C., Levine, J. E., Choi, S. W., Couriel, D., Reddy, P., Ferrara, J. L., & Paczesny, S. (2013). ST2 as a marker for risk of therapy-resistant graft-versus-host disease and death. *New England Journal of Medicine*, *369*(6), 529–539.

von Adrian, U. H., & Mempel, T. R. (2003). Homing and cellular traffic in lymph nodes. *Nature Reviews Immunology*, *3*, 867.

Wajant, H. (2013). The TWEAK-Fn14 system as a potential drug target. *British Journal of Pharmacology*, *170*(4), 748–764.

Wajant, H. (2016). Therapeutic targeting of CD70 and CD27. *Expert Opinion on Therapeutic Targets*, *20*(8), 959–973.

Waldman, E., Lu, S., Hubbard, V., Kochman, A., Eng, J., Terwey, T., Muriglan, S., Kim, T., Heller, G., Murphy, G. F., Liu, C., Alpdogan, O., & Van Den Brink, M. R. M. (2006). Absence of β7 integrin results in less graft-versus-host disease because of decreased homing of alloreactive T cells to intestine. *Blood*, *107*(4), 1703–1711.

Wall, W. J., Carruthers, G., & Howson, W. (1981). Measurement of CyA by Radioimmunoassay (RIA)' o Immunological Monitoring of the Transplant Recipient Clinical and Immunological Course Post-transplant. *The Lancet*, 686–689.

Wen, T., Bukczynski, J., & Watts, T. H. (2002). 4-1BB Ligand-Mediated Costimulation of Human T Cells Induces CD4 and CD8 T Cell Expansion, Cytokine Production, and the Development of Cytolytic Effector Function. *The Journal of Immunology*, *168*(10), 4897–4906.

Yu, X., Albert, M., Martin, P., & Anasetti, C. (2004). CD28 ligation induces transplantation tolerance by IFN gamma dependent depletion of T cells that recognized alloantigens. *J Clin Invest*, *113*(1624–30).

Zak, K., Grudnik, P., Magiera, K., Dömling, A., Dubin, G., & Holak, T. (2017). Structural Biology of the Immune Checkpoint Receptor PD-1 and Its Ligands PD-L1/PD-L2. *Structure Cell Press*, *25*(8), 1163–1174.

Zeiser, R., & Blazar, B. (2016). Preclinical models of acute and chronic graft-versus-host disease: how predictive are they for a successful clinical translation? *Blood*, *127*(25), 3117–3127.

Zeiser, R., & Blazar, B. (2017). Acute Graft-versus-Host Disease - Biologic Process, Prevention, and Therapy. *New England Journal of Medicine*, *377*(22), 2167–2179.

Zeiser, R., Socie, G., & Blazar, B. (2016). Pathogenesis of acute graft-versus-host disease: from intestinal microbiota alterations to donor T cell activation. *Br J Haematol.*, *175*(2), 191–207.

Zundler, S., Fischer, A., Schillinger, D., Binder, M. T., Atreya, R., Rath, T., Lopez-Pósadas, R., Voskens, C. J., Watson, A., Atreya, I., Neufert, C., & Neurath, M. F. (2017). The 4β1 Homing Pathway Is Essential for Ileal Homing of Crohn's Disease Effector T Cells in Vivo. *Inflammatory Bowel Diseases*, *23*, 379–391.

16 Appendix

16.1 Sequences

The following chapter contain the amino acid sequences of the:

DATK32 V_L

M N F G F S L I F L V L V L K G V Q C E VK L V P R Q L D Y K D D D D K E L
D I Q M T H S P S S M S A S L G D T V T I T C L A S Q D I G N Y L S W Y Q Q
K P G R S P K L M I Y A A T N L E D G V P S R F S G S R S G S D Y S L T I N
S L G Y D D E G I Y H C H Q Y Y E Y P Y T F G S G T K L E I K G S E I K R T
V A A P S V F I F P P S D E Q L K S G T A S V V C L L N N F Y P R E A K V Q
W K V D N A L Q S G N S Q E S V T E Q D S K D S T Y S L S S T L T L S K A
D Y E KH K V Y A C E V T H Q G L S S P V T K S F N R G E C

DATK32 V_H

X E L S G - L E N P L L T G L S K L I R L T I G R P K L Q N M N F G F S L I F
L V L V L K G V Q C E V K L V P R Q L D Y K D D D D K E L E V Q L V E S G
G G L V Q P G T S L K L S C V A S G F T F S D Y W M S W V R Q T P G K T M
E W I G D I K Y D G S Y P N Y A P S L K N R F T I S R D N A K N T L Y L Q M
S N V R S E D T A T Y Y C T R D D P Y F D Y W G Q G V M V T V S S

MAdCAM-1(ed, mu)

L S G - L E N X L L T G L S K L I R L T I G R P K L M E S I L A L L L A L A L
V P Y Q L S R G Q S F Q V N P P E S E V A V A M G T S L Q I T C S M S C D
E G V A R V H W R G L D T S L G S V Q T L P G S S I L S V R G M L S D T G
T P V C V G S C G S R S F Q H S V K I L V Y A F P D Q L V V S P E F L V P G
Q D Q V V S C T A Q E G T P L F R M T Q R W R L P S L G T P A P P A L H C
Q V T M Q L P K L V L T H R X E I P V L Q S Q T S P K P P N T T S A E P Y I
L T S S S T A E A V S T G L N I T T L P S A P P Y P K L S P R T L S S E G P
C R P K I H Q D L E A G W E L L C E A S C G P G X T V R W T L A P G D L A
T Y H K R E A G X Q A W L N V L P P G P X

P-Selectin(ed, mu)

E L S G X L E N P L L T G L S K L I R L T I G R P K L M A G C P K G S W T P
R L R S V I L G G A Q L I W F S A L I S E L V N Q K E V A A W T Y N Y S T K
A Y S W N N S R V F C R R H F T D L V A I Q N K N E I A H L N D V I P F F N
S Y Y W I G I R K I N N K W T W V G T N K T L T E E A E N W A D N E P N N
K K N N Q D C V E I Y I K S N S A P G K W N D E P C F K R K R A L C Y T A
S C Q D M S C S N Q G E C I E T I G S Y T C S C Y P G F Y G P E C E Y V K
E C G K V N I P Q H V L M N C S H P L G E F S F N S Q C T F S C A E G Y E
L D G P G E L Q C L A S G I W T N N P P X C D A V Q C Q S L E A P P H G T
M A C M H P Y R R F R L R F F L - N L N V

16.2 List of Publication

Published

Bäuerlein CA*, *Qureischi M**, Mokhtari Z, Tabares P, Brede C, Jordán-Garrote A, Riedel S, Chopra M, Reu S, Mottok A, Arellano-Viera E, Graf C, Kurzwart M, Schmiedgen K, Einsele H, Wölfl M, Schlegel PG and Beilhack A (2021). A Four T cell Surface Marker Panel Predicts Murine Acute Graft-versus-Host Disease**.** Frontiers in Immunology.

Xiao Y*, *Qureischi M**, Dietz* L, Vaeth M, Vallabhapurapu S, Klein-Hessling S, Klein M, Chuanguang L, Koenig A, Serfling E, Mottok A, Bopp T, Rosenwald A, Buttmann M, Berberich I, Beilhack A and Berberich-Siebelt F (2020). Lack of NFATc1 SUMOylation prevents autoimmunity and alloreactivity. Journal of Experimental Medicine.

Ottmüller K, Mokhtari M, Scheller L, Hartweg L, Thusek S, Le DD, Ranecky M, Shaikh H, *Qureischi M*, Heinze K, Beilhack A (2018). Photoconversion of alloreactive T cells in Peyer's patches during acute GvHD: Tracking the homing route of highly proliferative cells in vivo. Frontiers Immunology.

Ankenbrand MJ, Pfaff S, Teerhoeven N, *Qureischi M*, Gündel M, Weiss CL, Hackl T, Förster F (2018). Chloroextractor: Extraction and Assembly of The Chloroplast Genome From Whole Genome Shotgun Data. Journal of Open Source Software.

Klein-Hessling S, Muhammad K, Pusch T, Klein M, Rudolf R, Flöter J, *Qureischi M,* Beilhack A, Vaeth M, Kummerow C, Backes C, Schoppmeyer R, Hahn U, Hoth M, Bopp T, Berberich-Siebelt F, Patra A, Avots A, Müller N, Schulze A, Serfling E. (2017). NFATc1 controls the cytotoxicity of $CD8^+$ T cells on multiple levels. Nature Communications.

*equal contribution